DEVELOPMENTAL REFINEMENTS IN TEMPORALLY PRECISE AUDITORY BRAINSTEM CIRCUITS

DELWEN L. FRANZEN

Graduate School of
Systemic Neurosciences
LMU Munich

Dissertation der Graduate School of Systemic Neurosciences der
Ludwig-Maximilians-Universität München

24th July 2017

Delwen L. Franzen: *Developmental refinements in temporally precise auditory brainstem circuits*

Reviewer 1: Prof. Dr. Felix Felmy
Reviewer 2: Prof. Dr. Benedikt Grothe
Reviewer 3: Prof. Ian Forsythe
Date of oral defense: 02.11.2017

To my friends and family,

SUMMARY

The ability to localise sound sources is crucial to the survival of many species, and underlies a wide range of complex behaviours such as conspecific communication and prey – predator interactions. A combination of monaural and binaural cues is used to localise sound sources in the environment. These cues are initially encoded by highly specialised neurons in the auditory brainstem.

The ventral nucleus of the lateral lemniscus (VNLL) is a largely monaural nucleus in the auditory brainstem thought to be involved in analysing the temporal structure of sounds. Spherical VNLL neurons respond to the onset of acoustic stimuli with remarkably short latency and low temporal jitter, suggesting they are specialised to encode the onset of sounds. To gain insight into how VNLL neurons acquire their high temporal precision, we characterised developmental changes in intrinsic membrane properties in the VNLL of Mongolian gerbils, a well established model of human hearing. Our findings show how developmental changes in passive and active membrane properties interact to promote the emergence of temporally precise responses in mature VNLL neurons. Our results also highlight the relative contribution of passive membrane properties to different aspects of neuronal excitability upon varying stimulus conditions. The developmental maturation of intrinsic properties ensures that VNLL neurons are ideally suited to provide fast, broadband onset inhibition to the inferior colliculus.

As in other sensory systems, the establishment of auditory brainstem circuits is guided by sensory experience. Neurons of the medial superior olive (MSO) encode differences in the arrival time of sounds at the two ears (interaural time differences, ITDs) in the order of microseconds by integrating bilateral excitatory and inhibitory inputs with high precision. Shortly after hearing onset, glycinergic inputs to the MSO undergo a structural refinement which requires normal acoustic experience. To explore the mechanisms underlying circuit refinements in the MSO, we assessed whether calcium is developmentally regulated in the MSO of gerbils from before hearing onset to maturity. We show that the developmental profile of calcium signalling in MSO neurons supports the existence of a short time window after hearing onset for calcium-dependent circuit refinements. Given that masking binaural cues with omnidirectional white noise has previously been shown to disrupt the refinement of glycinergic inputs to the MSO, we assessed whether the same paradigm similarly affects the development of calcium signalling. Our findings are discussed in the context of how different features of sensory experience may differentially influence the refinement of neural circuits.

Taken together, the studies described in this thesis illustrate how membrane properties refine during development to fulfill distinct functional demands on the circuit. While the membrane properties of immature neurons reflect the need to establish a precise, functional circuit, they must rapidly refine to achieve the high temporal precision required of the mature system.

CONTENTS

1

INTRODUCTION

1.1 SOUND LOCALISATION

1.1.1 *Sound transduction and the mammalian ascending auditory pathway*

Changes in air pressure travel through the ear canal and induce mechanical deflections of the tympanic membrane. In turn, the ossicles of the middle ear vibrate and transmit amplified sound vibrations to the fluid filled cochlea. These vibrations elicit travelling waves along the basilar membrane of the cochlea. The width and stiffness of the basilar membrane change along its length. As a result, the frequency of a sound determines the position along the basilar membrane that vibrates maximally, generating a tonotopic map in the cochlea (von Békésy, 1956). On the basilar membrane lies the sensory epithelium, the Organ of Corti, where inner hair cells transduce mechanical energy into electrical signals. This activity is conveyed in the form of action potentials (APs) via the auditory nerve to the cochlear nucleus (CN) of the auditory brainstem (Grothe et al., 2010). Auditory nerve fibres converge onto several types of cells in the CN, some of which exhibit remarkably high temporal precision (Golding et al., 1995; Oertel, 1997; Oertel et al., 2000). The temporal information of sounds is preserved both at the level of the auditory nerve and in the CN. For low-frequency sounds, this is achieved by phase-locking to the fine structure of sounds (Rose et al., 1967; Rhode et al., 1983; Smith et al., 1991; Joris et al., 1994; Oertel, 1999). At high frequencies, neurons retain the temporal structure of sounds by phase locking to the envelope of acoustic signals (Rhode and Greenberg, 1994).

Different ascending streams originate from the CN, and can be subdivided into monaural and binaural pathways. Monaural pathways are formed by different cell types in the ventral and dorsal CN that project contralaterally to the lateral lemniscus and then to the inferior colliculus (IC), or to the IC directly. Binaural pathways originate in specialised bushy cells in the ventral CN (VCN), which combine the input from several auditory nerve fibres, and project to the principal nuclei of the superior olivary complex (SOC) on both sides (Stotler, 1953; Lindsey, 1975). In turn, SOC nuclei project to the dorsal nucleus of the lateral lemniscus (DNLL) and to the IC (Adams, 1979). Monaural and binaural pathways converge in the IC, which then targets the thalamus and auditory cortex (Grothe et al., 2010). One exception is the nucleus of the central acoustic tract, which circumvents the IC and projects directly onto the suprageniculate nucleus and then onto the frontal auditory cortex (Behrend and Schuller, 2000; Grothe and Park, 2000).

1.1.2 *Monaural and binaural cues used for sound localisation*

In the auditory system, the location of a sound source is not encoded at the level of sensory receptors. Rather, the auditory system exploits spectral and binaural cues in the environment, which are then processed in the brain to localise sounds. When broadband sound reaches the outer ear, its spectrum is altered at specific frequencies in a manner that depends on the elevation of the sound source. This monaural cue largely depends on the interaction of sound with the pinna and the ear canal, and is used to localise sounds in the vertical plane (Grothe et al., 2010). The auditory system also makes use of binaural cues to localise sounds in the horizontal plane. First, high frequencies with a wavelength equal or shorter than the diameter of the head are attenuated by the head, generating a shadowing effect that is largest at the ear furthest away from the sound source (Figure 1.1). This shadowing effect leads to differences in sound intensity level at the two ears (interaural level differences (ILDs)), which vary depending on the frequency and location of sounds. Second, low frequencies that are not reflected by the head can be localised based on the difference in the arrival time of sound at the two ears (interaural time differences, ITDs) (Figure 1.1). The demonstration that humans could detect interaural phase differences led to the duplex theory of sound localisation: ILDs are used to localise high-frequency sounds while ITDs are used to localise low-frequency sounds (Rayleigh, 1907). Binaural cues are initially processed in distinct nuclei of the auditory brainstem: ILDs are encoded by the lateral superior olive (LSO) and ITDs are encoded by the medial superior olive (MSO). While all terrestrial mammals exploit ILDs for sound localisation, their use of ITDs depends on their hearing range and the presence of a well-developed MSO (Grothe, 2000; Grothe and Pecka, 2014).

1.1.3 *A nucleus in a monaural pathway: the VNLL*

The ventral nucleus of the lateral lemniscus (VNLL) is a group of cells embedded in the fibres of the lateral lemniscus, a major part of the ascending auditory pathway. The cytoarchitecture and organisation of the VNLL varies between species. In bats, the VNLL is a hypertrophied structure, which can be subdivided into a columnar region (VNLLc) that comprises a homogeneous group of globular cells, and a region containing multipolar cells (Covey and Casseday, 1986; Huffman and Covey, 1995; Vater et al., 1997). VNLL cells of bats are monaural, as they are driven by sound presented to the contralateral ear (Covey and Casseday, 1991). Consistent with this, the major input to the VNLL originates in the contralateral VCN (Zook and Casseday, 1985; Covey and Casseday, 1986; Zook and Casseday, 1987; Huffman and Covey, 1995), with an additional inhibitory projection from the ipsilateral medial nucleus of the trapezoid body (MNTB) (Zook and Casseday, 1987; Grothe et al., 1994; Huffman and Covey, 1995). A minor projection from the ipsilateral lateral nucleus of the trapezoid body (LNTB) and the ventral periolivary nucleus has also been reported in the big brown bat (Huffman and Covey, 1995). Globular VNLLc neurons are broadly tuned, and respond to acoustic stimuli with a single AP precisely timed to the onset of the stimulus. Remarkably, VNLLc neurons display onset responses with extremely short latencies which are independent of sound level

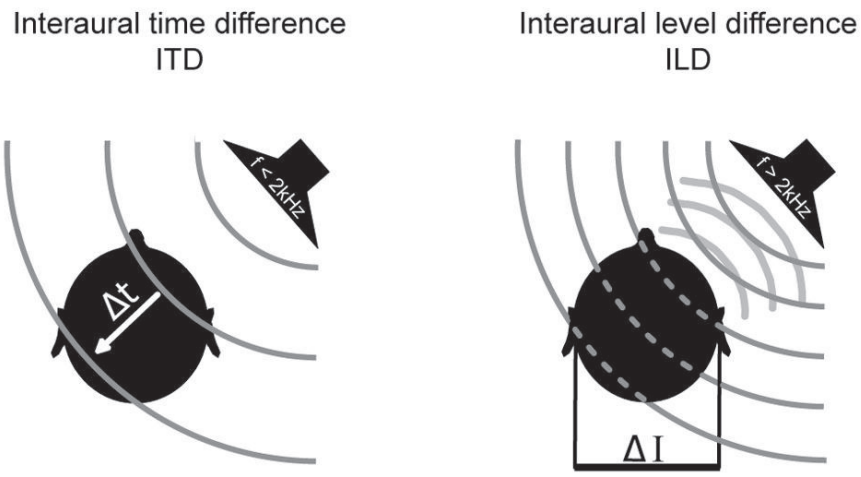

Figure 1.1: *Left*: Interaural time differences (ITDs) occur when a sound source arrives at one ear before the other, and are used to localise low-frequency sounds (<2 kHz). *Right*: The shadowing effect of the head creates differences in sound level between the two ears (interaural level differences (ILDs), which are used to localise high-frequency sounds (>2 kHz). Reproduced with permission from Grothe and Pecka (2014).

or frequency (Covey and Casseday, 1991). Furthermore, VNLLc neurons are innervated by large calyces (Zook and Casseday, 1985; Covey and Casseday, 1986; Vater and Feng, 1990; Vater et al., 1997), which ensure high fidelity synaptic transmission. Thus, globular VNLLc neurons are specialised to encode the onset of sounds with high precision and are thought to play a role in the spectral and temporal analysis of acoustic signals.

In other terrestrial mammals, the major excitatory projection to the VNLL also originates in the contralateral VCN (Stotler, 1953; Glendenning et al., 1981; Friauf and Ostwald, 1988; Schofield and Cant, 1997; Kelly et al., 2009). Moreover, VNLL neurons also receive an inhibitory projection from the ipsilateral MNTB (Glendenning et al., 1981; Spangler et al., 1985; Sommer et al., 1993; Smith et al., 1998; Kelly et al., 2009), which in turn is driven by sound at the contralateral ear (Figure 1.2). Although the VNLL is less well defined than in bats, a population of globular cells has been consistently observed in other mammals, and appears to be restricted to the ventral region of the VNLL (Adams, 1997; Schofield and Cant, 1997; Berger et al., 2014; Caspari et al., 2015). Similar to bats, globular VNLL cells are innervated by thick axons terminating in endbulbs (Stotler, 1953; Adams, 1979; Wu, 1999; Berger et al., 2014; Caspari et al., 2015). Evidence suggests that these endbulbs arise from octopus cells in the posterior VCN (Adams, 1997; Schofield and Cant, 1997) (Figure 1.2). Several endbulbs appear to converge onto single globular VNLL neurons (Adams, 1997; Smith et al., 2005; Berger et al., 2014). In vivo, VNLL neurons exhibit several response types, with a majority of onset and sustained responses (Aitkin et al., 1970; Batra and Fitzpatrick, 1999; Zhang and Kelly, 2006; Recio-Spinoso and Joris,

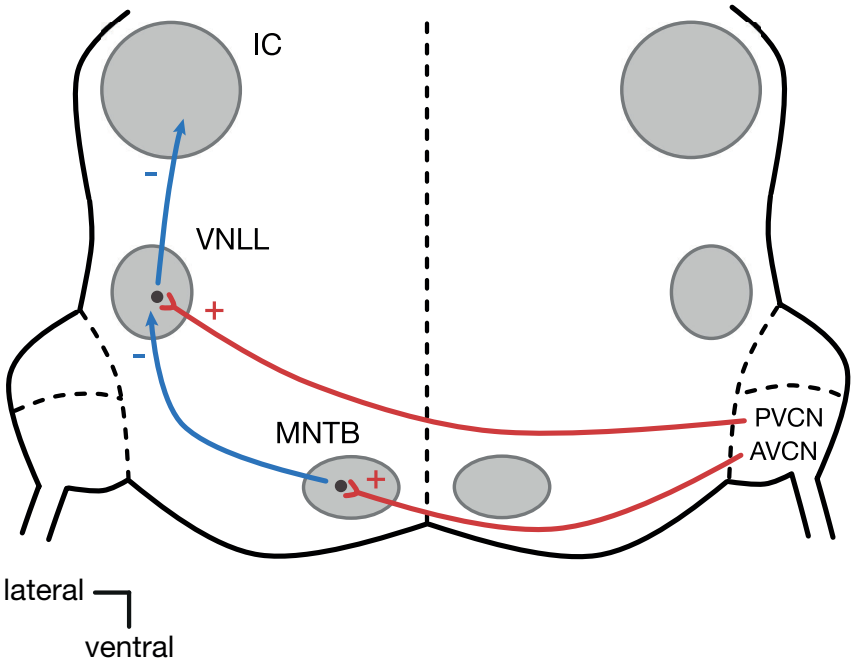

Figure 1.2: Simplified schematic of the input circuitry to globular neurons in the ventral region of the VNLL (the focus of our study). Globular VNLL neurons are innervated by endbulbs, most likely originating from the octopus cell area of the contralateral PVCN. Several endbulbs innervate a single globular VNLL neuron. VNLL neurons receive an inhibitory projection from the ipsilateral MNTB. VNLL neurons form a major inhibitory projection to the IC.

2014). Onset responses in particular are characterised by short first spike latencies and extremely low jitter, with a subset of onset neurons displaying constant latency responses as in the VNLLc of bats (Zhang and Kelly, 2006; Recio-Spinoso and Joris, 2014). Onset and sustained responses found in vivo correspond well with the onset and regular/irregular firing patterns observed in vitro (Wu, 1999; Irfan et al., 2005; Caspari et al., 2015), which have been attributed to cells with a bushy and stellate-like appearance, respectively (Zhao and Wu, 2001). In mice, while onset responses have been observed in calyx-receiving neurons in the ventral VNLL, another subset of cells in the dorsal VNLL also exhibits onset responses but possesses different intrinsic and synaptic properties (Caspari et al., 2015). The response properties of globular VNLL neurons are partly thought to reflect the remarkable temporal precision of their input, octopus cells, which are specialised to encode the timing of firing of many auditory nerve fibres (Oertel, 1999), and display broad tuning and onset responses (Godfrey et al., 1975; Rhode et al., 1983; Rhode and Smith, 1986).

One study reported that a subset of VNLL cells in rats respond to acoustic stimulation with an inhibitory postsynaptic potential (IPSP) preceding the first AP (Nayagam, 2005). Onset inhibition was suggested to arise from axon collaterals of globular VNLL neurons projecting back into the nucleus

(Zhao and Wu, 2001; Nayagam, 2005). However, broadband onset inhibition in VNLL neurons may be provided by multiple MNTB cells, a possibility supported by the anatomical projection from the MNTB to the VNLL in different species (Huffman and Covey, 1995; Spangler et al., 1985; Sommer et al., 1993; Smith et al., 1998; Kelly et al., 2009).

A large proportion of VNLL cells are immunoreactive for glycine and/or GABA (Saint Marie et al., 1997). Moreover, retrograde labelling studies have identified the VNLL as a major source of glycinergic projections to the ipsilateral IC (Saint Marie and Baker, 1990). Thus, the VNLL of bats and other mammals projects to the ipsilateral IC (Adams, 1979; Zook and Casseday, 1982; Nordeen et al., 1983; Zook and Casseday, 1987), where it generates precisely timed onset inhibition (Covey and Casseday, 1991; Nayagam, 2005) and shapes the response properties and tuning features of IC neurons (Pollak et al., 2011).

1.1.4 *A nucleus in a binaural pathway: the MSO*

The MSO is the primary site of binaural integration implicated in ITD processing in mammals. The ITD sensitivity of MSO neurons arises from the coincidence detection of precisely timed inputs from the two ears (Grothe et al., 2010). In most mammals ITDs are in the submillisecond range, illustrating the temporal resolution required for ITD encoding (Grothe and Pecka, 2014). Principal MSO neurons exhibit anatomical and biophysical specialisations which allow such small ITDs to be resolved (for review, see Grothe et al. (2010)). The MSO is tonotopically organised, with low-frequency tuned neurons located dorsally, and high-frequency tuned neurons located ventrally (Guinan et al., 1972). Principal MSO neurons are arranged along a single parasagittal plane and exhibit a bipolar dendritic morphology with their two primary dendrites extending orthogonally to the dorsoventral axis (Stotler, 1953; Rautenberg et al., 2009). MSO neurons receive bilateral, phase-locked excitation and inhibition via four distinct inputs. Spherical bushy cells (SBCs) in the ipsilateral and contralateral AVCN provide phase-locked excitation to the lateral and medial dendrites of MSO neurons respectively (Stotler, 1953; Warr, 1966; Lindsey, 1975; Smith et al., 1993). Thus, the synaptic inputs to the MSO are anatomically segregated. This arrangement, together with the thick bipolar dendrites of MSO neurons, is thought to facilitate coincidence detection (Agmon-Snir et al., 1998). Bilateral inhibition to the MSO is conveyed through two pathways. In the first pathway, globular bushy cells (GBCs) in the AVCN project to the contralateral MNTB via the Calyx of Held, one of the largest synaptic terminals in the mammalian brain (for review, see von Gersdorff and Borst (2002) and Schneggenburger and Forsythe (2006)). Glycinergic MNTB neurons convert temporally precise excitation into temporally precise inhibition, which is transmitted to the MSO on the same side (Kuwabara and Zook, 1992). The second source of inhibition to the MSO comes from the LNTB on the same side, which is innervated by GBCs in the ipsilateral AVCN (Cant and Hyson, 1992) (Figure 1.3). MSO neurons receive relatively few, but unusually strong excitatory and inhibitory inputs (Couchman et al., 2010). In mature MSO neurons, while excitatory inputs mainly innervate the dendrites, glycinergic synapses are restricted to the soma (Clark, 1969; Perkins, 1973; Kapfer et al., 2002; Werthat et al., 2008; Couchman et al., 2012).

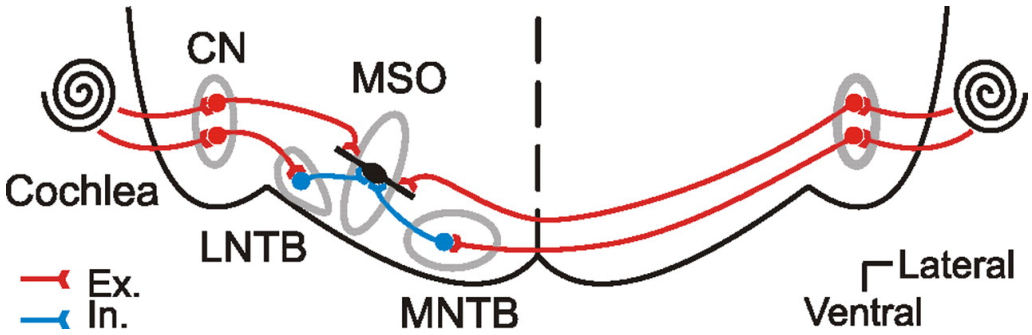

Figure 1.3: Scheme of the input circuitry to the MSO in the mammalian auditory brainstem. MSO neurons receive bilateral excitation and inhibition via four distinct inputs. Excitatory inputs are marked in red, inhibitory inputs in blue. See text for details. Reproduced with permission from Couchman et al. (2010).

MSO neurons typically respond best to contralateral-leading ITDs (Goldberg and Brown, 1969; Yin and Chan, 1990; Brand et al., 2002; Pecka et al., 2008; van der Heijden et al., 2013). Therefore, an internal delay must compensate for the difference in the arrival of sound at the two ears. Originally, it was proposed that systematic differences in the length of axons converging onto coincidence detector neurons within specific frequency channels compensate for different ITDs, generating a topographic map of azimuthal space (Jeffress, 1948). Although this model partially seems to hold true in birds (Ashida and Carr, 2011), it has become clear that differences in axon length alone are not sufficient to explain the diversity of best ITDs observed *in vivo* (Spitzer and Semple, 1995; McAlpine et al., 2001; Karino et al., 2011). In mammals with good low-frequency hearing, a relationship has consistently been found between the best ITD and tuning frequency, and best ITDs are mostly distributed outside the physiological range (McAlpine et al., 2001; Brand et al., 2002; Pecka et al., 2008). These findings support the idea that sound localisation in mammals is achieved by a population code, where the azimuthal location of a sound is encoded by the relative spike rate of two populations of broadly tuned neurons (Grothe, 2003; McAlpine and Grothe, 2003; Lesica et al., 2010; Grothe et al., 2010).

How exactly synaptic inputs are integrated *in vivo* in the MSO for ITD encoding in the order of microseconds is still under debate (Brand et al., 2002; Zhou et al., 2005; Pecka et al., 2008; Jercog et al., 2010; van der Heijden et al., 2013; Roberts et al., 2013; Myoga et al., 2014; Franken et al., 2015). Synaptic inhibition has been shown to tune the ITD sensitivity of MSO neurons *in vitro* and *in vivo* in Mongolian gerbils, a mammal with good low-frequency hearing (Brand et al., 2002; Pecka et al., 2008; Myoga et al., 2014). Crucially, blocking glycinergic inhibition *in vivo* was found to shift the peak of ITD functions towards the midline. Thus, glycinergic inhibition seems to adjust the maximal slope of ITD functions — where information encoding is high — within the physiological range (Brand et al., 2002; Pecka et al., 2008; Grothe, 2003). The preference of MSO neurons for contralateral ITDs was proposed to result from preceding contralateral inhibition relative to contralateral excitation

(Brand et al., 2002; Pecka et al., 2008), a prediction strongly supported by the anatomical and functional specialisations of the inhibitory pathway (Ford et al., 2015; Stange-Marten et al., 2017). While preceding inhibition was demonstrated in the MSO of immature (P15 – P20) gerbils *in vitro* using a thick slice preparation, it was found not to tune ITD functions (Roberts et al., 2013). However, a subsequent *in vitro* study in mature gerbils could show that a larger set of timing conditions together with the contribution of ipsilateral inhibition could dynamically tune coincidence detection, and agrees with the diversity of ITD functions recorded *in vivo* (Myoga et al., 2014). Other sources of internal delay have been proposed, including interaural disparities in EPSP slopes (Jercog et al., 2010) and an asymmetric origin of the axon (Zhou et al., 2005). However, these models have since been challenged (Rautenberg et al., 2009; Roberts et al., 2013). In turn, while conflicting findings have emerged from recent *in vivo* studies (van der Heijden et al., 2013; Franken et al., 2015), they have also provided new insights and remain under debate.

In support of the inhibition-based model of ITD encoding, the inhibitory pathway to the MSO exhibits remarkable functional and anatomical specialisations which ensure fast, stable and precise synaptic transmission. Specific adaptations in axonal properties and myelination pattern increase the conduction velocity of GBC axons compared to SBCs (Ford et al., 2015). The conduction velocity of GBC axons tuned to low frequencies is further enhanced through an increase in axon thickness, while a decrease in internode length towards the Calyx of Held ensures high action potential precision (Ford et al., 2015). Importantly, the anatomical specialisations of low-frequency tuned GBC axons are not found in mice, suggesting they represent a specific adaptation to meet the temporal precision required of ITD encoding (Stange-Marten et al., 2017). In turn, the Calyx of Held synapse ensures secure and reliable synaptic transmission at very high rates (Smith et al., 1998; Taschenberger and von Gersdorff, 2000; Englitz et al., 2009; Kopp-Scheinpflug et al., 2011) and fibres tuned to low frequencies have been shown to exhibit shorter and more stable synaptic delays (Stange-Marten et al., 2017). Similar to their inputs, low-frequency MNTB neurons exhibit phase-locking (Kopp-Scheinpflug et al., 2003), further preserving important temporal information. Finally, through an experience-dependent refinement around hearing onset, glycinergic synapses are confined to the soma and proximal dendrites of MSO neurons (Kapfer et al., 2002; Werthat et al., 2008). This refinement also appears to be a specific adaptation for ITD processing in mammals with good low-frequency hearing, and is thought to enhance the timing of inhibition (Kapfer et al., 2002; Grothe, 2003). Taken together, these adaptations suggest that the precise timing of inhibitory inputs is crucial to the computation of ITDs.

The high temporal precision required of the two circuits described above partly derives from their specialised inputs. However, the response properties of VNLL and MSO neurons are also highly dependent on their membrane properties. In the next section, I will discuss how passive and active membrane properties contribute to neuronal excitability and temporal precision.

1.2 BIOPHYSICAL PROPERTIES UNDERLYING NEURONAL EXCITABILITY & TEMPORAL PRECISION

What determines the excitability, precision, and operating mode of neurons? The next chapter will discuss how the response properties of neurons are modulated by (1) passive properties which result from the capacitative and resistive elements of their membranes; and (2) active properties which are voltage-dependent.

1.2.1 *Passive membrane properties*

The lipid bilayer of biological membranes not only contains conducting channels, but importantly also separates charge. Thus, biological membranes can be described as a resistor (R) in parallel with a capacitor (C), as shown in the equivalent circuit in Figure 1.4. A current injection will charge the capacitor and lead to a change in voltage. Once the capacitor is fully charged for that current injection, the voltage will have changed to a new steady state, V_{ss}, defined by Ohm's Law:

$$V = I \times R \tag{1.1}$$

While the capacitor is still charging, the voltage deflection at a given time, V(t), follows an exponential time course which is described by:

$$V(t) = V_{ss}(1 - e^{-\frac{t}{\tau}}) \tag{1.2}$$

where τ is the membrane time constant; τ is the linear product of the membrane resistance and the membrane capacitance:

$$\tau = R \times C \tag{1.3}$$

and therefore corresponds to the time point at which the voltage has reached 67% of the steady-state voltage (Figure 1.4).

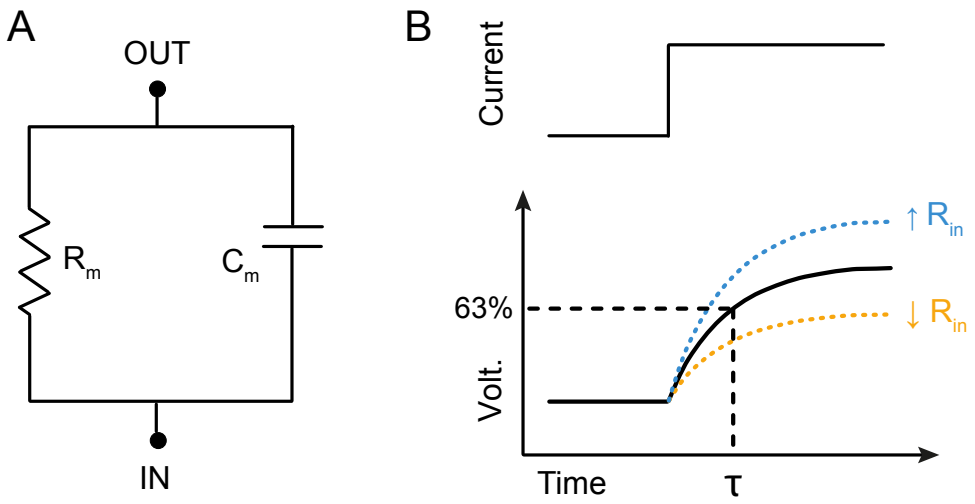

Figure 1.4: **A**. RC equivalent circuit representing the resistive and capacitative elements of a biological membrane. **B**. When a step current pulse is applied, the voltage changes with a time course τ that depends on RC.

In neurons, the input resistance (R_{in}) depends on the conductance through membrane ion channels. In turn, the total membrane capacitance (C_m) is proportional to the membrane surface area, and hence scales with cell size. Changes in morphology within neurons can lead to local alterations in both these parameters. Thus, leak conductances at rest (Berntson and Walmsley, 2008; Goldstein et al., 2001) and cell morphology (Agmon-Snir and Segev, 1993; Mainen and Sejnowski, 1996) can shape synaptic events, dendritic integration and neuronal excitability. In the MSO, differences in passive properties along dendrites enhance the amplitude of distal EPSPs, thereby compensating for passive attenuation and resulting in similar EPSP amplitudes at the soma regardless of synapse location (Winters et al., 2017).

Importantly, R_{in} and C_m directly affect the membrane time constant (τ_m), as the former determines the steady state voltage to be reached, while the latter affects the time needed to charge the membrane (Figure 1.4). In turn, τ_m partly determines the integration time window of synaptic inputs, and hence whether a cell operates more as a coincidence detector or an integrator (Geiger et al., 1997; König et al., 1996; Ratté et al., 2013). Neurons with a short τ_m exhibit rapid voltage signalling, imposing a narrow temporal window for synaptic inputs to summate and reach the threshold for AP generation. In contrast, neurons with a long τ_m display slower voltage responses, allowing non-coincident inputs to summate more readily. Thus, coincidence detectors are inherently more sensitive to the temporal structure of afferent activity. In turn, R_{in} also confers sensitivity to the timing of afferent stimulation by influencing the size of voltage events. Octopus cells, the input to globular VNLL neurons, exhibit an extremely low R_{in}, which causes voltage responses to be small. As a result, several inputs arriving

simultaneously are required to reach threshold (Golding et al., 1995). Thus, the passive properties of octopus cells make them ideally suited to detect the coincident activation of auditory nerve fibres (Golding et al., 1995; Oertel, 1997). Similarly, mature MSO neurons exhibit an extremely low R_{in} and short τ_m (Scott et al., 2005; Couchman et al., 2010), largely due to two well-balanced conductances at rest: a hyperpolarisation-activated mixed-cation conductance (g_h) and a low-threshold potassium conductance (g_{KLVA}) (Scott et al., 2005; Khurana et al., 2011; Baumann et al., 2013). The specialised passive membrane properties of mature MSO neurons promote fast voltage signalling, which is necessary for the high temporal resolution of ITD encoding (Scott et al., 2005; Grothe et al., 2010).

While R_{in} and C_m are thought to shape neuronal excitability through their effect on τ_m, the relative importance of each membrane property in determining the firing pattern, excitability and precision of neurons in the auditory brainstem has not been assessed in detail. Given that R_{in} and C_m dominate different parts of the voltage response of neurons, the relative contribution of R_{in} and C_m to excitability likely depends on the stimulation time course.

1.2.2 *Active membrane properties*

The excitability, temporal precision and operating mode of neurons are also dynamically adjusted by voltage-gated conductances, which can exert a variety of effects depending on the properties and distribution of ion channels. The onset firing pattern characteristic of temporally precise auditory neurons is thought to be mediated by a low voltage-activated potassium current (I_{KLVA}), which counteracts depolarisation sufficiently to prevent multiple APs in response to a single synaptic stimulus (Brew and Forsythe, 1995; Bal and Oertel, 2001; Dodson et al., 2002; Svirskis et al., 2002; Barnes-Davies et al., 2004; Leão et al., 2004; Scott et al., 2005; Cao et al., 2007). In turn, a high voltage-activated potassium current rapidly repolarises APs, enabling some neurons to sustain high-frequency firing (Brew and Forsythe, 1995; Cao et al., 2007). Although mature VNLL neurons display onset responses (rats: Wu (1999); mice: Caspari et al. (2015)), VNLL neurons of juvenile gerbils respond to long current injections with a slow membrane depolarisation followed by delayed continuous firing (Berger et al., 2014). The lack of onset AP partly results from the presence of a rapidly inactivating A-type potassium current (Berger et al., 2014). Moreover, VNLL neurons exhibit a high current threshold at immature stages. As a result, VNLL neurons respond preferentially to the summation of two inputs arriving in close temporal register, and as such, behave as coincidence detectors (König et al., 1996; Berger et al., 2014).

Beyond contributing strongly to the resting membrane conductance, I_{KLVA} along with a hyperpolarisation-activated mixed-cation current (I_h) also affect the shape of synaptic events. As I_{KLVA} and I_h are both activated in the subthreshold range, they actively shorten synaptic responses and sharpen the time window for coincidence detection (Kuba et al., 2002; Svirskis et al., 2003; Scott et al., 2005; Yamada, 2005; Mathews et al., 2010; Khurana et al., 2011; Baumann et al., 2013). In the gerbil MSO, low voltage-activated potassium channels in the soma and proximal dendrites reduce the duration

of EPSPs in a voltage-dependent manner, thereby compensating for distortions induced by dendritic cable filtering as voltage signals propagate from the dendrites to the soma (Mathews et al., 2010).

The distribution of voltage-gated channels also influences the active propagation of voltage signals throughout the neuron, which influences synaptic integration and synaptic plasticity (Johnston et al., 1996; Johnston et al., 2003; Gulledge et al., 2005). While voltage-gated sodium and calcium channels serve to amplify distal synaptic events, potassium channels dampen excitability (Hoffman et al., 1997). In the MSO of gerbils, APs are strongly attenuated as they backpropagate into the soma and dendrites (Scott et al., 2007). The limited backpropagation in MSO neurons has been attributed to several factors: K_v1 channels in the soma and proximal dendrites, a distance-dependent decrease in dendritic sodium currents, and an unusually hyperpolarised steady-state inactivation of somatic sodium channels (Scott et al., 2005; Scott et al., 2010). However, the extent of AP backpropagation in MSO neurons was assessed after hearing onset, when somatic APs start to decrease rapidly in amplitude (Scott et al., 2005), raising the possibility that APs may backpropagate more effectively before hearing onset.

1.3 Developmental refinements in the auditory brainstem

In contrast to mature stages, the membrane properties and responses of immature neurons are not as specialised. The developmental change in membrane properties may reflect a switch in the demands on the circuit at different developmental stages. While immature membrane properties may promote the establishment of a functional circuit, they are not well suited to the high temporal precision required of the mature system. Assessing which characteristics are refined or retained over the course of development also reveals their functional contribution to the mature circuit. The next section provides examples of key structural and functional refinements during development in the auditory brainstem.

1.3.1 *Functional refinements*

The development of several auditory brainstem nuclei is characterised by a considerable acceleration of voltage signalling, as shown by a decrease in membrane time constant and input resistance (Ahuja and Wu, 2000; Magnusson et al., 2005; Chirila et al., 2007; Ammer et al., 2012). In the MSO, this is largely achieved by a substantial developmental increase in I_h and I_{KLVA} (Scott et al., 2005; Khurana et al., 2012). At the level of synapses, the NMDAR-mediated component of the EPSC decreases in amplitude and acquires faster decay kinetics during development (Futai et al., 2001; Franks and Isaacson, 2005; Joshi and Wang, 2002). However, NMDARs are still maintained at mature stages in the MNTB and MSO (Steinert et al., 2010; Couchman et al., 2012). Together with the acceleration of the AMPAR-mediated EPSC, these developmental alterations increase the fidelity of synaptic

transmission (Taschenberger and von Gersdorff, 2000; Koike-Tani et al., 2005). In turn, glycinergic IPSC kinetics accelerate markedly during the first few postnatal weeks (Smith et al., 2000; Magnusson et al., 2005). Developmental changes in synaptic transmission are further complemented by changes in the contribution of voltage-gated calcium channels (VGCCs) mediating neurotransmitter release (Iwasaki and Takahashi, 1998; Iwasaki et al., 2000). Finally, changes in the expression of voltage-gated ion channels contribute to the development of neuronal excitability and the acquisition of specific types of firing pattern and operating mode (Scott et al., 2005; Hoffpauir et al., 2010; Khurana et al., 2012).

1.3.2 *Structural refinements*

A hallmark of circuit assembly in several systems is the elaboration and subsequent pruning of exuberant connections. Together with changes in the complexity of dendritic arbors, these refinements sculpt the precise connectivity of the mature circuit. Such refinements take place in the LSO and MSO during late postnatal development. In LSO neurons, dendritic arbors refine along the tonotopic axis through a loss of dendritic endpoints (Sanes et al., 1992b; Rietzel and Friauf, 1998). While the pruning of distal dendritic branches is most prominent before hearing onset (~P12) in the LSO of rats (Rietzel and Friauf, 1998), it has been observed during the second and third postnatal week in the LSO of gerbils (Sanes et al., 1992b). Functionally, these dendritic refinements coincide with an enhancement of frequency selectivity (Sanes et al., 1992b; Rietzel and Friauf, 1998). The dendritic complexity of MSO neurons also decreases from before hearing onset (Chirila et al., 2007) up until the end of the third postnatal week (Rogowski and Feng, 1981; Rautenberg et al., 2009). In turn, the cell volume continues to increase several weeks beyond hearing onset, largely due to an increase in dendritic diameter (Rautenberg et al., 2009). In parallel to changes in dendritic complexity, axonal arbors which initially grow many collaterals (Kandler and Friauf, 1993) are subsequently refined along the tonotopic axis after hearing onset (Sanes and Siverls, 1991). Taken together, considerable structural and functional refinements begin or continue after hearing onset, suggesting they are susceptible to changes in acoustic experience.

A key structural change in MSO neurons is the developmental refinement of inhibitory synapses to the soma. While glycinergic synapses initially innervate both the dendrites and soma of MSO cells, they refine to the soma in an experience-dependent manner after hearing onset (Kapfer et al., 2002; Werthat et al., 2008). This structural refinement is accompanied by a developmental decrease in the size of evoked inhibitory postsynaptic currents (IPSCs), and a decrease in the frequency of miniature IPSCs (Magnusson et al., 2005). Thus, the number of glycinergic synapses appears to decrease during development, with those remaining confined to the soma. Functionally, these refinements are thought to enhance the timing of inhibition for ITD encoding (Kapfer et al., 2002; Magnusson et al., 2005; Myoga et al., 2014). The role of activity in guiding this refinement will be discussed in the next section.

1.4 THE ROLE OF ACTIVITY IN GOVERNING DEVELOPMENTAL REFINEMENTS

The establishment of precise, functional neural circuits during development is a complex task that requires coordinated molecular and activity-dependent processes. Sensory systems are ideally suited to study the role of activity in shaping neuronal circuits during development (Katz and Shatz, 1996). In the next section, I will first provide example of how (1) activity-independent processes, (2) spontaneous activity, and (3) sensory-evoked experience guide the development of neuronal circuits. Next, I will discuss the more specific case of how sensory-evoked experience influences the refinement of inhibitory synapses in MSO neurons, and the implications for the maturation of ITD tuning.

1.4.1 *The kind of activity matters*

In the auditory brainstem, axons from the CN innervate the correct targets within the SOC as early as embryonic day 18 (Kandler and Friauf, 1993; Kil et al., 1995). Starting before birth, specific complexes of axon guidances molecules direct axons across the midline and ensure the correct target is innervated in such a way that the basic tonotopy is already present (Huffman and Cramer, 2007; Howell et al., 2007; Nakamura et al., 2012; Cramer and Gabriele, 2014). Unilateral cochlear ablation in neonatal gerbils causes the CN of the unablated side to innervate SOC nuclei normally innervated by the CN on the ablated side. These ectopic projections are tonopically organised, suggesting the involvement of molecular cues (Kitzes et al., 1995). Signalling molecules also regulate the development of the size, monoinnervation and efficiency of the calyx of Held terminal (Xiao et al., 2013). Thus, activity-independent processes play an important role in establishing initial connectivity.

In the developing visual system, blocking neural activity in the retina before the onset of vision disrupts the segregation of retinal ganglion cell axons in different layers in the lateral geniculate nucleus (Shatz and Stryker, 1988). Moreover, selectively increasing spontaneous activity levels in one retina increases the territory occupied by its inputs at the expense of the less active retina, suggesting the existence of a competitive mechanism (Stellwagen and Shatz, 2002). Thus, patterned spontaneous activity shapes the assembly of complex neural circuits (Kirkby et al., 2013). In the auditory system, ATP released by transient supporting cells in the cochlea elicits bursts of calcium APs in inner hair cells, which propagate throughout the auditory pathway as early as postnatal day 1 (Tritsch et al., 2007; Tritsch et al., 2010). A mouse model of congenital deafness, in which auditory nerve activity is absent, has shed insight onto how prehearing activity regulates the expression of ion channels. In the MNTB, a loss of prehearing activity increases neuronal excitability (Leão et al., 2004), disrupts a tonotopic gradient of LVA and HVA potassium currents (Leão et al., 2006), and increases the frequency of glycinergic mIPSCs (Leao, 2003). Furthermore, inducing deafness with bilateral cochlear ablations before hearing onset alters chloride homeostasis and cotransporter function, leading to unbalanced excitatory – inhibitory responses (Vale and Sanes, 2002; Vale et al., 2003; Shibata et al., 2004). Spontaneous activity also contributes to the refinement of tonotopic

maps. Before hearing onset, LSO neurons are functionally disconnected from a large proportion of their inputs, while remaining inputs are strengthened (Kim and Kandler, 2003; Kim and Kandler, 2010). Selectively changing the temporal pattern of spontaneous activity disrupts this sharpening of MNTB–LSO topography (Clause et al., 2014).

With the onset of hearing, circuits rely less on spontaneous activity and more on sensory-evoked experience. Unilateral cochlear ablation disrupts the tonotopic sharpening of MNTB–LSO connections that normally occurs after hearing onset, as shown by the larger area innervated by MNTB arbors along the tonotopic axis of the LSO (Sanes and Siverls, 1991; Sanes et al., 1992a; Sanes and Takács, 1993). Across sensory systems the role of sensory-evoked experience in shaping the maturation of circuits has been assessed by (a) changing the overall amount of activity or by (b) disrupting the pattern of activity. For example, while prolonged dark rearing decreases the segregation of ocular dominance columns in the primary visual cortex (Swindale, 1981; Jaffer et al., 2012), rearing cats with strabismus (misalignment of the two eyes) enhances their segregation (Hubel and Wiesel, 1965). Furthermore, dark rearing prolongs the critical period, allowing plasticity to be reintroduced during adulthood (Cynader and Mitchell, 1980). Similarly, exposuring juvenile rats to continuous white noise delays the maturation of tonotopicity in the primary auditory cortex and delays the closure of the critical period (Chang and Merzenich, 2003). These findings illustrate the sensitivity of neuronal circuits to the overall activity and stimulus statistics provided by sensory-evoked experience. The following section discusses a key developmental refinement in MSO neurons which depends on normal acoustic experience.

1.4.2 *Experience-dependent refinement of glycinergic synapses in the MSO*

The refinement of glycinergic synapses to the soma of MSO neurons is a key example of how acoustic experience shapes the function of circuits in the developing auditory brainstem. The rearrangement of glycinergic synapses to the soma of MSO neurons is disrupted following unilateral cochlear ablation or by raising gerbils in omnidirectional white noise, both of which interfere with normal binaural cues (Kapfer et al., 2002). Exposure to omnidirectional white noise also prevents the normal decrease in the size of evoked IPSCs and the decrease in mIPSC frequency (Magnusson et al., 2005). Taken together, these findings suggest that normal acoustic experience guides a process of inhibitory synapse elimination, whereby glycinergic synapses become confined to the soma of MSO neurons. These refinements coincide with a developmental maturation of ITD functions in the DNLL, a direct output of MSO neurons (Seidl, 2005). In juvenile gerbils, best ITDs peak around zero ITD with the slope not yet adjusted to the physiological range. In contrast, adult gerbils exhibit contralateral-leading best ITDs, shifting the slope within the physiological range. Interestingly, gerbils exposed to omnidirectional white noise during a limited period of development display immature-like ITD functions as adults, without any change in other response characteristics (Seidl, 2005). In fact, ITD functions following noise rearing resemble those in the MSO following inhibition blockade (Brand et al., 2002; Pecka et al., 2008). Although correlative, these findings raise the possibility that binaural cues during a critical window of development orchestrate a structural rearrangement of glycinergic

synapses, which enhances the timing of inhibition and tunes ITD functions to the physiologically relevant range (Grothe, 2003). The refinement of glycinergic synapses to the soma of MSO neurons does not occur in species with poor low-frequency hearing, suggesting that it is a specific adaptation in species which use ITDs for sound localisation (Kapfer et al., 2002). This observation further supports the idea that the developmental refinement of inhibition is important for ITD tuning.

A common feature underlying activity-dependent refinements is the involvement of calcium, an important second messenger in neurons. The following section will discuss different sources of calcium, and the role of calcium in circuit refinements.

1.5 THE ROLE OF CALCIUM IN ACTIVITY-DEPENDENT REFINEMENTS

1.5.1 *Sources of calcium: a focus on voltage-gated calcium channels*

Calcium is a very important second messenger involved in almost every aspect of neuronal function. A low intracellular calcium concentration is maintained by ATP-dependent pumps and exchangers which actively extrude calcium, or sequester calcium into intracellular organelles (Clapham, 2007). The main sources of external calcium entry are: (1) calcium permeable ligand-gated ion channels (LGICs) such as AMPARs and NMDARs, which are activated upon presynaptic glutamate release during synaptic activity (Jonas and Burnashev, 1995), and (2) VGCCs driven by voltage changes such as APs (Catterall, 2011). Calcium in the extracellular environment can also enter through nicotinic acetylcholine receptors (Shen and Yakel, 2009). The focus of this thesis is calcium entry through VGCCs.

VGCCs comprise a pore-forming $\alpha 1$ subunit in association with $\alpha 2$, β, γ, and δ subunits. Ten different calcium channel genes encoding a different $\alpha 1$ subunit have been identified, and can be grouped into three broad subfamilies based on similarity: Ca_v1 (L-type), Ca_v2 (P/Q-, N- and R-type), and Ca_v3 (T-type) (Catterall, 2005). VGCCs differ in their kinetics, voltage dependence and pharmacological properties. A broad categorisation can be made based on their activation voltage: (1) high voltage-activated (HVA) such as L-, P/Q-, N- and R-type channels; and (2) low voltage-activated (LVA) such as T-type channels. L-type currents exhibit a large single channel conductance and slow voltage-dependent inactivation (Catterall, 2011). In turn, T-type currents are generally distinguished by their rapid voltage-dependent inactivation, slow deactivation and small single channel conductance, although differences exist between subtypes (Carbone and Lux, 1984; Swandulla and Armstrong, 1988; Talavera and Nilius, 2006). Furthermore, T-type channels require a prior hyperpolarisation to relieve them from steady-state inactivation at rest (Figure 1.5) (Cueni et al., 2009). Finally, N- and P/Q-type calcium currents display intermediate voltage dependence and kinetics (Nowycky et al., 1985; Catterall, 2011). The different calcium channel subtypes can be

differentiated based on their sensitivity to specific blockers, allowing their relative contribution to the total calcium current to be estimated.

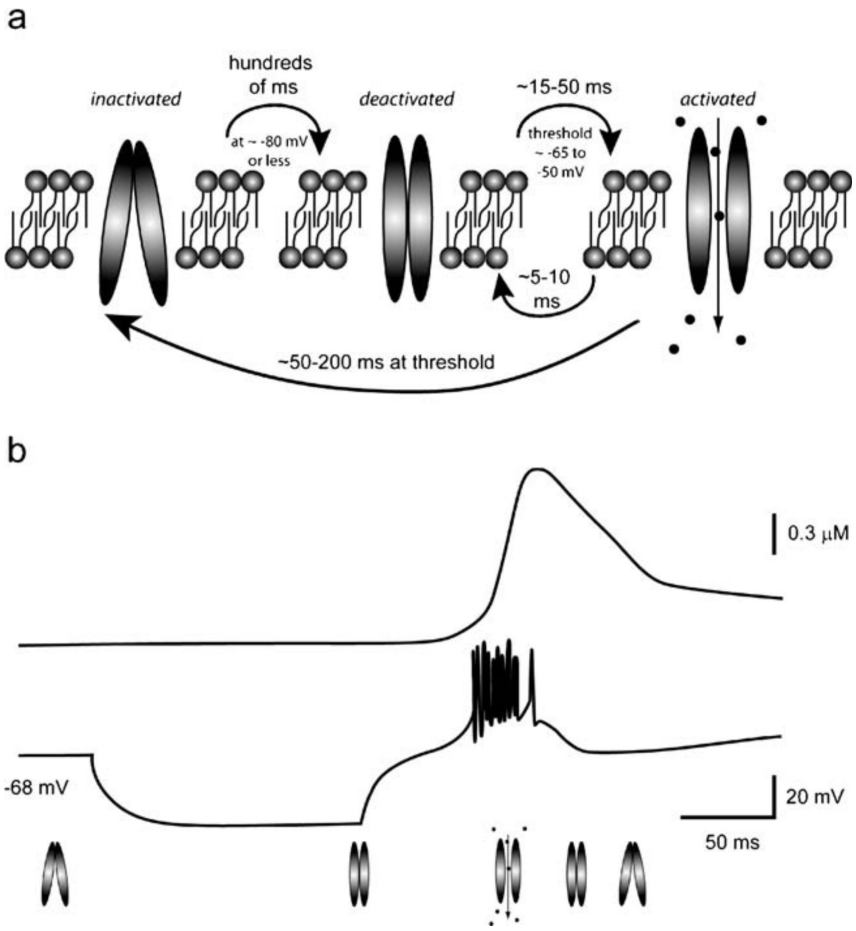

Figure 1.5: **a)** Scheme of T-Type calcium channel gating properties. T-Type channels transition between inactivation, deactivation and activation states. **b)** Calcium transient (*top*) elicited by a rebound low-threshold burst following a brief membrane hyperpolarisation (*bottom*) to relieve steady-state inactivation. Reproduced with permission from Cueni et al. (2009).

As LVA calcium channels are activated at more hyperpolarised potentials, they can serve to amplify subthreshold voltage events. In several cell types, T-type channels are expressed in distal dendrites, where they mediate local increases in calcium in response to subthreshold synaptic inputs (Christie et al., 1995; Magee et al., 1995; Crandall et al., 2010; Rudolph et al., 2015). In contrast, the activation of HVA calcium channels requires larger changes in potential, such as that evoked by APs (Markram et al., 1995; Magee and Johnston, 1995). The entry of calcium during an AP depends strongly on the

AP waveform (McCobb and Beam, 1991). Given the slower activation kinetics of VGCCs compared to sodium channels, VGCCs generally contribute little to the rising phase of the AP. Rather, large calcium tail currents are evoked upon repolarisation to rest, when the driving force for calcium is high (Bean, 2007). In turn, calcium entry through VGCCs can influence the repolarisation and afterhyperpolarisation of APs through calcium-activated potassium channels (Berridge, 1998; Cueni et al., 2009).

In neurons, N-, R- and P/Q-type calcium channels are thought to be expressed presynaptically where they mediate calcium entry required for exocytosis and synaptic transmission. In turn, L-type channels are generally localised on the soma or proximal dendrites, where they facilitate activity-dependent gene transcription (Greer and Greenberg, 2008). Finally, the kinetics of T-type channels make them ideally suited to uniquely influence neuronal excitability. T-type channels are strongly developmentally regulated in some cell types, and have been implicated in a number of processes including rhythmic bursts, dendritic integration, neural development and long-term synaptic plasticity (for review see Cueni et al. (2009) and Leresche and Lambert (2016)). Besides triggering a number of signalling pathways, calcium entry through VGCCs can also promote the release of calcium from intracellular stores by directly or indirectly activating ryanodine and IP_3 receptors on the membrane of the endoplasmic reticulum. Calcium induced calcium release can shape calcium signals, influence neuronal excitability and recruit calcium signalling pathways involved in synaptic plasticity (Rose and Konnerth, 2001; Verkhratsky, 2002; Bardo et al., 2006). The amplitude and spatio-temporal profile of calcium signals is further fine-tuned by calcium buffers (Berridge et al., 2003).

1.5.2 *Calcium and the development of the auditory brainstem*

Calcium is essential for the normal development of the auditory system. The inner hair cells of $Ca_v1.3^{-/-}$ mice lack spontaneous calcium spikes and exhibit disrupted neurotransmitter release onto afferent auditory nerve fibres before hearing onset (Brandt et al., 2003). Moreover, the normal development of the topographic organisation and cytoarchitecture of the SOC also requires activity-dependent calcium signalling (Lohmann et al., 1998). $Ca_v1.2^{-/-}$ and $Ca_v1.3^{-/-}$ mice exhibit neuronal loss and a substantial decrease in the volume of several auditory nuclei (Hirtz et al., 2011; Ebbers et al., 2015). Loss of $Ca_v1.3$ channels also increases the proportion of LSO cells displaying a firing pattern with multiple APs, through a reduction in a LVA potassium current (Hirtz et al., 2011). Similarly, depolarisation-induced calcium signalling via VGCCs and intracellular stores regulates the expression of voltage-gated potassium channels in cultured MNTB neurons, thereby influencing their excitability (Tong et al., 2010). The importance of calcium homeostasis during critical phases of development is further emphasised by the strong developmental regulation of calcium binding proteins across several auditory brainstem nuclei (Friauf, 1993; Lohmann and Friauf, 1996; Felmy and Schneggenburger, 2004). Therefore, activity patterns which change the development of calcium signalling are likely to influence important aspects of circuit formation.

1.5.3 *Calcium mediates synaptic plasticity mechanisms*

Given its role as a major second messenger which can activate a myriad of downstream signalling cascades, calcium is ideally suited to underlie many forms of synaptic plasticity (Malenka and Bear, 2004). The amplitude and profile of calcium events is one of the critical factors determining whether synaptic plasticity results in potentiation or depression (Malenka et al., 1988; Lisman, 1989; Cormier et al., 2001; Ismailov, 2004). While excitatory neurotransmission can readily elicit calcium influx through glutamate receptors or indirectly via VGCCs, less is known about how inhibitory synapses activate calcium signalling pathways involved in synaptic plasticity. In spike timing dependent plasticity (STDP), the sign of plasticity depends critically on the order and timing of pre- and postsynaptic activity (Zhang et al., 1998; Feldman, 2012). Information about postsynaptic activity is conveyed to the activated synapse by backpropating APs (bAPs), which activate dendritic VGCCs and mediate calcium entry (Markram, 1997; Magee and Johnston, 1997). Thus, dendritic calcium signals through VGCCs are a retrograde indicator of postsynaptic activity. In classical STDP, a pre-leading-post spike order leads to synaptic strengthening, as the EPSP coincides with the bAP to generate supralinear calcium signals. Conversely, a post-leading-pre spike order only elicits moderate calcium influx and leads to synapse depression. Beyond amplifying calcium influx through AMPARs and NMDARs, calcium via VGCCs or internal stores can contribute to signalling cascades downstream of activated metabotropic receptors (Feldman, 2012). The tuning asymmetry of MSO neurons has been suggested to emerge from a STDP learning rule during a critical window of development (Leibold and Hemmen, 2005). However, whether such a learning rule exists remains an open question.

1.6 ANIMAL MODEL

All experiments in this thesis were performed on Mongolian gerbils (Meriones unguiculatus), a well established animal model of human hearing. Similar to humans, gerbils expanded their hearing into the low-frequency range, with comparable thresholds between 1 – 10 kHz (Ryan, 1976; Grothe and Pecka, 2014). Gerbils use both ILDs and ITDs for sound localisation (Heffner and Heffner, 1988; Tolnai et al., 2017) and can accurately discriminate sound sources separated by as little as 23 – 27° in the case of broad-band noise (Heffner and Heffner, 1988; Maier and Klump, 2006; Maier et al., 2008). Moreover, as in humans, gerbils exhibit localisation dominance in the context of the precedence effect (Wolf et al., 2010), further underscoring their validity as an animal model to study the neural mechanisms underlying sound localisation. Finally, hearing onset occurs around P12 – P13 in gerbils (Finck et al., 1972; Ryan et al., 1982; Woolf and Ryan, 1984; Smith and Kraus, 1987). This developmental profile provides the opportunity to assess how changes in acoustic experience affect the development of neurons and circuits in the auditory system.

1.7 OVERVIEW

The central theme of this thesis is how developmental changes in membrane properties and ion channel expression mediate the transition between the need to establish a functional circuit and the need to acquire high temporal precision. In the first study, we assessed the relative contribution of passive and active membrane properties to the development of temporal precision in VNLL neurons. First, we characterised the development of membrane properties in response to short and long current injections. Second, we assessed the relative contribution of the input resistance and the membrane capacitance to these developmental changes. The specific contribution of the input resistance was isolated by comparing neuronal responses in the presence of a leak conductance applied with conductance clamp. Our findings show that passive and active membrane properties act in concert to achieve the high temporal precision of mature VNLL neurons, and that the relative contribution of passive membrane properties largely depends on the stimulation time course.

The goal of the second study was to assess whether calcium signalling is developmentally regulated in MSO neurons. Given its role as a major second messenger, developmental changes in intracellular calcium should provide insight into the cellular mechanisms available for activity-dependent circuit refinements around hearing onset. Our findings show that large dendritic calcium signals before and at hearing onset are rapidly downregulated within a week after hearing onset. Furthermore, raising gerbils in omnidirectional white noise appeared to accelerate the maturation of calcium signalling in MSO neurons. Thus, the developmental profile of calcium signalling in MSO neurons supports the existence of a short time window for calcium-dependent circuit refinements around the onset of acoustic experience.

2

DEVELOPMENT AND MODULATION OF INTRINSIC MEMBRANE PROPERTIES CONTROL THE TEMPORAL PRECISION OF AUDITORY BRAIN STEM NEURONS

2.1 CONTRIBUTIONS

Franzen, D. L.*, Gleiss, S. A.*, Berger C.*, Kümpfbeck, F. S., Ammer, J. J. & Felmy, F. (2015). **Development and modulation of intrinsic membrane properties control the temporal precision of auditory brain stem neurons**. *J. Neurophysiol. 113(2)*, pp. 524-36. doi: 10.1152/jn.00601.2014.

The contributions of the authors Delwen L. Franzen (DLF), Sarah A. Gleiss (SAG), Christina Berger (CB), Franziska S. Kümpfbeck (FSK), Julian J. Ammer (JJA) and Felix Felmy (FF) to the study included in this thesis are as follows:

DLF, SAG, CB, FSK, JJA, and FF designed the research; DLF, SAG, CB, JJA, and FF performed the experiments; DLF, SAG, CB, FSK, JJA, and FF analysed the data and interpreted the results of the experiments; DLF, SAG, CB, FSK, and FF prepared the figures; DLF, JJA, and FF drafted the manuscript; DLF, SAG, CB, FSK, JJA, and FF edited and revised the manuscript; DLF, SAG, CB, FSK, JJA, and FF approved the final version of the manuscript.

J Neurophysiol 113: 524–536, 2015.
First published October 29, 2014; doi:10.1152/jn.00601.2014.

Development and modulation of intrinsic membrane properties control the temporal precision of auditory brain stem neurons

Delwen L. Franzen,[1,2]* Sarah A. Gleiss,[1,2]* Christina Berger,[1]* Franziska S. Kümpfbeck,[1] Julian J. Ammer,[1,2] and Felix Felmy[1,3]

[1]*Division of Neurobiology, Department Biology II, Ludwig-Maximilians-Universität München, Planegg-Martinsried, Germany;* [2]*Graduate School of Systemic Neurosciences, Ludwig-Maximilians-Universität München, Planegg-Martinsried, Germany; and* [3]*BioImaging Center, Ludwig-Maximilians-Universität München, Planegg-Martinsried, Germany*

Submitted 12 August 2014; accepted in final form 24 October 2014

Franzen DL, Gleiss SA, Berger C, Kümpfbeck FS, Ammer JJ, Felmy F. Development and modulation of intrinsic membrane properties control the temporal precision of auditory brain stem neurons. *J Neurophysiol* 113: 524–536, 2015. First published October 29, 2014; doi:10.1152/jn.00601.2014.—Passive and active membrane properties determine the voltage responses of neurons. Within the auditory brain stem, refinements in these intrinsic properties during late postnatal development usually generate short integration times and precise action-potential generation. This developmentally acquired temporal precision is crucial for auditory signal processing. How the interactions of these intrinsic properties develop in concert to enable auditory neurons to transfer information with high temporal precision has not yet been elucidated in detail. Here, we show how the developmental interaction of intrinsic membrane parameters generates high firing precision. We performed in vitro recordings from neurons of *postnatal days 9–28* in the ventral nucleus of the lateral lemniscus of *Mongolian gerbils*, an auditory brain stem structure that converts excitatory to inhibitory information with high temporal precision. During this developmental period, the input resistance and capacitance decrease, and action potentials acquire faster kinetics and enhanced precision. Depending on the stimulation time course, the input resistance and capacitance contribute differentially to action-potential thresholds. The decrease in input resistance, however, is sufficient to explain the enhanced action-potential precision. Alterations in passive membrane properties also interact with a developmental change in potassium currents to generate the emergence of the mature firing pattern, characteristic of coincidence-detector neurons. Cholinergic receptor-mediated depolarizations further modulate this intrinsic excitability profile by eliciting changes in the threshold and firing pattern, irrespective of the developmental stage. Thus our findings reveal how intrinsic membrane properties interact developmentally to promote temporally precise information processing.

ventral nucleus of the lateral lemniscus; postnatal development; neuronal excitability; cholinergic modulation

THE ABILITY OF A NEURON TO generate action potentials with high temporal precision depends on the interaction of passive and active membrane properties (Ammer et al. 2012; Axmacher and Miles 2004; Berntson and Walmsley 2008; Fricker and Miles 2000; Gittelman and Tempel 2006; Kuba et al. 2002). Furthermore, these intrinsic membrane properties define the firing behavior of neurons, as different conductance states support, for example, either coincidence-detector or integrator-operating modes (Ratte et al. 2013). Intrinsic membrane properties depend, in turn, on leak currents (Berntson and Walmsley 2008; Goldstein et al. 2001), cell morphology (Mainen and Sejnowski 1996), and voltage-gated channels (Fricker and Miles 2000; Gittelman and Tempel 2006; Johnston et al. 2010) and are subject to neuromodulatory influences.

Changes in passive and active membrane properties, as well as in neuronal morphology, are widespread among neurons in auditory brain stem nuclei during late postnatal development. Across these nuclei, a reduction in input resistance generates shorter membrane time constants, promoting fast and temporally precise integration (Ahuja and Wu 2000; Ammer et al. 2012; Kandler and Friauf 1995; Kuba et al. 2002; Scott et al. 2005; Wu and Oertel 1987). A reduction in dendritic arborization (Rautenberg et al. 2009; Rietzel and Friauf 1998; Rogowski and Feng 1981; Sanes et al. 1992) decreases the cell capacitance, also leading to faster voltage signaling. Additional changes in active membrane properties result in enhanced excitability, as indicated by the shape and threshold of action potentials (Ahuja and Wu 2000; Ammer et al. 2012; Scott et al. 2005; Taschenberger and von Gersdorff 2000). Thus the regulation of these features during late postnatal development tunes the response properties of neurons in the auditory brain stem.

The ventral nucleus of the lateral lemniscus (VNLL) relays auditory information with exceptional temporal precision, particularly at the onset of sounds (Adams 1997; Covey and Casseday 1991; Recio-Spinoso and Joris 2014; Zhang and Kelly 2006). This temporal precision is attributed to globular cells in the ventral region of the adult rodent and cat VNLL (Adams 1997; Recio-Spinoso and Joris 2014; Zhang and Kelly 2006) and in the columnar region of bats (Covey and Casseday 1991). Around hearing onset, these neurons typically generate onset action potentials in response to prolonged current injections in rats (Zhao and Wu 2001). However, onset firing is lacking at threshold in this cell type before hearing onset in gerbils (Berger et al. 2014), suggesting a change in the firing pattern of globular cells during late postnatal development. Consistent with the mature onset firing pattern, the expression of Kv1.1, a low voltage-activated potassium channel, has been reported in adult bats (Rosenberger et al. 2003). At the circuit level, the temporal fidelity of globular VNLL neurons is critical to generate a prominent, feed-forward onset inhibition to the inferior colliculus (Nayagam et al. 2005; Pollak et al. 2011). Thus globular VNLL neurons constitute an ideal system

* D. L. Franzen, S. A. Gleiss, and C. Berger contributed equally.

Address for reprint requests and other correspondence: F. Felmy, BioImaging Center, Dept. Biology II, Ludwig-Maximilians-Universität München, Grosshadernerstr. 2, D-82152 Planegg-Martinsried, Germany (e-mail: felmy@zi.biologie.uni-muenchen.de).

to evaluate the developing contribution of intrinsic properties to precise action-potential generation. Therefore, we characterized the developmental profile of intrinsic properties of globular VNLL neurons from before hearing onset to maturity to unravel their contribution to action-potential generation and precision.

Our findings reveal that the suprathreshold responsiveness of VNLL neurons emerges from the specific interaction between passive and active membrane properties during late postnatal development. Notably, these alterations generate the emergence of coincidence-detector properties (Ratte et al. 2013), which are crucial to relay auditory information with high temporal precision.

MATERIALS AND METHODS

Preparation. All experiments complied with institutional guidelines and national and regional laws. Animal protocols were reviewed and approved by the Regierung of Oberbayern (according to the Deutsches Tierschutzgesetz). Mongolian gerbils (*Meriones unguiculatus*), of either sex and of *postnatal day 9* (P9)–P28, were anesthetized with isoflurane and then decapitated. This age range was chosen to evaluate the late postnatal refinement before and after the onset of hearing, which occurs at P12–P13 in gerbils (Finck et al. 1972; Ryan et al. 1982; Smith and Kraus 1987). Brains were removed in dissection solution containing (in mM) 50–120 sucrose, 25 NaCl, 27 $NaHCO_3$, 2.5 KCl, 1.25 NaH_2PO_4, 3 $MgCl_2$, 0.1 $CaCl_2$, 25 glucose, 0.4 ascorbic acid, 3 myoinositol, and 2 Na-pyruvate (pH was 7.4 when bubbled with 95% O_2 and 5% CO_2), and 180–200 μm-thick transverse slices containing the VNLL were cut with a VT1200S Vibratome (Leica Microsystems GmbH, Wetzlar, Germany). Slices were incubated for 45 min at 34.5°C in extracellular recording solution (same as dissection solution but with 125 mM NaCl, no sucrose, 1.2 mM $CaCl_2$, and 1 mM $MgCl_2$). All recordings were carried out at near-physiological temperature (34–36°C).

Electrophysiology. Globular VNLL neurons were visualized and imaged with a 60 × 1 numerical aperture (NA) objective with a microscope (BX51WI or BX50WI; Olympus, Center Valley, PA) equipped with gradient contrast illumination, a 1.4-NA oil-immersion condenser, and a TILL Photonics imaging system (FEI Munich GmbH, Munich, Germany) composed of a charge-coupled device (TILL-Imago VGA or Retiga 2000DC) camera and a monochromator (Polychrome IV or V). Recordings were performed using an EPC 10/2 amplifier [HEKA Elektronik, Lambrecht (Pfalz), Germany]. Data were acquired at 100 kHz for current-clamp and 50 kHz for voltage-clamp recordings and filtered at 3 kHz. In whole-cell, current-clamp recordings, the bridge balance was set to 100% after estimation of the series resistance and was monitored repeatedly during recordings. The series resistance during whole-cell, voltage-clamp recordings was compensated to a constant residual of 2–3 MΩ. The liquid junction potential (LJP) was not corrected for any of the solutions. For current-clamp experiments, the internal recording solution consisted of (in mM) 145 K-gluconate, 4.5 KCl, 15 HEPES, 2 Mg-ATP, 2 K-ATP, 0.3 Na_2-GTP, 7.5 Na_2-phosphocreatine, 5 K-EGTA, and 20–50 μM Alexa Fluor 568 (pH adjusted with KOH to 7.3; LJP ~16 mV). To reduce the driving force during recordings of whole-cell potassium currents, the potassium reversal potential was elevated to −71.5 mV by the following internal solution (in mM): 65 K-gluconate, 80 Na-gluconate, 4.5 KCl, 15 HEPES, 2 Mg-ATP, 2 K-ATP, 0.3 Na_2-GTP, 7.5 Na_2-phosphocreatine, 5 Na-EGTA, and 20–50 μM Alexa Fluor 568 (pH adjusted with NaOH to 7.3; LJP ~14 mV). In addition, the external potassium concentration was raised to 5 mM and the calcium concentration reduced to 1 mM. Potassium currents were isolated in the presence of 1 μM TTX, 100 μM Cd^{2+}, 50 μM ZD 7288, 10 μM SR95531, 0.5 μM Strychnine, 20 μM 6,7-dinitroquinoxaline-2,3-dione, and 50 μM D-2-amino-5-phosphonopentanoate. The reduction of the extracellular calcium concentration, together with the use of micromolar concentration of Cd^{2+}, largely prevented precipitation. The cell compartment, type, and location were morphologically verified for all recordings.

Conductance-clamp recordings were made with a SM-1 conductance-clamp amplifier (Cambridge Conductance, Royston, UK) with added linear conductances. The reversal potential of the leak current was set to the resting membrane potential of each cell. Leak conductances, ranging from 2 to 20 nS, were applied to evaluate the impact of decreasing the input resistance on cellular properties in globular VNLL neurons of P9 and >P25 animals. The range of applied background conductances was based on the developmental change of the input resistance observed in these neurons.

Cholinergic responses were evoked by local application of carbachol (500 μM) and oxotremorine (0.5 or 1 mM), dissolved in extracellular recording solution, and loaded into a patch-pipette connected to a dispense system (Picospritzer III; Parker, Cleveland, OH). Pipettes of equal size were consistently placed ~200 μm from the soma of the recorded neuron. The agonist was applied using a 100-ms pulse at 15–20 lb./in^2. The resting membrane potential was recorded for ~2.5 min, following agonist application to test for recovery. Changes in the current threshold and the firing pattern induced by cholinergic agonists were evaluated using a short (0.5 ms) and a long (200 ms) current injection before and after agonist application.

Morphology. Immunohistochemistry was performed on brain tissue from animals aged P9 and P26. Animals were anesthetized using 200 mg/kg body wt pentobarbital (Narcoren; Merial GmbH, Hallbergmoos, Germany) via intraperitoneal injection. The animals were perfused transcardially with Ringer solution, supplemented with 0.1% heparin (Meditech Vertriebs GmbH, Parchim, Germany) for 5 min, followed by 4% paraformaldehyde for 30 min. The brains were removed and postfixed overnight at 4°C. Brains were washed three times in PBS, and coronal brain stem slices of 50–60 μm thickness were taken using a VT1200S Vibratome (Leica Microsystems GmbH). Standard immunohistochemical procedures were performed after 1 h incubation in blocking solution (0.3% Triton, 0.1% saponin, 1% BSA in PBS) on free-floating slices using the anti-microtubule-associated protein 2 (MAP2) antibody (chicken polyclonal; 1:1,000; Neuromics, Edina, MN). The secondary antibody was applied after 2 days of incubation for 3 h at room temperature and was conjugated with aminomethylcoumarin (anti-chicken; 1:100; Dianova, Hamburg, Germany). Finally, the slices were mounted in Vectashield medium (H-100; Vector Laboratories, AXXORA, Enzo Life Sciences GmbH, Lörrach, Germany).

Data analysis and statistics. The cell diameter of VNLL neurons was analyzed in ImageJ software on confocal image stacks with a voxel size of 320 × 320 × 335 nm. These images were acquired with a 63× objective (1.32 NA) and a 1.5 zoom on a Leica SP5 system. To obtain an unbiased estimate of the cell diameter, the maximal length and width were measured from maximal projections of all imaged neurons in the ventral VNLL, irrespective of a specific morphological subpopulation. Electrophysiological data were analyzed with custom-written IGOR Pro procedures (WaveMetrics, Lake Oswego, OR) and in Microsoft Excel. Results are reported as mean ± SE. Statistical significance was determined with either a paired or unpaired Student's *t*-test in Excel, and the significance level was defined as $P < 0.05$. Linear correlation analysis was performed using Pearson's *r* in Prism.

RESULTS

Here, we characterized the developmental changes in passive and active membrane properties, as well as in the firing pattern of visually identified, globular VNLL neurons from P9 to P28. Specifically, we addressed how the developing interaction between these membrane properties pro-

vides mature VNLL neurons with temporally precise responses characteristic of coincidence-detector neurons. Finally, we examined how depolarizations induced by endogenous cholinergic modulation further promote such response properties.

Development of the resting membrane properties. Voltage signaling in neurons depends on both passive and active membrane properties. To gain insight into the developmental regulation of voltage signaling in VNLL neurons, we first estimated their passive membrane properties, namely, the resting potential, membrane time constant, resting input resistance, and effective capacitance. These membrane parameters were analyzed from the average voltage response to 40–60 repetitions of 200 ms-long step current injections of −10 pA (Fig. 1*A*; $n = 75$) (Ammer et al. 2012; Berger et al. 2014; Couchman et al. 2010; Porres et al. 2011). The use of such a small current amplitude kept the resulting voltage deflection minimal and hence minimized the activation or deactivation of additional voltage-dependent conductances close to the neuron's resting state. These current injections generated voltage responses within the range of the observed resting voltage fluctuations of a cell (Fig. 1*A*). Therefore, this paradigm allows the passive membrane properties of these neurons to be approximated at rest. Among the intrinsic membrane parameters at rest, only the membrane potential remained similar between P9 ($n = 11$) and ≥P25 ($n = 7$; P9: −64.6 ± 1.0 mV; ≥P25: −63.9 ± 1.1 mV, $P > 0.05$; Fig. 1*B*). In contrast, the membrane time constant and the resting input resistance decreased significantly from 13.1 ± 1.0 ms and 254.6 ± 30.9 MΩ to 3.6 ± 0.5 ms and 108.3 ± 13.7 MΩ, respectively, between P9 and ≥P25 (all $P < 0.05$; Fig. 1*B*). As a result, the estimated effective resting capacitance decreased by 40% from 55.2 ± 5.5 to 33.8 ± 2.5 pF ($P < 0.05$) over this developmental period (Fig. 1*B*). This reduction in the effective capacitance could result from morphological alterations or a reduction in spatial charging efficacy, resulting from a decrease in input resistance.

To ascertain whether anatomical changes occur in the VNLL during postnatal development, we quantified the cell size of VNLL neurons from MAP2 stainings at P9 and P26 (Fig. 1, *C–E*). The average soma diameter decreased significantly from 15.6 ± 0.3 μm at P9 ($n = 52$; three sections from three animals) to 13.9 ± 0.4 μm at P26 ($n = 31$; three sections from three animals, $P < 0.05$; Fig. 1*E*). The calculation of a spherical surface from the measured soma diameter leads to an estimated reduction in soma size of ~20%. Thus the developmental reduction in soma diameter explains ~50% of the decrease in effective capacitance. The remaining reduction in the effective capacitance is likely due to a refinement in the dendritic arbor, a process known to occur in the auditory brain stem (Rautenberg et al. 2009; Rietzel and Friauf 1998; Rogowski and Feng 1981; Sanes et al. 1992), and a reduction in spatial charging efficacy. Importantly, the refinement of passive membrane properties occurs predominantly before, but continues for a short time after hearing onset, as illustrated by

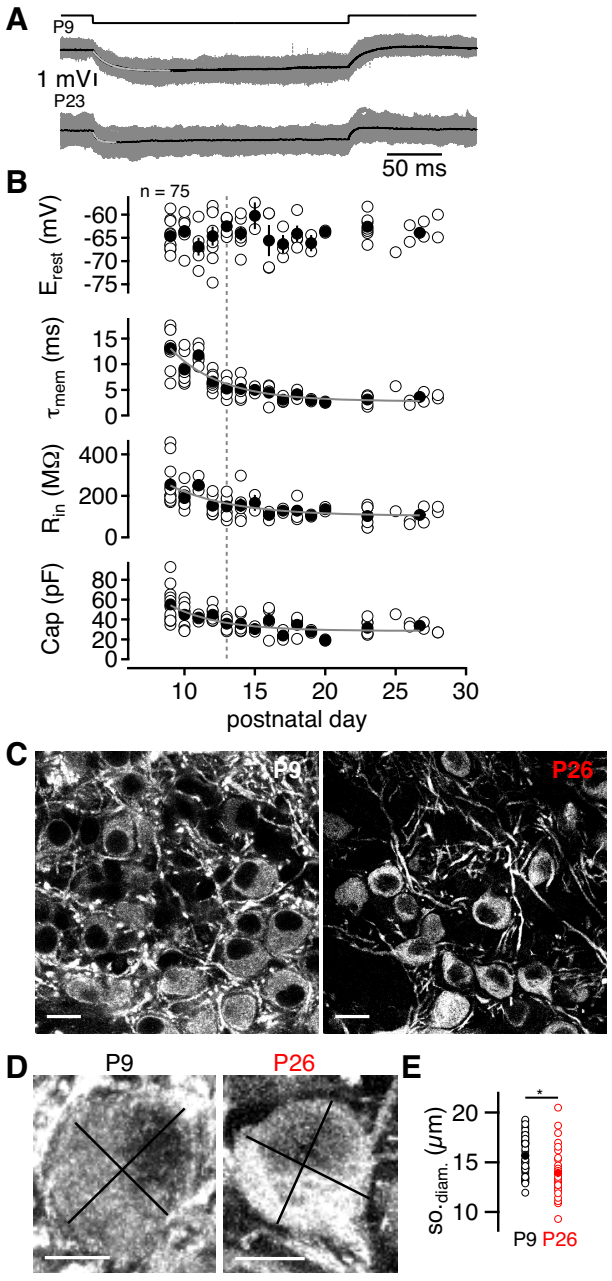

Fig. 1. Developmental changes in resting membrane properties accelerate voltage signaling in ventral nucleus of the lateral lemniscus (VNLL) neurons. *A*: voltage deflection in response to a −10-pA current injection of 200 ms (*top*) in a *postnatal day 9* (P9; *middle*) and in a P23 (*bottom*) neuron. Single trials are in gray; average in black. A single exponential function was fitted to the onset of the average voltage response (light gray). *B*: change in passive membrane properties during late postnatal development. Open circles denote single cells ($n = 75$); closed circles represent averages at the respective postnatal day. *Top:* the resting membrane potential (E_{rest}) was measured from the average membrane potential before the current injection. *Upper middle:* membrane time constant (τ_{mem}), measured from the exponential fits shown in *A*. *Lower middle:* resting input resistance (R_{in}), calculated from the steady-state voltage deflection in *A* and the applied current amplitude. *Bottom:* effective membrane capacitance (Cap), calculated from R_{in} and τ_{mem}. A single exponential function was fitted to the development of each measured parameter (gray). The dotted line indicates the onset of hearing (P13). *C*: microtubule-associated protein 2 staining in the VNLL of a P9 (*left*) and a P26 (*right*) animal. Scale bars, 20 μm. *D*: maximal projections of a P9 and a P26 neuron. Scale bars: 10 μm. To estimate the soma diameter, the length (defined as the longest possible straight line through the soma) and width (longest possible straight line through the soma orthogonal to the length) were measured and averaged for each cell in 3 confocal image stacks obtained from 3 animals at P9 and P26. *E*: soma diameter ($SO._{diam.}$) was obtained as depicted in *D*. Open circles denote single cells; closed circles represent the averages of all cells in 1 age group. P9 is black; P26 is red. *Significance at the $P < 0.05$ level.

the exponential fits (decay time of 3.6 days for the membrane time constant, 4.5 days for the resting input resistance, and 3.5 days for the estimated capacitance; Fig. 1*B*). Taken together, changes in resting membrane properties, such as the input resistance and the cell capacitance, effectively decrease the membrane time constant, thus shortening the somatic integration time window of VNLL neurons during late postnatal development.

Development of firing properties. Short integration times are characteristic features of an operating mode of coincidence detection (Ratte et al. 2013), well suited to achieve the temporal precision required for auditory processing. However, the late and sustained firing pattern of VNLL neurons in juvenile gerbils is inconsistent with this operating mode (Berger et al. 2014). To investigate whether the refinement in passive membrane properties is accompanied by a change in operating mode, we characterized the firing pattern of VNLL neurons in response to 500 ms-long current injections at different stages of late postnatal development ($n = 75$; Fig. 2). In P9 animals, these neurons responded with continuous firing after an initial silent period (Fig. 2*A*). In P13 animals, the threshold current generated an action potential at stimulus onset. Further increasing the current amplitude led to an action potential at stimulation onset, followed by continuous firing (Fig. 2*A*). This firing pattern is also found in P12–P16 rat VNLL neurons (Zhao and Wu 2001). Finally, at P26, only the action potential at stimulation onset remained (Fig. 2*A*). The current threshold in response to these long injections increased during late postnatal development (P9: 0.28 ± 0.04 nA; ≥P25: 0.42 ± 0.04 nA, $P < 0.05$; Fig. 2*B*). As the firing pattern changed, the maximal number of action potentials increased between P9 (78.6 ± 7.9, $n = 11$) and ~P13 (108.2 ± 13.4, $n = 6$) before rapidly declining to three action potentials maximally, from ≥P25 onward (1.8 ± 0.3, $n = 7$; Fig. 2*B*). The time to the first elicited action potential also decreased from 172.8 ± 28.6 ms to 1.6 ± 0.1 ms (Fig. 2*B*), between P9 and ≥P25. This decrease was not limited to the switch from continuous firing to an onset response but continued between P13 and P28 for the action potentials at stimulation onset (Fig. 2*B*). The developmental change in firing pattern and particularly, the generation of a single spike at stimulation onset are consistent with the emergence of intrinsic coincidence-detector properties (Ratte et al. 2013).

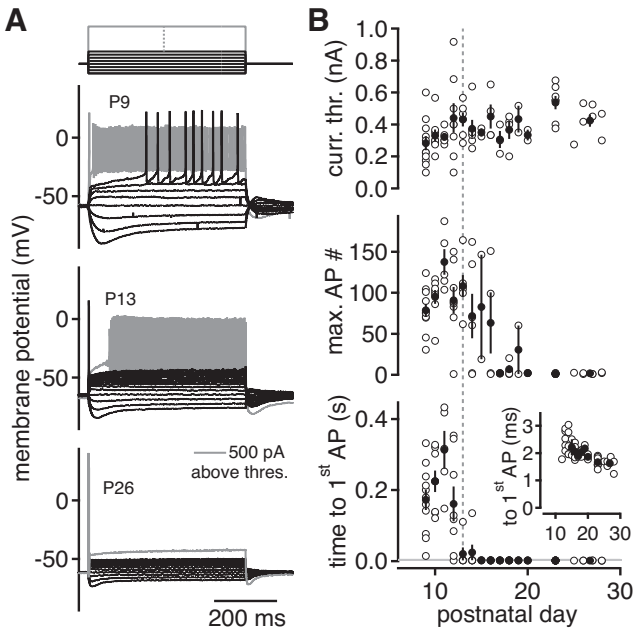

Fig. 2. Developmental regulation of the firing pattern. *A*: voltage deflections in response to hyperpolarizing and depolarizing 500 ms current injections, incremented in 100 pA steps (*top*) in P9, P13, and P26 VNLL neurons. All subthreshold and the 1st suprathreshold traces are displayed in black. Gray traces denote the firing behavior 500 pA above the action-potential current threshold. *B*, *top*: the action-potential current threshold derived from long current injections as a function of age. Open circles denote single cells ($n = 75$); closed circles represent averages at the respective postnatal day. *Middle:* the maximal number of action potentials (max. AP) decreased during development. *Bottom*: the time to the 1st action potential decreased with age. The area shaded in gray corresponds to action-potential latencies <3 ms and is enlarged in the *inset*. The dotted line indicates the onset of hearing (P13). *Inset*: enlarged view of the gray area showing the development of the time to the 1st action potential.

Next, we determined the relative contribution of the effective capacitance and the resting input resistance to the change in the firing properties of VNLL neurons during postnatal development. During long current injections, cellular voltage responses reach steady state, and therefore, the input resistance should dominate the neuronal output. Indeed, in response to these long current injections, the current threshold correlated significantly with the input resistance ($r = -0.5069$, $P < 0.0001$) but not with the cell capacitance ($r = -0.06653$, $P = 0.057$; Fig. 3*A*). To probe whether the input resistance can directly influence the firing behavior of VNLL neurons, we performed conductance-clamp recordings in juvenile animals. In these experiments, the input resistance of recorded cells was artificially lowered by applying a background leak conductance. We then quantitatively characterized the input-output functions of P9 neurons in response to 200 ms current injections (Fig. 3*B*). The input resistance during the application of the additional background conductance was estimated at rest, as for control conditions, illustrated in Fig. 1*A*. At decreased input resistances, P9 cells now generated an action potential at stimulation onset at threshold (Fig. 3*B*). However, a further increase in the stimulation intensity still resulted in action potentials late during stimulation (Fig. 3*B*), contrasting the mature firing pattern of VNLL neurons (Fig. 2*A*). Nevertheless, the current threshold increased considerably upon lowering the input resistance in P9 neurons ($n = 7$; Fig. 3*C*). This increase matched the relationship between the current threshold and the input resistance of cells throughout the developmental period (Fig. 3*C*). The maximal number of action potentials evoked in P9 neurons also decreased upon the application of a background conductance, even leading to the generation of only a single action potential at stimulation onset in two out of seven neurons, similar to mature neurons (Fig. 3*D*). Furthermore, the imposed reduction in input resistance consistently shortened the time to the first action potential (Fig. 3*E*). To conclude, an experimental decrease in input resistance in P9 neurons induces a firing pattern similar to that at more mature stages. Thus the developmental alteration in input resistance largely promotes the developmental change in firing pattern. Yet, further refinement of active membrane properties appears required to explain fully the emergence of the mature firing pattern.

Development of whole-cell potassium currents. Since lowering the input resistance could not fully explain the maturation

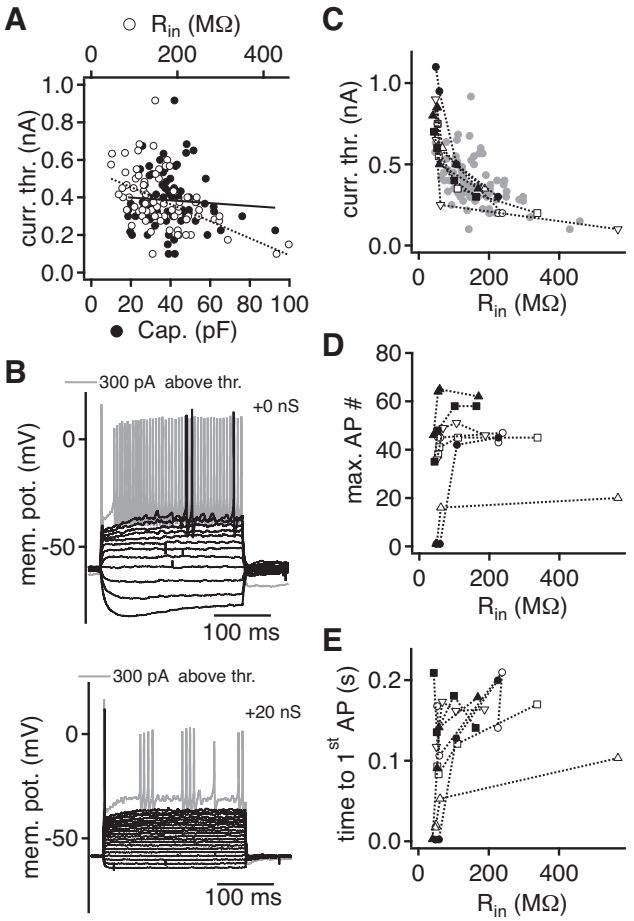

Fig. 3. The developmental change in input resistance contributes to the emergence of the mature firing pattern. *A*: the action-potential current threshold in response to long current injections plotted against the input resistance (open circles, dashed linear fit) and the cell capacitance (closed circles, solid linear fit, $n = 75$). *B*: P9 neurons exhibit buildup firing at threshold and an action potential at stimulus onset at higher current amplitudes (gray) in response to 200 ms step current injections incremented in 50 pA steps from −150 pA. Black traces represent all subthreshold and the 1st suprathreshold trials. Gray traces denote the firing behavior of neurons, 300 pA above threshold. The addition of 20 nS background leak conductance promoted an action potential at stimulus onset at threshold in P9 neurons. *C*: action-potential current threshold as a function of the input resistance induced by the addition of a background leak conductance in P9 neurons ($n = 7$). The different black and white symbols represent different cells. The current threshold increased considerably upon lowering the input resistance in P9 neurons. Data points obtained from the same cell are connected with dotted lines. Gray symbols reiterate the developmental relationship between the input resistance and the current threshold in *A* and are replotted here for comparison. *D*: the maximal number of action potentials decreased, along with the reduction in input resistance induced by the added background leak conductance in P9 neurons ($n = 7$). Symbols are as in *C*. *E*: the time to the 1st action potential in P9 neurons decreased along with the artificial reduction in input resistance. Symbols are as in *C*.

of the firing pattern (Fig. 3), a developmental change in the active membrane properties might be required to generate additional outward current. Therefore, we analyzed pharmacologically isolated, voltage-dependent, whole-cell potassium currents at P9–P11 ($n = 13$) and in animals >P22 ($n = 9$). Potassium currents were elicited with step potentials ranging from −70 mV to +70 mV, following a 500-ms conditioning potential at −80 mV (Fig. 4*A*). The peak potassium current at a step potential of +70 mV was slightly larger in mature animals (17.6 ± 1.47 nA, $n = 9$) compared with that in juvenile P9–P11 animals (14.4 ± 0.87 nA, $n = 13$, $P < 0.05$; Fig. 4, *A* and *B*). However, as the effective capacitance of VNLL neurons decreased during late postnatal development (Fig. 1), the potassium current density provided a more meaningful basis for comparison. We used the compensated capacitance values to normalize the potassium current to the cell size. The compensated cell capacitance was 1.6-fold larger in P9 (23.7 ± 1.6 pF, $n = 13$) than in >P22 neurons (15.5 ± 1.4 pF, $n = 9$, $P < 0.05$), corroborating the 40% developmental reduction observed in current-clamp recordings (Fig. 1). Based on the calculated current densities, the peak and steady-state potassium flux were substantially larger in >P22 neurons compared with those in P9 neurons (peak: 1.18 ± 0.12 nA/pF,

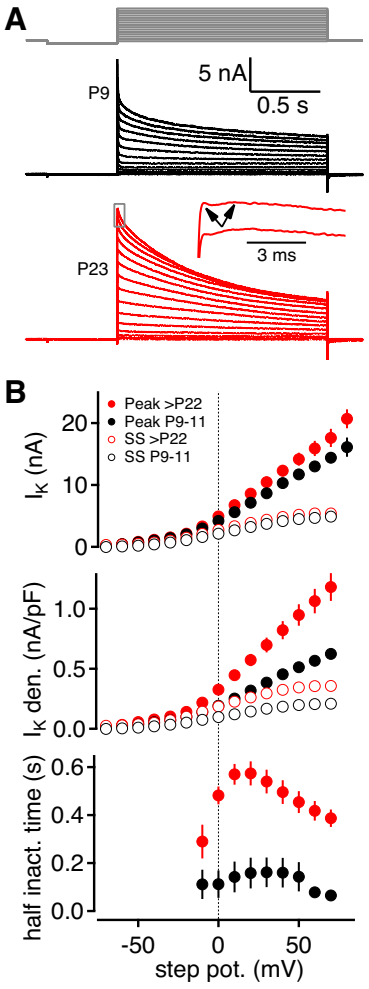

Fig. 4. The whole-cell potassium current is developmentally regulated. *A*: pharmacologically isolated whole-cell potassium current in response to voltage steps, ranging from −70 to +80 mV (*top*) in a P9 (*middle*) and P23 (*bottom*) neuron. *Inset*: the onset of the responses marked by the boxed area at P23, indicating the presence of different subtypes (arrows) within the whole-cell potassium current. *B*, *top*: average peak (closed circles) and steady-state (SS; open circles) potassium current (I_K) as a function of applied step potential in P9–P11 neurons ($n = 13$; black) and in >P22 neurons ($n = 9$; red). *Middle*: average peak and steady-state potassium current normalized to the cell capacitance (I_K den.) as a function of the applied step potential in P9–P11 neurons ($n = 13$) and in >P22 neurons ($n = 9$). Symbols are as in *Top*. *Bottom*: inactivation time course in P9–P11 neurons (black, $n = 13$) and in >P22 neurons (red, $n = 9$), measured as ½ inactivation of the whole-cell potassium current.

$n = 9$, vs. 0.62 ± 0.04 nA/pF, $n = 13$, at a step potential of +70 mV, $P < 0.05$; Fig. 4*B*). Thus the relative amount of potassium current increased during late postnatal development in VNLL neurons.

Importantly, the inactivation time course of potassium currents differed substantially between the two age groups (Fig. 4*A*). As these whole-cell potassium currents appeared to be based on a mixed subset of channel types (Fig. 4*A*), the inactivation kinetics could not be described accurately using exponential decays. Therefore, we quantified the half inactivation time between peak and steady-state current. Our half inactivation time analysis revealed a four-fold difference ($P < 0.05$) in the maximal inactivation time in P9 of 0.16 ± 0.06 s ($n = 13$) compared with 0.57 ± 0.05 s ($n = 9$) in >P22 animals (Fig. 4*B*). The lack of ongoing activity in the firing pattern of adult animals is consistent with a larger density of slowly inactivating potassium outward currents.

Development of action-potential properties. So far, we characterized the developmental changes and relative contributions of passive and active conductances to the firing pattern using step protocols between 200 and 500 ms. However, action potentials in the auditory brain stem are usually triggered by 0.5–2 ms fast synaptic α-amino-3-hydroxy-5-methyl-4-isoxazolepropionic acid conductances (Ammer et al. 2012; Couchman et al. 2010; Porres et al. 2011; Taschenberger and von Gersdorff 2000; Yang and Xu-Friedman 2009) rather than by prolonged depolarization plateaus. Thus the development of the relevant action-potential properties cannot be extracted using long current injections.

To unravel the developmental interplay of cell intrinsic factors toward action-potential generation and precision, we injected currents approximating the excitatory postsynaptic current (EPSC) shape in juvenile VNLL neurons (Berger et al. 2014). This physiologically relevant current injection of 180 μs rise and 500 μs decay time was incremented in steps of 100 pA (Fig. 5, *A* and *B*). Parameters describing the shape of the action potential were averaged from the first suprathreshold event over two to three repetitions/cell (Fig. 5). During late postnatal development, the action-potential size, measured from the resting membrane potential, remained constant, from 86.6 ± 2.4 mV at P9 ($n = 11$) to 88.7 ± 3.2 mV at ≥P25 ($n = 7$, $P < 0.05$; Fig. 5*C*). The duration of the action potential—determined as the action-potential half-width—decreased significantly over the same developmental period (529 ± 34 μs to 189 ± 14 μs, $P < 0.05$), with a time constant of 4.3 days (Fig. 5*C*). In line with the reduced half-width, the speed of action-potential depolarization and repolarization increased significantly throughout development (depolarization P9: 416 ± 30 mV/ms, ≥P25: 814 ± 75 mV/ms, $P < 0.05$; repolarization P9: −176 ± 15 mV/ms, ≥P25: −610 ± 63 mV/ms, $P < 0.05$), with developmental time constants of 9.3 and 11.7 days, respectively (Fig. 5*C*). Importantly, the developmental increase of the repolarization speed of the action potential exceeded that of its depolarization, as indicated by a significant decrease in the ratio of depolarization over repolarization speed (P9: 2.42 ± 0.14; ≥P25: 1.35 ± 0.04, $P < 0.05$; Fig. 5*C*). This developmental alteration occurred with a time constant of 5 days. The differential acceleration of action-potential kinetics supports a change in active membrane properties during late postnatal development. Specifically, the larger acceleration of action-potential repolarization is consistent with the larger whole-cell potassium current density in mature animals. Notably, the refinement of active membrane parameters clearly persists after hearing onset (Fig. 5) and appears to succeed the refinement of passive properties, as judged from the exponential fits (Figs. 1 and 5).

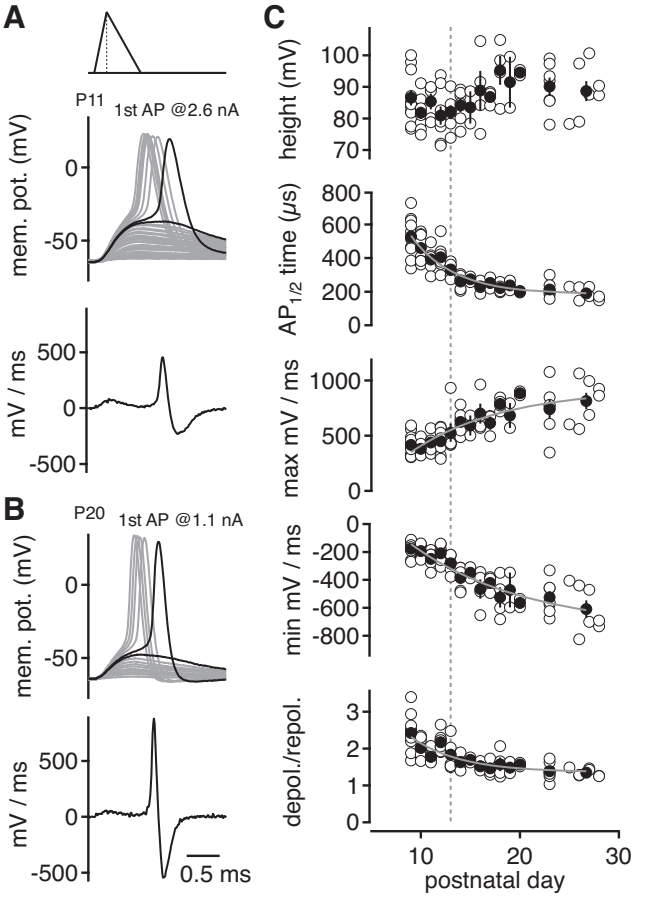

Fig. 5. The action-potential waveform is developmentally regulated in VNLL neurons. *A*: sub- and suprathreshold voltage deflections (*middle*) of a P11 neuron in response to excitatory postsynaptic current (EPSC)-approximating current injections (*top*), incremented in 100 pA steps. The last subthreshold trial and the 1st suprathreshold trial are shown in black. The 1st evoked action potential was used for further analysis (as shown in *C*). *Bottom:* 1st derivative of the 1st suprathreshold voltage response, indicating the speed of action-potential depolarization and repolarization. *B*: same as in *A, middle* and *bottom*, in a P20 neuron. (The stimulation paradigm, illustrated in *A*, *top*, also accounts for *B*.) *C*: developmental profile of the action-potential waveform. Open circles denote single cells ($n = 75$); closed circles represent averages at the respective postnatal day. *Top*: action-potential height measured from the resting membrane potential before the current injection. *Upper middle*: the action-potential ½-width (AP $^1/_2$ time) was measured at ½ of the action-potential height. *Middle* and *lower middle*: speed of action-potential depolarization and repolarization measured from the maxima and minima of the 1st derivative of the action potential, respectively. *Bottom*: ratio of action-potential depolarization to repolarization speed. A single exponential function was fitted to the development of each measured parameter (gray lines). The dotted line indicates the onset of hearing (P13).

To address further the mechanism of action-potential initiation, we investigated the developmental regulation of the action-potential current and voltage threshold in response to EPSC-approximating stimuli. In contrast to the increase in the current threshold to long current injections, both the current and voltage threshold decreased significantly in VNLL neurons between P9 ($n = 11$) and ≥P25 ($n = 7$; 3.18 ± 0.24 nA to 1.22 ± 0.11 nA, $P < 0.05$; −35.8 ± 1.6 mV to −43.2 ± 1.4

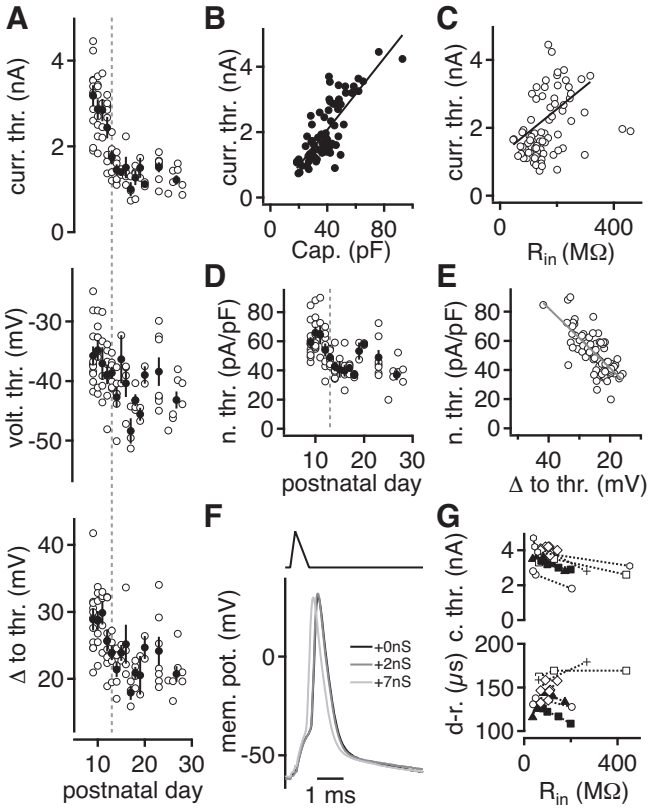

Fig. 6. A developmental decrease in the action-potential current and voltage thresholds in response to short current injections suggests an increase in excitability. *A*, *top*: action-potential current threshold, measured as the current required to elicit the 1st suprathreshold response, as a function of age. Open circles denote single cells ($n = 75$); closed circles represent averages at the respective postnatal day. *Middle*: the voltage threshold, considered as the voltage at which the 1st suprathreshold response was evoked, as a function of age. *Bottom*: Δ to threshold, measured as the difference in membrane potential between the resting membrane potential and the voltage threshold, as a function of age. The dotted line indicates the onset of hearing (P13). *B*: relationship between the action-potential current threshold and the effective capacitance fitted linearly. *C*: relationship between the action-potential current threshold and the input resistance fitted linearly. The black lines represent the linear fit. *D*: decrease in the action-potential current threshold normalized to the cell capacitance (n. thr.) over the same age range. Open circles denote single cells ($n = 75$); closed circles represent averages at the respective postnatal day. The dotted line indicates the onset of hearing (P13). *E*: decrease in the normalized current threshold as a function of the Δ to threshold ($n = 75$). The gray line indicates a linear fit. *F*: the 1st suprathreshold event in a P10 neuron in response to a short EPSC-approximating current injection (*top*) in control (black) and with the addition of 2 nS (dark gray) and 7 nS (light gray) background leak conductance using conductance clamp. *G*, *top*: the action-potential current threshold (c. thr.) as a function of the input resistance induced by the addition of a background leak conductance in P9–P10 neurons. *Bottom*: the time between the maximal speed of action-potential depolarization and repolarization (d-r.) as a function of artificially induced changes in input resistance. The different symbols correspond to different cells. Dotted lines connect data points obtained from the same cell.

mV, $P < 0.05$; Fig. 6*A*). Furthermore, since the resting membrane potential remained constant (Fig. 1*B*), the decrease in the voltage threshold effectively reduced the potential difference that needs to be crossed from rest to the voltage threshold from P9 ($n = 11$) to ≥P25 ($n = 7$; 28.9 ± 1.6 mV to 20.7 ± 1.2 mV, $P < 0.05$; Fig. 6*A*). Taken together, the development of the suprathreshold response of VNLL neurons indicates a change in active membrane properties.

Interplay of active and passive membrane properties during development. The developmental changes described so far prompted us to examine the interactions and contributions of passive/resting and active membrane properties in regulating changes in the suprathreshold response of VNLL neurons during late postnatal development. We quantified the relation of the action-potential current threshold to the effective capacitance and the resting input resistance (Fig. 6, *B* and *C*). The action-potential threshold in response to EPSC-approximating current injections now correlated more strongly with the cell's effective capacitance ($r = 0.797$, $P < 0.0001$) than with its input resistance ($r = 0.3759$, $P = 0.0009$; Fig. 6, *B* and *C*). The strong correlation between the current threshold and the capacitance can be explained by the fact that these short current injections of ~0.5 ms fall within 5–10% of the membrane time constant. The voltage response in this initial part of the membrane time constant is largely determined by the cell's capacitance, since the charging current dominates over the current flowing through the resistive element of the membrane. Thus the developmental change in effective capacitance potentially mediates the change in action-potential current threshold. To evaluate this hypothesis further, the current threshold was normalized to the estimated capacitance (Fig. 6*D*). This normalized current threshold only displayed a 1.6-fold decrease (Fig. 6*D*) compared with the 2.6-fold decrease in the absolute current threshold over the investigated age range (Fig. 6*A*). Therefore, the change in capacitance, a passive membrane property, partially drives the developmental decrease in current threshold and hence influences the integrational properties of VNLL neurons.

However, the current threshold also depends on a cell's active membrane properties. Thus the developmental decrease in the current threshold might result from concurrent changes in the active membrane properties, more likely represented by the voltage threshold (Fig. 6*A*). To ascertain how current and voltage thresholds relate to each other during development, the current threshold normalized to the estimated effective capacitance was correlated to the difference in membrane potential required to reach the voltage threshold (Δ to threshold; Fig. 6*E*). As indicated by the linear fit, a 10-mV change in the Δ to threshold corresponded to a reduction of almost 20 pA/pF. The 8-mV decrease in the Δ to threshold between P9 and ≥P25 is therefore enough to explain the 22 pA/pF drop in the normalized current threshold over the same developmental period. Taken together, the reduction in the effective capacitance and the change in active membrane properties explain the large drop in the current threshold during late postnatal development. Thus the effective capacitance and active membrane properties govern the output of a neuron to short EPSC-approximating stimuli.

If responses to EPSC-approximating stimuli in the soma are controlled by the capacitance, as well as by the active membrane properties of a cell, then the decrease in input resistance during development should not strongly affect the action-potential current threshold in response to these very short stimuli. To assay directly the role of the input resistance in determining the current threshold, the effects of applying a background leak conductance were, once more, investigated in P9–P10 animals (Fig. 6, *F* and *G*). As before, the current threshold was assessed using an EPSC-approximating current injection, incremented in 100 pA steps. The current threshold

was measured for the different input resistances within a given neuron (Fig. 6*F*). In agreement with our previous results, the increase of the leak—and thus decreasing the input resistance—only slightly increased the current threshold in P9 neurons ($n = 7$; Fig. 6*G*). Furthermore, the decrease in input resistance did not affect the action-potential waveform (Fig. 6*G*). To conclude, these findings confirm our prediction that the observed developmental reduction in the current threshold in response to short current injections cannot be explained by the decrease in input resistance but is rather largely mediated by the reduction in cell capacitance.

Input resistance controls action-potential precision. At the end of a current injection, the time course with which a charged membrane relaxes back to the resting potential also depends on the membrane resistance. Thus we hypothesize that the membrane resistance influences the time the membrane potential spends close to the action-potential threshold. Since action-potential precision is influenced by the time the membrane spends close to threshold (Ammer et al. 2012; Rodriguez-Molina et al. 2007), the input resistance should affect the precision of action-potential generation to short current injections. Therefore, we assessed whether action-potential precision is developmentally regulated in the VNLL and how it is affected by changes in input resistance.

Action-potential precision is classically assessed in terms of action-potential latency and jitter. To measure these parameters, the injected, short EPSC-approximating current was scaled to evoke action potentials in ~40% of the trials (Fig. 7*A*) (Ammer et al. 2012; Cathala et al. 2003; Fricker and Miles 2000; Lehnert et al. 2014). As in the DNLL (Ammer et al. 2012), action-potential latency and jitter decreased significantly between P9 ($n = 11$) and P25 ($n = 10$; latency P9: 1.15 ± 0.05 ms, P25: 1.00 ± 0.04 ms, $P < 0.05$; jitter P9: 0.17 ± 0.02 ms, P25: 0.12 ± 0.01 ms, $P < 0.05$; Fig. 7*B*) in VNLL neurons. This type of stimulation close to threshold confirmed the age dependency of the current threshold to short current injections (P9: 3.13 ± 0.15 nA; P25: 1.00 ± 0.06 nA, $P < 0.05$; Fig. 7*B*). To assess whether the observed developmental increase in action-potential precision is driven by changes in input resistance, a constant background conductance was again added to the EPSC-approximating current injections (Fig. 7*A*) to reduce artificially the input resistance of recorded cells. As indicated by the linear regression analysis, the application of this background conductance reduced the latency and jitter of evoked action potentials within single cells and over the population of juvenile and mature VNLL neurons (latency P9: $r = 0.4669$, $P = 0.0036$, P25: $r = 0.663$, $P = 0.0006$; jitter P9: $r = 0.5864$, $P = 0.0001$, P25: $r = 0.4969$, $P = 0.0159$; Fig. 7, *A* and *B*). Interestingly, the imposed leak changed the latency and jitter to such an extent that these parameters in P9 neurons adopted the same dependency on the input resistance than at P25 (Fig. 7*B*). Thus leak appears not only important but also sufficient to regulate action-potential precision. Consistent with our previous results (Fig. 6*G*), the imposition of a leak conductance increased the current threshold to short current injections rather slightly (P9: $r = 0.01229$, $P = 0.9425$; P25: $r = -0.08852$, $P = 0.6880$; Fig. 7*B*). Finally, the lowering of the input resistance did not affect the ratio of the action-potential de- and repolarization speed in either age group tested (P9: $r = 0.2582$, $P = 0.1229$; P25: $r =$

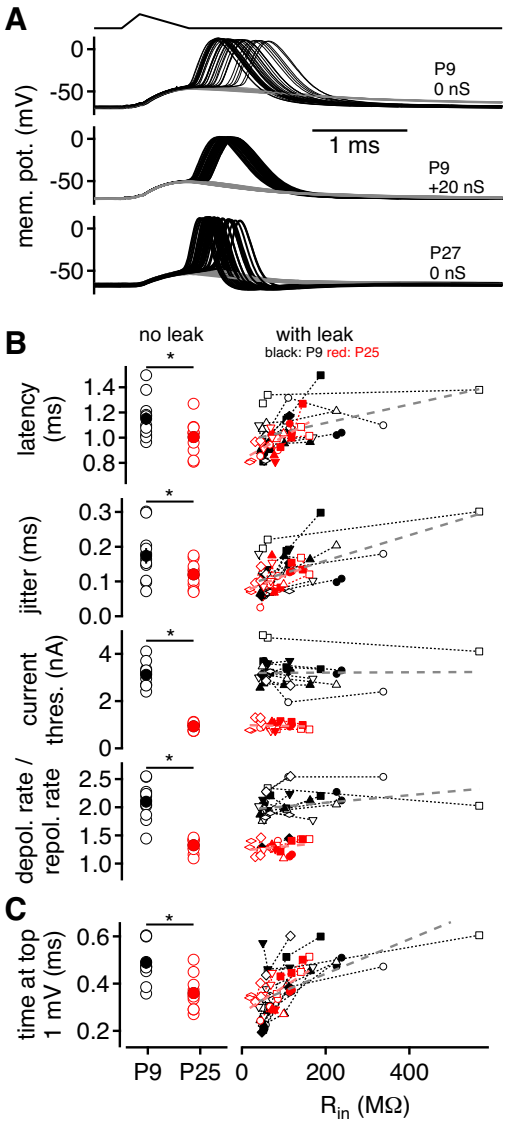

Fig. 7. A reduction in input resistance decreases the latency and jitter of evoked action potentials in VNLL neurons. *A*, *top*: sub (gray)- and suprathreshold (black) voltage deflections in a P9 neuron in response to EPSC-approximating current injections scaled to evoke an action potential in 40% of trials. *Middle*: the addition of 20 nS background leak conductance decreased action-potential jitter in the same P9 neuron. *Bottom*: sub- and suprathreshold responses in a P27 neuron in the absence of a background leak conductance. *B*, *top left*: latency of action-potential generation in P9 neurons (black open circles, $n = 11$) and in P25 neurons (red open circles, $n = 10$) without the addition of a background leak conductance. Closed black and red circles denote averages at P9 and P25, respectively. *Significance at the $P < 0.05$ level. *Top right*: a decrease in input resistance induced by the addition of a leak conductance decreased action-potential latency in P9 neurons (black symbols, $n = 11$). Action-potential latency was measured from the onset of the current injection. The different symbols correspond to different cells at P9 (black) and P25 (red). *Upper middle*: compared with P25 neurons (red open circles, $n = 10$), suprathreshold responses in P9 neurons (black open circles, $n = 11$) displayed significantly higher jitter, which could be reduced with the addition of a background leak conductance (*right*). Action-potential jitter was calculated as the SD of action-potential response latency. *Lower middle* and *bottom*: both the current threshold and the ratio of action-potential depolarization and repolarization speed were not affected by the addition of the background leak conductance. As above, symbols on the *right* represent single cells. *C*: subthreshold voltage responses in P9 neurons (black open circles, $n = 11$) spent significantly more time within 1 mV below threshold compared with P25 neurons (red open circles, $n = 10$), both of which decreased along with a reduction in input resistance induced by the application of a background leak conductance (*right*). As above, different symbols correspond to different cells at P9 (black) and P25 (red).

0.2478, $P = 0.2542$; Fig. 7*B*), indicating that these properties indeed depend on active properties.

Consistent with the developmental increase in precision, P9 neurons ($n = 11$), with a higher input resistance, generated membrane deflections that remained close to action-potential threshold for longer than those in P25 neurons ($n = 10$; P9: 0.49 ± 0.03 ms; P25: 0.36 ± 0.02 ms, $P < 0.05$; Fig. 7*C*). The time the voltage deflection spent within 1 mV below threshold was reduced significantly with the addition of a background conductance, hence, by decreasing the input resistance (time at top 1 mV, P9: $r = 0.6045$, $P < 0.0001$; P25: $r = 0.5983$, $P = 0.0026$; Fig. 7*C*). As a result, P9 neurons adopted the same relationship between the input resistance and the time the membrane potential spent close to threshold, as found in P25 neurons. Thus the time window for action-potential generation decreased in an input resistance-dependent manner. Taken together, our data show that during development, the action-potential current threshold is strongly affected by the cell's effective capacitance, whereas the precision of action-potential generation is controlled by the cell's input resistance. Thus action-potential generation elicited with brief EPSC-approximating current injections is controlled differentially by the two major passive membrane properties.

Cholinergic modulation enhances excitability. From our findings, we would expect a depolarization to reduce the current threshold to EPSC-approximating injections through a decrease in the Δ to the action-potential voltage threshold (Fig. 6*E*). Moreover, predepolarizations were shown previously to change the firing pattern of VNLL neurons (Berger et al. 2014). Thus endogenous neuromodulations that lead to a depolarization should facilitate the generation of action potentials and alter the firing pattern of VNLL neurons. A strong candidate for generating endogenous depolarizations in the VNLL is acetylcholine, as suggested by the expression of acetylcholine receptors in this nucleus (Happe and Morley 2004). Furthermore, cholinergic modulation has been reported previously to alter neuronal excitability (Gulledge et al. 2009; Smith and Araneda 2010; Stiefel et al. 2008) and in the case of the auditory system, has been described in the cochlear nucleus (Fujino and Oertel 2001; He et al. 2014). Therefore, we examined whether cholinergic neuromodulators could generate depolarization-induced changes in excitability in P9–P10 and P19–P21 VNLL neurons, thereby altering the neurons' response profiles. First, we tested whether cholinergic agonists could evoke voltage responses in juvenile VNLL neurons. Puff application of carbachol (500 μM for 4 s), a rather unselective acetylcholine agonist, evoked a clear membrane depolarization in a P9 neuron (Fig. 8*A*). The same neuron was subsequently challenged with a puff application of external recording solution, which did not elicit a voltage response (Fig. 8*A*). Therefore, our pressure application itself did not induce voltage responses. Finally, puff application of oxotremorine (500 μM), a muscarinic acetylcholine receptor agonist, elicited a membrane depolarization in VNLL neurons (Fig. 8*A*). In the next set of experiments, we assessed whether depolarizations elicited by cholinergic agonists can be evoked at mature stages. A brief, 100-ms pressure application of 500 μM carbachol induced a robust depolarization in all four P9–P10 (7.6 ± 1.2 mV) and in all six P19–P21 (5.1 ± 0.5 mV) cells. An even more pronounced depolarization was evoked by the application of 1 mM oxotremorine for 100 ms (P9–P10: 11.9 ± 3.6 mV, $n = 4$; P19–P21: 9.8 ± 2.7 mV, $n = 3$). Thus VNLL neurons are likely subject to a developmentally independent form of neuromodulation mediated through metabotropic acetylcholine receptors.

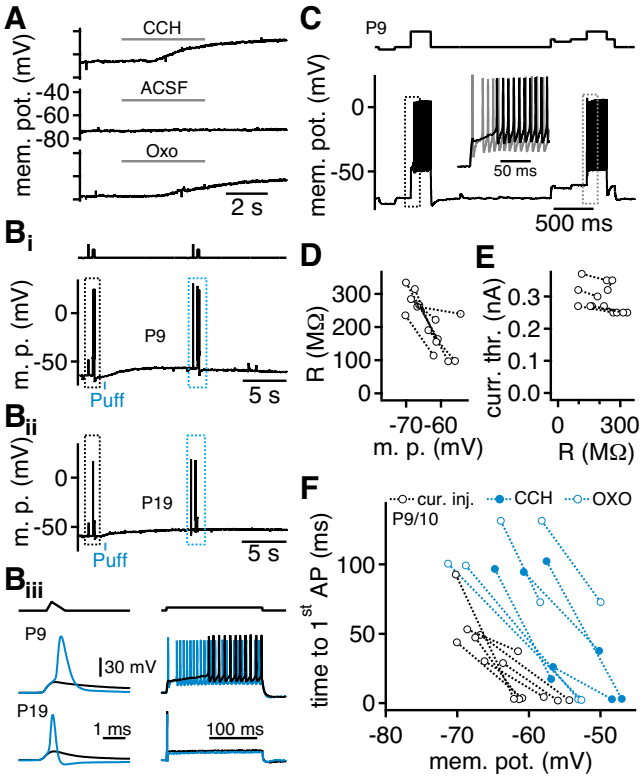

Fig. 8. Depolarization induced by cholinergic modulation changes the excitability of VNLL neurons. *A*: effect of puff applications of 500 μM carbachol (CCH), extracellular recording solution [artificial cerebrospinal fluid (ACSF)], and 1 mM oxotremorine (Oxo) on the membrane potential of a P9 neuron. *Bi* and *Bii*: puff application of 500 μM carbachol (blue bar) in both P9 and P19 neurons combined with the injection of a short and a long current stimulus. The stimulus trace is displayed above the voltage deflection in *Bi*. m. p., membrane potential. *Biii*: overlays of the traces in *Bi* and *Bii* in the regions highlighted by the dashed boxes. Control responses are shown in black; responses following puff application in blue. The depolarization affected the excitability of both P9–P10 and ≥P19 neurons in response to EPSC-approximating current injections and altered the firing pattern of P9–P10 neurons. *Left:* a stimulus, previously evoking a subthreshold response (black trace), elicited an action potential following agonist application (blue trace) in the P9 and P19 neurons. *Right:* in response to longer current injections (200 ms), an action potential could be elicited at stimulation onset at threshold in P9–P10 neurons following agonist application (blue trace). The firing pattern of ≥P19 neurons remained unchanged by the agonist application. The profile of the stimulation current is displayed above the corresponding voltage deflections. *C*: P9 neurons elicited low-frequency firing after an initial silent period in response to 200 ms current injections (*left*). A predepolarization induced by a +70-pA current injection promoted an action potential at stimulation onset directly at threshold (*right*). The stimulus is depicted above the voltage responses. *Inset*: an enlarged view of the regions highlighted by the dashed boxes: firing pattern in the absence (black) and in the presence (gray) of the predepolarization. *D*: the membrane resistance (R) as a function of the membrane potential at rest and during the predepolarization. Open circles denote single cells ($n = 7$). *E*: the current threshold obtained with and without the predepolarization as a function of the input resistance ($n = 7$). *F*: effect of the predepolarization (black circles, $n = 7$) and the application of cholinergic agonists (blue circles, $n = 8$) on the time to the 1st action potential in P9–P10 neurons.

The effect of metabotropic acetylcholine receptor activation on excitability was assayed further by applying short and long current injections before and after agonist application in these

P9–P10 (Fig. 8*Bi*) and P19–P21 (Fig. 8*Bii*) neurons. The injected current was adjusted to evoke a voltage deflection ~10% below action-potential threshold in response to the short current injections and a response just above threshold during the long current injections. The subthreshold event in response to short current injections became suprathreshold following agonist application in both P9–P10 and P19–P21 animals (Fig. 8*Biii*). Furthermore, cholinergic modulation elicited changes in the firing pattern of P9 neurons in response to long current injections. This change was manifested as a decrease in the time to the first action potential and in some cases, as the generation of an action potential at stimulation onset (Fig. 8, *Biii* and *F*). The onset voltage response to long current injections remained largely unchanged in P19–P21 neurons (Fig. 8*Biii*). Thus the generation of action potentials, the firing pattern, and the integrational properties of ventral VNLL neurons can be dynamically adjusted by slow, endogenous neuromodulation.

Next, we evaluated the contribution of the membrane resistance to depolarization-induced changes in firing pattern. To generate a change in excitability similar to that elicited by cholinergic neuromodulation, we introduced a predepolarization using a current injection of +70 pA for 800 ms. The membrane resistance during the predepolarization was measured with a nested, 200-ms hyperpolarization step, induced by a −15-pA current injection (Fig. 8*C*). The neuron's input-output function was subsequently determined using a 300-ms test injection incremented in 100-pA steps (Fig. 8*C*). The predepolarization raised the membrane potential by 8.42 ± 0.76 mV in P9–P10 neurons ($n = 7$) and promoted an action potential at stimulus onset (Fig. 8*C*). The predepolarization also reduced the membrane resistance of P9–P10 neurons (270 ± 18 MΩ to 156 ± 22 MΩ, $n = 7$, $P < 0.05$; Fig. 8*D*). This decrease in membrane resistance coincided with a slight but insignificant increase in the current threshold induced by the predepolarization (286 ± 18 pA to 299 ± 15 pA, $n = 7$, $P < 0.05$; Fig. 8*E*), in agreement with previous results (Fig. 6). Finally, both the application of acetylcholine agonists and depolarizations induced by current injection appeared similarly effective in decreasing the latency to the first action potential (Fig. 8*F*). Again, this decrease in action-potential latency was similar to that induced by artificial reductions in membrane resistance (Fig. 6), supporting the contribution of the membrane resistance to depolarization-induced changes in excitability. To conclude, depolarizations induced by cholinergic modulation result in changes in the excitability and firing pattern of VNLL neurons, largely predicted by concomitant changes in membrane resistance.

DISCUSSION

Here, we examined the interaction of passive and active membrane properties in establishing the temporal precision of mature VNLL neurons during late postnatal development. The maturation of these intrinsic properties leads to shorter integration time windows and enhanced precision of action-potential firing. These developmental changes form the basis of an operating mode characteristic of intrinsic coincidence detectors, optimized for precise information processing. Moreover, the activation of metabotropic acetylcholine receptors depolarizes VNLL neurons in a developmentally independent manner, promoting the generation of suprathreshold responses with high precision. Importantly, our data show that passive and active membrane properties work in synergy during development to establish the physiologically relevant features of auditory neurons.

The role of passive membrane parameters in the development of excitability. By estimating the passive membrane properties close to the resting membrane potential, we show that during late postnatal development, VNLL neurons become leakier and smaller, the latter being corroborated anatomically. Besides leading to a shorter integration time constant, these changes interact with active membrane properties to determine the threshold and precision of action-potential generation as well as the firing pattern. Interestingly, the input resistance and the capacitance contribute to VNLL excitability in different ways. Our findings also suggest that the relative contribution of these membrane properties depends critically on the stimulus duration. For very short EPSC-approximating stimuli, lasting <10% of the membrane time constant, the capacitance dominates the voltage response that leads to action-potential generation. In contrast, a decrease in input resistance alone is sufficient to shorten the time the voltage response spends close to threshold. Thus the capacitance could control the reaching of the action-potential threshold, while a decrease in input resistance alone was sufficient to enhance action-potential precision by shortening the subthreshold integration time window. This finding is consistent with the view that the shape of subthreshold events controls action-potential precision (Ammer et al. 2012; Axmacher and Miles 2004; Cathala et al. 2003; Cudmore et al. 2010; Fricker and Miles 2000; Rodriguez-Molina et al. 2007; Zsiros and Hestrin 2005). For long-lasting stimuli, the input resistance is the dominating membrane property, as it determines the membrane potential that is reached in steady state. Under these stimulation conditions, VNLL neurons displayed a developmental shift in operating mode from buildup to firing only at stimulation onset. The latter type of firing pattern is inherent to the operating mode of coincidence-detector neurons (Ratte et al. 2013). To conclude, our data illustrate the importance of the stimulation time course, as the response to different stimulus durations differentially depends on the capacitance or the input resistance.

Contribution of potassium currents to the development of action-potential firing. In the auditory brain stem, developmental changes in voltage-gated potassium channels (Bortone et al. 2006; Garcia-Pino et al. 2010; Hardman and Forsythe 2009; Liu and Kaczmarek 1998; Nakamura and Takahashi 2007; Scott et al. 2005) are well documented. Here, we describe how developmental changes in the whole-cell potassium current interact with alterations in passive membrane properties to mediate this change in firing behavior. Mature VNLL neurons exhibited a larger potassium current density than juvenile neurons. This difference resulted from a slight developmental increase in the absolute current amplitude and most importantly, from a concurrent reduction in the effective capacitance. This particular interaction of passive and active membrane properties can largely explain the developmental change in action-potential kinetics. Notably, the potassium current also acquired slower inactivation kinetics. Together with the developmental decrease in input resistance, the prolonged potassium current could mediate the outward drive required for the firing pattern of coincidence-detector neurons (Ratte et al. 2013).

Hence, these findings, once more, illustrate the importance of the interaction of passive and active membrane properties. Thus the developing interaction of these intrinsic properties is crucial in establishing physiologically relevant firing properties.

Cholinergic-induced depolarizations modulate the excitability of VNLL neurons. Besides being developmentally regulated, neuronal firing properties are tightly controlled by neuromodulations. Here, we provide evidence of a strong excitatory drive provided by the activation of muscarinic acetylcholine receptors. Depolarizations induced by muscarinic acetylcholine receptor agonists facilitated the generation of action potentials. Similar depolarizations induced by current injections also reduced the input resistance, suggesting that cholinergic modulation could enhance temporal precision. Importantly, these cholinergic-mediated depolarizations could be elicited regardless of the developmental stage, similar to glutamatergic modulation in the cochlear nucleus (Chanda and Xu-Friedman 2011). Thus rather than driving developmental processes, this modulation might support the faithful transfer of suprathreshold information. For example, the activation of this excitatory drive during periods of high activity might further enable cells to sustain high firing rates with high precision, possibly even counteracting synaptic depression.

Time course of developmental alterations. As in the dorsal nucleus of the lateral lemniscus (Ammer et al. 2012) and in the medial superior olive (Chirila et al. 2007; Magnusson et al. 2005; Scott et al. 2005), the maturation of passive membrane properties in the gerbil VNLL precedes that of active membrane properties. The delayed development of active properties could result from a more extensive requirement of sensory experience in regulating channel expression. Whereas the maturation of the input resistance and the capacitance is complete at ~P15 in the VNLL and in the dorsal nucleus of the lateral lemniscus (Ammer et al. 2012), changes in these features persist until P17–P20 in the medial superior olive (Chirila et al. 2007; Magnusson et al. 2005; Scott et al. 2005). Active membrane properties based on action-potential properties mature until ~P18 in the VNLL and in the dorsal nucleus of the lateral lemniscus (Ammer et al. 2012) compared with ~P22 in the medial superior olive (Scott et al. 2005). From the comparison of these developmental profiles (Ammer et al. 2012; Chirila et al. 2007; Magnusson et al. 2005; Scott et al. 2005), it is tempting to speculate that the time course of refinement is related to the complexity of the integrational task of a neuron. Neurons in the medial superior olive integrate excitation and inhibition with active conductances with submillisecond precision (Golding and Oertel 2012; Grothe 2003; Myoga et al. 2014). Although the integration of excitation and inhibition is also of functional relevance in the dorsal nucleus of the lateral lemniscus, the timing is less exquisite, as it operates within tens of milliseconds (Burger and Pollak 2001; Pecka et al. 2007; Siveke et al. 2006; Yang and Pollak 1994). Finally, VNLL neurons predominantly integrate excitation within the millisecond time range (Adams 1997; Covey and Casseday 1991; Recio-Spinoso and Joris 2014; Zhang and Kelly 2006). Thus the differential time course of developmental maturation across auditory nuclei might reflect the amount of sensory experience required to achieve different integration complexities.

Functional implications for globular VNLL neurons. The emergence of precise action-potential firing and an intrinsic operating mode of coincidence detection observed here is well suited to the functional requirements of mature VNLL neurons. The predominant excitatory input to globular VNLL neurons originates from the octopus cell area and is capable of generating high firing rates (Oertel et al. 2000). In turn, VNLL neurons give rise to rapid-onset inhibition in the inferior colliculus (Nayagam et al. 2005; Pollak et al. 2011). Thus mature VNLL neurons are expected to be capable of following high stimulation rates and generate action potentials with high temporal precision. Here, we show mechanistically how biophysical adaptations allow VNLL neurons to achieve the temporal precision of this signal-processing task.

In juvenile VNLL neurons, the temporal precision of information transfer relies on the coincidental activation of synaptic inputs (Berger et al. 2014). Here, we describe how the development of intrinsic features further supports precise information transfer by shaping the neurons' operating mode to that of an intrinsic coincidence detector. Thus we propose that the basis for temporally precise information transfer, depending initially on the coactivation of synaptic inputs, is complemented by the emergence of intrinsic coincidence-detector properties in mature VNLL neurons.

ACKNOWLEDGMENTS

The authors thank Rainer Uhl and Benedikt Grothe for support, Mike Burger and Mike Myoga for comments on the manuscript, and Christian Leibold for discussions.

GRANTS

Funds for this work were provided by the Deutsche Forschungsgemeinschaft (DFG; FE789/3-1). F. Felmy and S. A. Gleiss were funded by the Elisabeth and Helmut Uhl Foundation, C. Berger by the DFG (FE789/3-1), D. L. Franzen by the DFG Research Training Group (GRK) 1091, J. J. Ammer by the Bundesministerium für Bildung und Forschung through the Bernstein Fokus 01GQ0981, and F. S. Kümpfbeck by the DFG SFB870.

DISCLOSURES

The authors declare no competing financial interests.

AUTHOR CONTRIBUTIONS

Author contributions: D.L.F., S.A.G., C.B., F.S.K., J.J.A., and F.F. conception and design of research; D.L.F., S.A.G., C.B., J.J.A., and F.F. performed experiments; D.L.F., S.A.G., C.B., F.S.K., J.J.A., and F.F. analyzed data; D.L.F., S.A.G., C.B., F.S.K., J.J.A., and F.F. interpreted results of experiments; D.L.F., S.A.G., C.B., F.S.K., and F.F. prepared figures; D.L.F., J.J.A., and F.F. drafted manuscript; D.L.F., F.S.K., J.J.A., and F.F. edited and revised manuscript; D.L.F., S.A.G., C.B., F.S.K., J.J.A., and F.F. approved final version of manuscript.

REFERENCES

Adams JC. Projections from octopus cells of the posteroventral cochlear nucleus to the ventral nucleus of the lateral lemniscus in cat and human. *Audit Neurosci* 3: 335–350, 1997.

Ahuja TK, Wu SH. Developmental changes in physiological properties in the rat's dorsal nucleus of the lateral lemniscus. *Hear Res* 149: 33–45, 2000.

Ammer JJ, Grothe B, Felmy F. Late postnatal development of intrinsic and synaptic properties promotes fast and precise signaling in the dorsal nucleus of the lateral lemniscus. *J Neurophysiol* 107: 1172–1185, 2012.

Axmacher N, Miles R. Intrinsic cellular currents and the temporal precision of EPSP-action potential coupling in CA1 pyramidal cells. *J Physiol* 555: 713–725, 2004.

Berger C, Meyer EM, Ammer JJ, Felmy F. Large somatic synapses on neurons in the ventral lateral lemniscus work in pairs. *J Neurosci* 34: 3237–3246, 2014.

Berntson AK, Walmsley B. Characterization of a potassium-based leak conductance in the medial nucleus of the trapezoid body. *Hear Res* 244: 98–106, 2008.

Bortone DS, Mitchell K, Manis PB. Developmental time course of potassium channel expression in the rat cochlear nucleus. *Hear Res* 211: 114–125, 2006.

Burger RM, Pollak GD. Reversible inactivation of the dorsal nucleus of the lateral lemniscus reveals its role in the processing of multiple sound sources in the inferior colliculus of bats. *J Neurosci* 21: 4830–4843, 2001.

Cathala L, Brickley S, Cull-Candy S, Farrant M. Maturation of EPSCs and intrinsic membrane properties enhances precision at a cerebellar synapse. *J Neurosci* 23: 6074–6085, 2003.

Chanda S, Xu-Friedman MA. Excitatory modulation in the cochlear nucleus through group I metabotropic glutamate receptor activation. *J Neurosci* 31: 7450–7455, 2011.

Chirila FV, Rowland KC, Thompson JM, Spirou GA. Development of gerbil medial superior olive: integration of temporally delayed excitation and inhibition at physiological temperature. *J Physiol* 584: 167–190, 2007.

Couchman K, Grothe B, Felmy F. Medial superior olivary neurons receive surprisingly few excitatory and inhibitory inputs with balanced strength and short-term dynamics. *J Neurosci* 30: 17111–17121, 2010.

Covey E, Casseday JH. The monaural nuclei of the lateral lemniscus in an echolocating bat: parallel pathways for analyzing temporal features of sound. *J Neurosci* 11: 3456–3470, 1991.

Cudmore RH, Fronzaroli-Molinieres L, Giraud P, Debanne D. Spike-time precision and network synchrony are controlled by the homeostatic regulation of the D-type potassium current. *J Neurosci* 30: 12885–12895, 2010.

Finck A, Schneck CD, Hartman AF. Development of cochlear function in the neonate Mongolian gerbil (*Meriones unguiculatus*). *J Comp Physiol Psychol* 78: 375–380, 1972.

Fricker D, Miles R. EPSP amplification and the precision of spike timing in hippocampal neurons. *Neuron* 28: 559–569, 2000.

Fujino K, Oertel D. Cholinergic modulation of stellate cells in the mammalian ventral cochlear nucleus. *J Neurosci* 21: 7372–7383, 2001.

Garcia-Pino E, Caminos E, Juiz JM. KCNQ5 reaches synaptic endings in the auditory brainstem at hearing onset and targeting maintenance is activity-dependent. *J Comp Neurol* 518: 1301–1314, 2010.

Gittelman JX, Tempel BL. Kv1.1-containing channels are critical for temporal precision during spike initiation. *J Neurophysiol* 96: 1203–1214, 2006.

Golding NL, Oertel D. Synaptic integration in dendrites: exceptional need for speed. *J Physiol* 590: 5563–5569, 2012.

Goldstein SA, Bockenhauer D, O'Kelly I, Zilberberg N. Potassium leak channels and the KCNK family of two-P-domain subunits. *Nat Rev Neurosci* 2: 175–184, 2001.

Grothe B. New roles for synaptic inhibition in sound localization. *Nat Rev Neurosci* 4: 540–550, 2003.

Gulledge AT, Bucci DJ, Zhang SS, Matsui M, Yeh HH. M1 receptors mediate cholinergic modulation of excitability in neocortical pyramidal neurons. *J Neurosci* 29: 9888–9902, 2009.

Happe HK, Morley BJ. Distribution and postnatal development of alpha 7 nicotinic acetylcholine receptors in the rodent lower auditory brainstem. *Brain Res Dev Brain Res* 153: 29–37, 2004.

Hardman RM, Forsythe ID. Ether-a-go-go-related gene K+ channels contribute to threshold excitability of mouse auditory brainstem neurons. *J Physiol* 587: 2487–2497, 2009.

He S, Wang YX, Petralia RS, Brenowitz SD. Cholinergic modulation of large-conductance calcium-activated potassium channels regulates synaptic strength and spine calcium in cartwheel cells of the dorsal cochlear nucleus. *J Neurosci* 34: 5261–5272, 2014.

Johnston J, Forsythe ID, Kopp-Scheinpflug C. Going native: voltage-gated potassium channels controlling neuronal excitability. *J Physiol* 588: 3187–3200, 2010.

Kandler K, Friauf E. Development of electrical membrane properties and discharge characteristics of superior olivary complex neurons in fetal and postnatal rats. *Eur J Neurosci* 7: 1773–1790, 1995.

Kuba H, Koyano K, Ohmori H. Development of membrane conductance improves coincidence detection in the nucleus laminaris of the chicken. *J Physiol* 540: 529–542, 2002.

Lehnert S, Ford MC, Alexandrova O, Hellmundt F, Felmy F, Grothe B, Leibold C. Action potential generation in an anatomically constrained model of medial superior olive axons. *J Neurosci* 34: 5370–5384, 2014.

Liu SJ, Kaczmarek LK. The expression of two splice variants of the Kv3.1 potassium channel gene is regulated by different signaling pathways. *J Neurosci* 18: 2881–2890, 1998.

Magnusson AK, Kapfer C, Grothe B, Koch U. Maturation of glycinergic inhibition in the gerbil medial superior olive after hearing onset. *J Physiol* 568: 497–512, 2005.

Mainen ZF, Sejnowski TJ. Influence of dendritic structure on firing pattern in model neocortical neurons. *Nature* 382: 363–366, 1996.

Myoga MH, Lehnert S, Leibold C, Felmy F, Grothe B. Glycinergic inhibition tunes coincidence detection in the auditory brainstem. *Nat Commun* 5: 3790, 2014.

Nakamura Y, Takahashi T. Developmental changes in potassium currents at the rat calyx of Held presynaptic terminal. *J Physiol* 581: 1101–1112, 2007.

Nayagam DA, Clarey JC, Paolini AG. Powerful, onset inhibition in the ventral nucleus of the lateral lemniscus. *J Neurophysiol* 94: 1651–1654, 2005.

Oertel D, Bal R, Gardner SM, Smith PH, Joris PX. Detection of synchrony in the activity of auditory nerve fibers by octopus cells of the mammalian cochlear nucleus. *Proc Natl Acad Sci USA* 97: 11773–11779, 2000.

Pecka M, Zahn TP, Saunier-Rebori B, Siveke I, Felmy F, Wiegrebe L, Klug A, Pollak GD, Grothe B. Inhibiting the inhibition: a neuronal network for sound localization in reverberant environments. *J Neurosci* 27: 1782–1790, 2007.

Pollak GD, Gittelman JX, Li N, Xie R. Inhibitory projections from the ventral nucleus of the lateral lemniscus and superior paraolivary nucleus create directional selectivity of frequency modulations in the inferior colliculus: a comparison of bats with other mammals. *Hear Res* 273: 134–144, 2011.

Porres CP, Meyer EM, Grothe B, Felmy F. NMDA currents modulate the synaptic input-output functions of neurons in the dorsal nucleus of the lateral lemniscus in Mongolian gerbils. *J Neurosci* 31: 4511–4523, 2011.

Ratte S, Hong S, De Schutter E, Prescott SA. Impact of neuronal properties on network coding: roles of spike initiation dynamics and robust synchrony transfer. *Neuron* 78: 758–772, 2013.

Rautenberg PL, Grothe B, Felmy F. Quantification of the three-dimensional morphology of coincidence detector neurons in the medial superior olive of gerbils during late postnatal development. *J Comp Neurol* 517: 385–396, 2009.

Recio-Spinoso A, Joris PX. Temporal properties of responses to sound in the ventral nucleus of the lateral lemniscus. *J Neurophysiol* 111: 817–835, 2014.

Rietzel HJ, Friauf E. Neuron types in the rat lateral superior olive and developmental changes in the complexity of their dendritic arbors. *J Comp Neurol* 390: 20–40, 1998.

Rodriguez-Molina VM, Aertsen A, Heck DH. Spike timing and reliability in cortical pyramidal neurons: effects of EPSC kinetics, input synchronization and background noise on spike timing. *PLoS One* 2: e319, 2007.

Rogowski BA, Feng AS. Normal postnatal development of medial superior olivary neurons in the albino rat: a Golgi and Nissl study. *J Comp Neurol* 196: 85–97, 1981.

Rosenberger MH, Fremouw T, Casseday JH, Covey E. Expression of the Kv1.1 ion channel subunit in the auditory brainstem of the big brown bat, *Eptesicus fuscus*. *J Comp Neurol* 462: 101–120, 2003.

Ryan AF, Woolf NK, Sharp FR. Functional ontogeny in the central auditory pathway of the Mongolian gerbil. A 2-deoxyglucose study. *Exp Brain Res* 47: 428–436, 1982.

Sanes DH, Song J, Tyson J. Refinement of dendritic arbors along the tonotopic axis of the gerbil lateral superior olive. *Brain Res Dev Brain Res* 67: 47–55, 1992.

Scott LL, Mathews PJ, Golding NL. Posthearing developmental refinement of temporal processing in principal neurons of the medial superior olive. *J Neurosci* 25: 7887–7895, 2005.

Siveke I, Pecka M, Seidl AH, Baudoux S, Grothe B. Binaural response properties of low-frequency neurons in the gerbil dorsal nucleus of the lateral lemniscus. *J Neurophysiol* 96: 1425–1440, 2006.

Smith DI, Kraus N. Postnatal development of the auditory brainstem response (ABR) in the unanesthetized gerbil. *Hear Res* 27: 157–164, 1987.

Smith RS, Araneda RC. Cholinergic modulation of neuronal excitability in the accessory olfactory bulb. *J Neurophysiol* 104: 2963–2974, 2010.

Stiefel KM, Gutkin BS, Sejnowski TJ. Cholinergic neuromodulation changes phase response curve shape and type in cortical pyramidal neurons. *PLoS One* 3: e3947, 2008.

Taschenberger H, von Gersdorff H. Fine-tuning an auditory synapse for speed and fidelity: developmental changes in presynaptic waveform, EPSC kinetics, and synaptic plasticity. *J Neurosci* 20: 9162–9173, 2000.

Wu SH, Oertel D. Maturation of synapses and electrical properties of cells in the cochlear nuclei. *Hear Res* 30: 99–110, 1987.

Yang H, Xu-Friedman MA. Impact of synaptic depression on spike timing at the endbulb of Held. *J Neurophysiol* 102: 1699–1710, 2009.

Yang L, Pollak GD. The roles of GABAergic and glycinergic inhibition on binaural processing in the dorsal nucleus of the lateral lemniscus of the mustache bat. *J Neurophysiol* 71: 1999–2013, 1994.

Zhang H, Kelly JB. Responses of neurons in the rat's ventral nucleus of the lateral lemniscus to amplitude-modulated tones. *J Neurophysiol* 96: 2905–2914, 2006.

Zhao M, Wu SH. Morphology and physiology of neurons in the ventral nucleus of the lateral lemniscus in rat brain slices. *J Comp Neurol* 433: 255–271, 2001.

Zsiros V, Hestrin S. Background synaptic conductance and precision of EPSP-spike coupling at pyramidal cells. *J Neurophysiol* 93: 3248–3256, 2005.

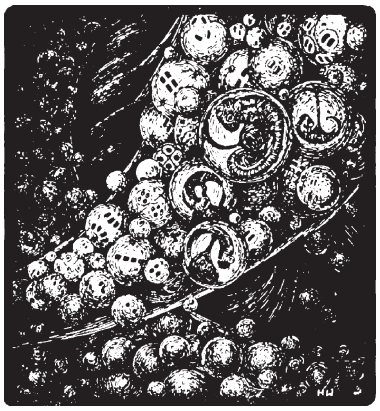

3

ACTIVITY-DEPENDENT CALCIUM SIGNALLING IN MSO NEURONS DURING LATE POSTNATAL DEVELOPMENT

3.1 CONTRIBUTIONS

Franzen, D. L., Kellner, C. J. & Felmy, F. **Activity-dependent calcium signalling in MSO neurons during late postnatal development**. Manuscript in preparation.

The contributions of the authors Delwen L. Franzen (DLF), Christian J. Kellner (CJK) and Felix Felmy (FF) to the study included in this thesis are as follows:

DLF and FF designed the research. DLF performed the experiments and analysed the electrophysiological and imaging data. CJK designed and implemented a custom–made program for the analysis of the imaging data. DLF drafted the manuscript included in this thesis with the help of FF.

Activity-dependent calcium signalling in MSO neurons during late postnatal development

Delwen L. Franzen[1,2,3], Christian J. Kellner[1,2], Felix Felmy[3]

[1] *Division of Neurobiology, Department Biology II, Ludwig-Maximilians-Universität München, Planegg-Martinsried, Germany*

[2] *Graduate School of Systemic Neurosciences, Department Biology II, Ludwig-Maximilians-Universität München, Planegg-Martinsried, Germany*

[3] *Stiftung Tierärtzliche Hochschule Hannover, Institut für Zoologie, Hannover*

Abstract

Neurons of the medial superior olive (MSO) in the auditory brainstem encode interaural time differences in the order of microseconds. MSO neurons undergo key structural and functional refinements around hearing onset (postnatal day (P) 12 - 13) which depend on normal acoustic experience. Given the role of calcium in activity-dependent refinements, we assessed whether calcium is developmentally regulated in MSO neurons. We performed in vitro electrophysiological recordings on Mongolian gerbils from P10 - P60. The whole-cell calcium current decreased progressively during development, and a low voltage-activated component was rapidly downregulated shortly after hearing onset. While action potentials elicited large, global dendritic signals before hearing onset, they decreased markedly in amplitude shortly after hearing onset. Masking binaural cues by raising gerbils in omnidirectional white noise accelerated the maturation of voltage-dependent calcium signalling, without altering other response properties. These findings suggest the presence of a short time window after hearing onset for calcium-dependent circuit refinements, which closes earlier upon high levels of acoustic activity.

1. Introduction

During development neurons must acquire their mature intrinsic membrane properties while integrating into a precise, functional circuit. Neurons in the auditory brainstem encode auditory cues with high precision, which requires a substantial acceleration of their voltage signalling during development (Scott, Mathews, et al., 2005; Chirila et al., 2007; Ammer et al., 2012; Franzen et al., 2015). Changes in passive and active membrane properties are paralleled by the elaboration and subsequent pruning of presynaptic inputs, as well as the development of their synaptic properties (Sanes and Siverls, 1991; Smith et al., 2000; Kim and Kandler, 2003; Magnusson et al., 2005; Werthat et al., 2008; Hoffpauir et al., 2010; Case et al., 2011). In several nuclei of the auditory brainstem, postnatal development is further characterised by changes in the expression and properties of voltage-gated ion channels (Iwasaki and Takahashi, 1998; Iwasaki, Momiyama, et al., 2000; Scott, Mathews, et al., 2005; Nakamura and Takahashi, 2007; Hoffpauir et al., 2010; Khurana et al., 2012) and ligand-gated ion channels (LGICs) (Taschenberger and von Gersdorff, 2000; Koike-Tani et al., 2005; Hassfurth et al., 2010; Steinert et al., 2010). Taken together, these developmental changes enable neurons to process sound localisation cues with high fidelity and precision.

Many developmental processes in neurons depend critically on calcium (Greer and Greenberg, 2008; Berridge, 1998; Berridge et al., 2003). Calcium signalling is required for neuronal growth and synapse formation (Spitzer et al., 2000; Michaelsen and Lohmann, 2010), the establishment and refinement of neuronal networks (Lohmann, Ilic, et al., 1998; Hirtz, Braun, et al., 2012), synaptic plasticity (Feldman, 2012; Horibe et al., 2014) and neuronal survival (Franklin and Johnson, 1992). Furthermore, activity can regulate gene transcription in a calcium-dependent manner during synapse development (Greer and Greenberg, 2008; Tong et al., 2010). In the auditory brainstem, voltage-gated calcium channels (VGCCs) have been shown to be necessary for the normal development of several nuclei (Lohmann, Ilic, et al., 1998; Hirtz, Boesen, et al., 2011; Ebbers et al., 2015). Furthermore, the expression of calcium binding proteins is developmentally regulated in the auditory brainstem, suggesting important developmental phases of calcium homeostasis (Friauf, 1993; Lohmann and Friauf, 1996; Felmy and Schneggenburger, 2004; Bazwinsky-Wutschke et al., 2016).

Extracellular calcium enters neurons in several ways (Gallin and Greenberg, 1995), two of which are: (1) synaptic activity leads to the release of glutamate from presynaptic terminals, which in turn leads to the opening of postsynaptic calcium permeable LGICs (Jonas and Burnashev, 1995);

(2) regenerative events such as action potentials (APs) lead to calcium entry through VGCCs (Markram et al., 1995; Simms and Zamponi, 2014). Global dendritic calcium signals elicited by backpropagating APs are a retrograde indicator of postsynaptic activity, whose timing relative to presynaptic activity can lead to changes in synaptic strength (Markram, 1997; Magee and Johnston, 1997; Feldman, 2012). Furthermore, synaptic plasticity mechanisms can require the coordinated entry of calcium through both LGICs and VGCCs following synaptic activity (Leresche and Lambert, 2016).

Neurons of the medial superior olive (MSO) of the auditory brainstem encode interaural time differences (ITDs), a binaural cue used to localise low-frequency sounds in the azimuthal plane (Grothe et al., 2010). MSO neurons receive bilateral excitatory and inhibitory inputs, which they integrate with high precision (Grothe, 2003). In the MSO of gerbils, glycinergic synapses refine to the soma in an experience-dependent manner shortly after hearing onset. This structural refinement appears to be a specific adaptation for ITD encoding in mammals with good low-frequency hearing (Kapfer et al., 2002). During critical periods of development, changes in the amount and/or pattern of sensory activity can alter the functional and structural organisation of neural circuits (Katz and Shatz, 1996; Hensch, 2005). Masking binaural cues with omnidirectional white noise or cochlear ablation prevents the somatic relocation of glycinergic synapses (Kapfer et al., 2002; Werthat et al., 2008) and disrupts the normal development of inhibitory synaptic transmission (Magnusson et al., 2005). Exposure to omnidirectional white noise also disrupts the normal development of ITD tuning in the dorsal nucleus of the lateral lemniscus (DNLL), which receives a direct input from the MSO (Seidl, 2005). Thus, normal acoustic experience during a restricted phase of development appears to instruct specific inhibitory refinements, which may be necessary for appropriate ITD tuning (Kapfer et al., 2002; Grothe, 2003; Seidl, 2005). Whether changes in the overall amount and/or pattern of acoustic activity similarly affect the refinement of excitation to the MSO is unknown.

Here, we assessed whether calcium influx into MSO neurons through postsynaptic VGCCs is developmentally regulated. Given the importance of calcium during neuronal development and plasticity, changes in calcium dynamics at the onset of sensory-evoked activity are expected to reveal important phases and mechanisms underlying circuit refinement and maturation. We found that a global calcium signal could be reliably elicited in MSO dendrites in response to trains of somatic APs before and at hearing onset. However, these dendritic calcium signals declined rapidly a few days after hearing onset, suggesting the existence of a short time window for sensory-driven, calcium-dependent refinements. Furthermore, MSO neurons of gerbils raised in omnidirectional white noise (OWN) displayed calcium signals characteristic of more mature stages. Our findings

raise the possibility that the refinement of excitation and the time window for calcium-dependent circuit refinements may be sensitive to overall levels of acoustic activity.

2. Methods

2.1 Preparation

All experiments complied with the institutional guidelines and national and regional laws. Animal protocols were reviewed and approved by the Regierung of Oberbayern (according to the Deutsches Tierschutzgesetz). Mongolian gerbils (Meriones unguiculatus) of either sex and of postnatal day (P) 10 - P60 were used in these experiments. The gerbils were anesthesized with isoflurane and then decapitated. Brains were removed in dissection solution containing (in mM) 50–120 sucrose, 25 NaCl, 27 $NaHCO_3$, 2.5 KCl, 1.25 NaH_2PO_4, 3 $MgCl_2$, 0.1 $CaCl_2$, 25 glucose, 0.4 ascorbic acid, 3 myoinositol, and 2 Na-pyruvate (pH was 7.4 when bubbled with 95% O_2 and 5% CO_2), and 110-200 µm-thick transverse (young) or horizontal (adult) slices containing the MSO were cut with a VT1200S Vibratome (Leica Microsystems GmbH, Wetzlar, Germany). Slices were incubated for 30 - 45 min at 34.5°C in extracellular recording solution (same as dissection solution but with 125 mM NaCl, no sucrose, 2 mM $CaCl_2$, and 1 mM $MgCl_2$). All recordings were carried out at near-physiological temperature (34 – 36°C).

2.2 Electrophysiology

MSO neurons were visualised and imaged with a 60 X 1 numerical aperture (NA) objective with a microscope (BX51WI or BX50WI; Olympus, Center Valley, PA) equipped with gradient contrast illumination, a 1.4-NA oil-immersion condenser, and a TILL Photonics imaging system (FEI Munich GmbH, Munich, Germany) composed of a charge-coupled device (Retiga 2000DC) camera and a monochromator (Polychrome IV or V). Recordings were performed using an EPC 10/2 amplifier [HEKA Elektronik, Lambrecht (Pfalz), Germany]. Data for both current-clamp and voltage-clamp recordings were acquired at 100 kHz, and filtered at 3 kHz. In current-clamp recordings, the bridge balance was set to 100% after estimation of the series resistance, which was monitored repeatedly during recordings. The series resistance during whole-cell voltage-clamp recordings was compensated to a constant residual of 2 MΩ. The liquid junction potential (LJP) was not corrected for any of the solutions. For current-clamp experiments, the internal recording solution consisted of (in mM) 145 K-gluconate, 4.5 KCl, 15 HEPES, 2 Mg-ATP, 2 K-ATP, 0.3 Na_2-GTP, 7.5 Na_2-phosphocreatine, 30 µM Oregon Green 488 BAPTA-1 and 50 µM Alexa

Fluor 594 (pH adjusted with KOH to 7.4). Inhibitory glycinergic and GABAergic currents were blocked with 0.5 µM Strychnine hydrochloride and 10 µM SR 95531 hydrobromide, respectively. In addition, alpha-amino-3-hydroxy-5-methyl-4-isoxazolepropionic acid (AMPA) receptors and N-methyl-D-aspartate (NMDA) receptors were blocked with 20 µM DNQX disodium salt and 50 µM D-AP5, respectively. For voltage-clamp experiments, the internal recording solution consisted of (in mM) 135 Cs-gluconate, 10 HEPES, 20 TEA-Cl, 3.3 $MgCl_2$, 2 Na_2-ATP, 0.3 Na_2-GTP, 3 Na_2-phosphocreatine, 5 Cs-EGTA, as well as 10 µM ZD7288 and 50 µM Alexa Fluor 568 or 594. Whole-cell calcium currents were isolated with 1 µM Tetrodotoxin (citrate) (TTX), 2 mM 4-Aminopyridine (4-AP), 10 mM Tetraethylammonium chloride (TEA), 50 µM ZD 7288, 20 µM DNQX disodium salt, 10 µM R-CPP, 10 µM SR 95531 hydrobromide, and 0.5 µM Strychnine hydrochloride. To increase the driving force for calcium, we used an external recording solution containing 2.5 mM $CaCl_2$ and 0.5 mM $MgCl_2$. Slices were also incubated in this solution.

2.3 Dendritic calcium imaging

The internal solution contained 30 µM Oregon Green 488 BAPTA-1 to visualize calcium transients as well as 50 µM Alexa Fluor 594. Images were acquired at a frame rate of 33 Hz (exposure time 20 ms, read-out time 10 ms). Binning was set to 4 x 4 to increase signal-to-noise and the window was chipped (Y=75) to increase the acquisition rate. Changes in calcium influx were recorded by acquiring a 300 ms baseline, shortly after which the cell was stimulated and imaged for a further 2400 ms (Figure 1). A small portion of the soma was always present in the iris to ensure that the imaging analysis was comparable across ages. Only trials within 7 minutes and 15 minutes of cell opening were considered for analysis, to restrict the impact of calcium channel rundown on the recorded transients. No holding current was applied at any time during the experiment, and only cells with a stable resting membrane potential were included. Trials which displayed failures during action potential trains were discarded from further analysis, as they could not be compared to other trials.

2.4 Noise exposure

A cage was placed in a 100 x 80 x 80 cm^3 sound-attenuated box in a quiet room. A 30 minute loop of white noise was generated with a Raspberry Pi and presented via 24 speakers: 12 low-frequency (100 Hz - 12 kHz) and 12 high-frequency (3.5 kHz - 30 kHz) speakers, 2 of each on all 6 sides of the box. Such a broadband, omnidirectional stimulus should mask most directional cues and spatially discrete sources (Withington-Wray et al., 1990). The amplitude of the noise in the centre

of the cage was adjusted to 75 dB SPL, a level that does not cause damage to the cochlea or to primary auditory centres (Withington-Wray et al., 1990). Litters with no fewer than 4 pups, and no more than 8 pups were used for these experiments. The male gerbil was separated from the female and the pups 1-2 days before noise exposure began at P8 - 9. The cage used for the noise exposure was devoid of a house to avoid additional reverberations, but sufficient nest material was provided. A 12h light/dark cycle was set up using a mechanical timer. The temperature and humidity were constantly monitored and stored using a temperature/humidity sensing unit. The temperature and humidity inside the noise box levelled at approximately 25°C and 40%, respectively. A humidifier ensured the humidity never fell below 30%. The mother was allowed to feed *ad libidum*, and fresh water was provided every few days. The mother and pups were monitored without distraction several times a day using an infrared camera. At P14 (or P13 in certain experiments), the first pup was briefly removed from the noise box for recordings, and so forth over the following days. Although experiments were mostly performed on a single pup each day, in some cases two pups were recorded from on the same day. These experiments were approved according to the German Tierschutzgesetz (TVA 55.2-1-54-2532-224-2013).

2.5 Analysis

Electrophysiological parameters were extracted from the current and voltage responses of cells using custom-written IGOR PRO procedures (WaveMetrics, Lake Oswego, OR) and Microsoft Excel. For the development of AP properties, the data of a given parameter was averaged across all single AP trials for each cell. For the imaging analysis, a region of interest including a small part of the soma and the length of visible dendrite was traced in ImageJ using a custom-made plugin. For each stimulation condition, ΔF/F values were calculated for each pixel in Python. ΔF/F values were then averaged across the length of the dendrite, and the peak between 360 ms and 720 ms was taken as the peak ΔF/F value per stimulation condition per cell (start of stimulation = 300 ms) (Figure 1). We imposed this time window to exclude occasional calcium signals that occurred much later than those evoked by the AP. Given that our analysis was based on averaging over the length of the dendrite, we discarded dendrites smaller than 35 µm. To quantify how ΔF/F signals varied along the dendrite, we averaged ΔF/F signals between 450 ms and 690 ms and plotted the ΔF/F over dendritic location for each repetition (Figure 1). These curves were box smoothed in Igor Pro and the peak location of all repetitions was averaged per cell. Data plotted are the median ± interquartile range as most of the data was found not to be normally distributed.

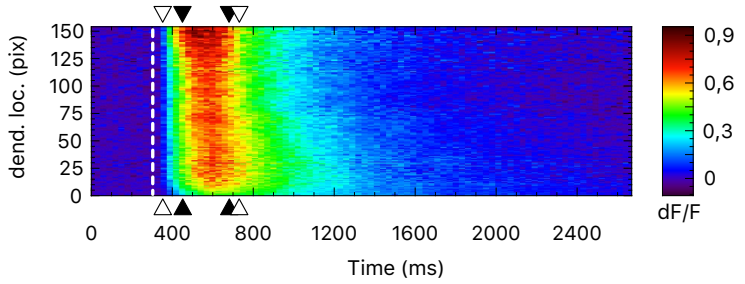

Figure 1. Example kymograph illustrating a calcium transient in response to 25 APs over time as a function of dendritic location from the soma (0). The dashed white line indicates the start of the stimulation at 300 ms. The white arrowheads depict the range used to detect the peak ΔF/F (360 - 720 ms). The black arrowheads depict the range used to analyse how ΔF/F signals vary across the dendrite (450 - 690 ms).

3. Results

We used a combination of patch-clamp electrophysiology and calcium imaging to characterise the developmental regulation of calcium signals in MSO neurons. As we were particularly interested in whether the onset of acoustic activity (P12 - P13) influences calcium signalling, we performed our experiments from before hearing onset (P10) to maturity (P60) with a focus on the week following hearing onset (P13 - P18). To induce a change in acoustic experience, we raised litters of gerbils in omnidirectional white noise and assessed the development of calcium signalling using daily recordings.

3.1 Developmental decrease in the whole-cell calcium current and loss of a T-Type component

We used whole-cell voltage-clamp to assess whether the whole-cell calcium current is developmentally regulated in MSO neurons. A 400 ms voltage step to -85 mV followed by a 400 ms voltage step from -70 mV to +56 mV in 7 mV increments was used to generate current-voltage (I-V) curves at P10 and P20 (Figure 2A - B). Comparing the I-V curves at P10 and P20 revealed two main differences. First, the peak of the whole-cell calcium current was larger in P10 neurons compared to that in P20 neurons. Second, at P10, the I-V curve indicated the presence of a low voltage-activated inward current (Figure 2A, arrow), such as that mediated by low voltage-activated T-Type calcium channels. T-Type channels display steady-state inactivation at rest (Cueni et al., 2009). Thus, we used a subtraction protocol to isolate this current: (i) we evoked a 150 ms prepulse to -85 mV to relieve T-Type channels from inactivation. This was followed by a 70 ms voltage step from -55 mV to -35 mV in 5 mV increments (Figure 2C); (ii) we evoked the same protocol in the absence of the prepulse i.e. only the fraction of channels open at rest pass current (Figure 2D). The

absolute T-Type current at -35 mV was calculated by subtracting (ii) from (i) for each cell.

To obtain a full developmental profile of the whole-cell calcium current and the T-Type calcium current in MSO neurons, we performed these experiments at different ages between P10 and P60 (n = 75). The whole-cell calcium current increased slightly between P10 (2 nA) and P13 (2.6 nA), before progressively decreasing to mature levels (P60: 1.1 nA) (Figure 2E). In turn, the peak T-Type current at a holding potential of -35 mV recorded at P10 was large (497.2 pA), but decreased rapidly at hearing onset until it was very small or no longer present from P15 onwards (53 pA) (n = 91) (Figure 2F). To assess whether the developmental regulation of the whole-cell calcium current is affected by changes in acoustic experience, we repeated these experiments in gerbils raised in OWN (peak current n = 43; T-Type n = 50). The whole-cell calcium current was significantly smaller at P13 (2 nA in OWN vs 2.6 nA in a normal acoustic environment (NAE); Unpaired T Test: p = 0.004) but not at other ages (P14: 2.1 nA in OWN vs 2.1 nA in NAE; P15: 2 nA in OWN vs 2.1 nA in NAE) (Figure 2E, yellow symbols). Similarly, the T-Type calcium current seemed to decrease slightly faster, with a significantly smaller evoked current at P14 (53.1 pA in OWN vs 101.1 pA in NAE, Mann Whitney: p = 0.032) but not at other ages (P13: 106 pA in OWN vs 115 pA in NAE; P15: 42.3 pA vs 53 pA in NAE) (Figure 2F, yellow symbols). Taken together, from before hearing onset to maturity the peak whole-cell calcium current decreases. In addition, a large T-Type component is rapidly downregulated shortly after hearing onset. Exposure to omnidirectional white noise appeared to accelerate the development of the peak whole-cell calcium current and the T-Type calcium current by approximately one day.

3.2 The whole-cell calcium current is largely mediated by P/Q-Type and L-Type channels

To assess the contribution of different calcium channel subtypes to the overall calcium current, we performed whole-cell voltage-clamp recordings of the whole-cell calcium current in the presence of various blockers of high voltage-activated calcium channels. We repeatedly evoked a 100 or 300 ms voltage step to 0 mV and quantified the decrease in the whole-cell calcium current after bath application (12 minutes) of 200 nM ω-Agatoxin IVA, 1 µM ω-conotoxin, or 50 µM Nifidepine (diluted in DMSO) to reveal the contribution of P/Q-, N-, and L-Type channels respectively (Figure 3A). Application of ω-Agatoxin IVA blocked 58% of the whole-cell calcium current in P13 - P15 MSO neurons (n = 6), demonstrating a large contribution of P/Q-Type channels to the overall calcium current. In turn, ω-conotoxin (n = 8) reduced the peak amplitude by $\sim$30% while Nifedipine blockade resulted in a 49% decrease in the whole-cell calcium current (n = 9) (Figure 3A). To take possible rundown of VGCCs into account, we repeated the same procedure in

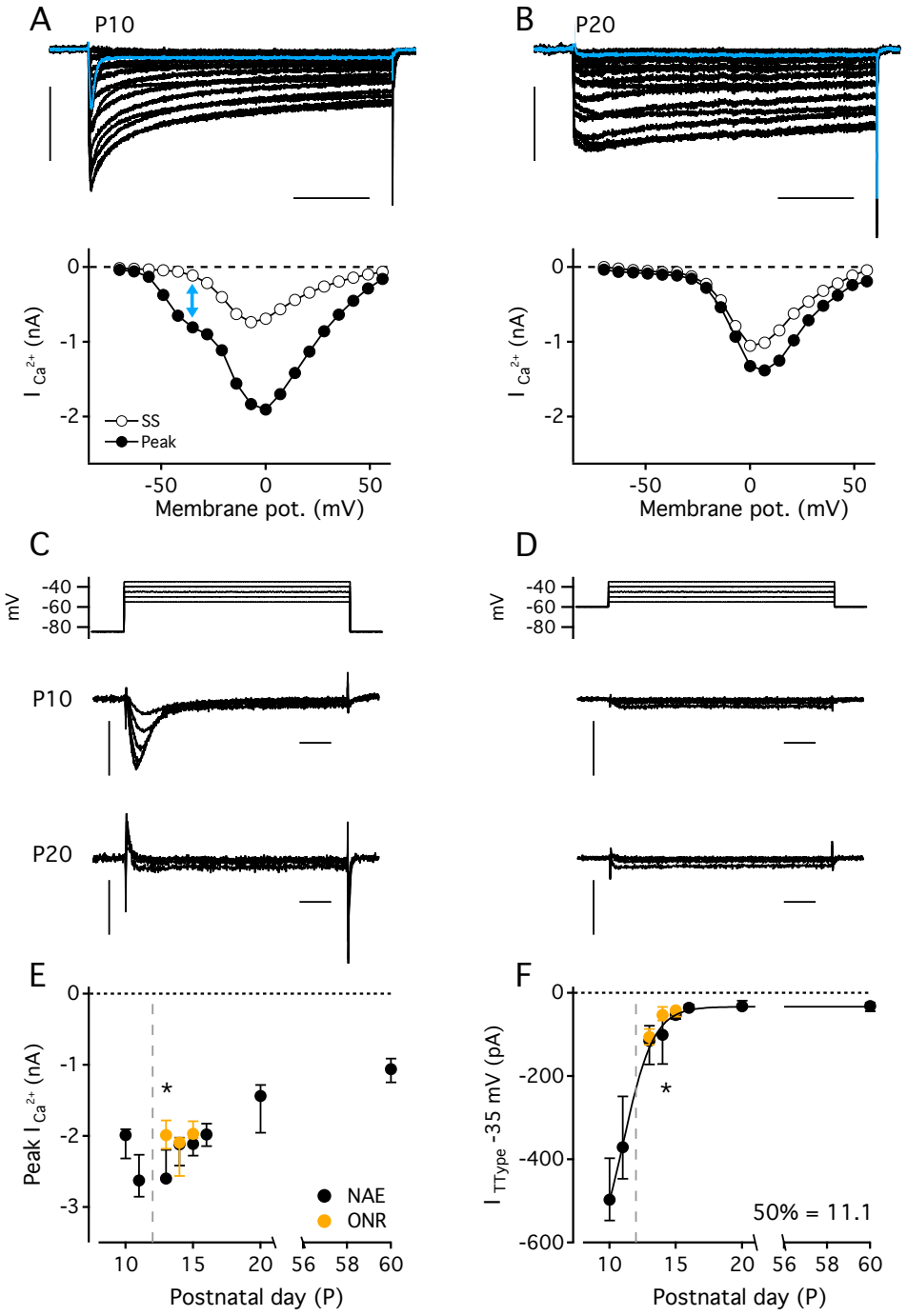

Figure 2. **A**. *Top*: Whole-cell calcium current in a P10 MSO neuron. Scale bar: 100 ms, 1 nA. The blue trace denotes the whole-cell current at a holding potential of -35 mV. *Below*: Voltage-dependent relationship of the whole-cell calcium current. The blue arrow denotes the low voltage-activated T-Type component at a holding potential of -35 mV. **B**. Same as in A in a P20 MSO neuron. Scale bar: 100 ms, 1 nA. **C**. Whole-cell calcium current evoked by a step command to -55 mV (incremented in 5 mV steps) when preceded by a prepulse to -85 mV to remove steady-state inactivation in a P10 (*top*) and P20 (*bottom*) MSO neuron. Scale bar: 10 ms, 500 pA. **D**. Whole-cell calcium current evoked by a step command to -55 mV (incremented in 5 mV steps) without a prepulse in a P10 (*top*) and P20 (*bottom*) MSO neuron. Scale bar: 10 ms, 500 pA. **E**. Change in the peak whole-cell calcium current during late postnatal development in gerbils raised in a NAE (black symbols) and gerbils raised in OWN (yellow symbols). The dashed line represents hearing onset (P12). **F**. Development of the T-Type calcium current at a holding potential of -35 mV, measured with a subtraction protocol during late postnatal development in gerbils raised in a NAE (black symbols) and in gerbils raised in OWN (yellow symbols). A sigmoid was fitted to the data. The dashed line represents hearing onset (P12). All symbols depict the median and the error bars represent the first and third quartiles. Significance at the $p < 0.05$ level is denoted by an asterisk.

the absence of any blockers (n = 8). The whole-cell calcium current decreased by 26% in 12 minutes (Figure 3B). Thus, the relative contribution of each channel type was adjusted for 26% rundown, leading to a contribution of 32% for P/Q-, 4% for N-, and 23% for L-Type channels (Figure 3C). The contribution of T-Type channels was directly estimated from a subtraction protocol based on their steady-state inactivation and activation at low voltages (Figure 2). At P13 and P14, T-Type calcium channels contributed on average 6.5% to the whole-cell calcium current. Considering the substantial developmental regulation of the T-Type current around hearing onset, the contribution stated here is subject to changes depending on the developmental period considered. Nonetheless, our recordings suggest it comprises between 5 - 8% of the total calcium current at P14 and P13, respectively. (Note that T-Type measurements displayed a high variability during development: at P13 the T-Type component comprised as little as 1.3% and as much as 41% (outlier) of the whole-cell current; at P14 the T-Type component comprised as little as 1.4% and 15.5% of the whole-cell current). Taken together, between P13 and P15 MSO neurons possess a majority of P/Q- and L-Type calcium channels, with a smaller contribution of N- and T-Type channels to the whole-cell calcium current (Figure 3C).

Next, we sought to confirm the contribution of different calcium channel subtypes to the whole-cell calcium current using a combination of calcium imaging and pharmacology. However, given that Nifedipine is light-sensitive and T-Type channel blockers had been found to have unspecific effects at the time of our experiments, we restricted this experiment to P/Q-Type channels (n = 5). We evoked trains of 3, 10 or 25 APs at 100 Hz using somatic step current injections of 3800 pA and simultaneously imaged dendritic calcium signals. We compared the magnitude of dendritic calcium signals at regular intervals before and after the application of 200 nM ω-Agatoxin IVA, a selective blocker of P/Q-Type channels. On average, the magnitude of the evoked $\Delta F/F$ decreased by 55.7% 10 minutes after the application of ω-Agatoxin IVA, confirming the presence of these channels (Figure 3D - E). However, this is likely an overestimation if both calcium channel rundown and bleaching are considered. The decrease in calcium signals occurred in the absence of large changes in the AP waveform (Figure 3F).

3.3 Passive and active membrane properties accelerate voltage signalling during late postnatal development

Depending on their voltage-dependence properties, VGCCs can be activated by subthreshold or suprathreshold voltage events, which propagate throughout neurons in a manner that largely depends on passive and active membrane properties. Thus, we used current-clamp to characterise the development of voltage signalling in MSO neurons from P10 to P60 in gerbils raised in a

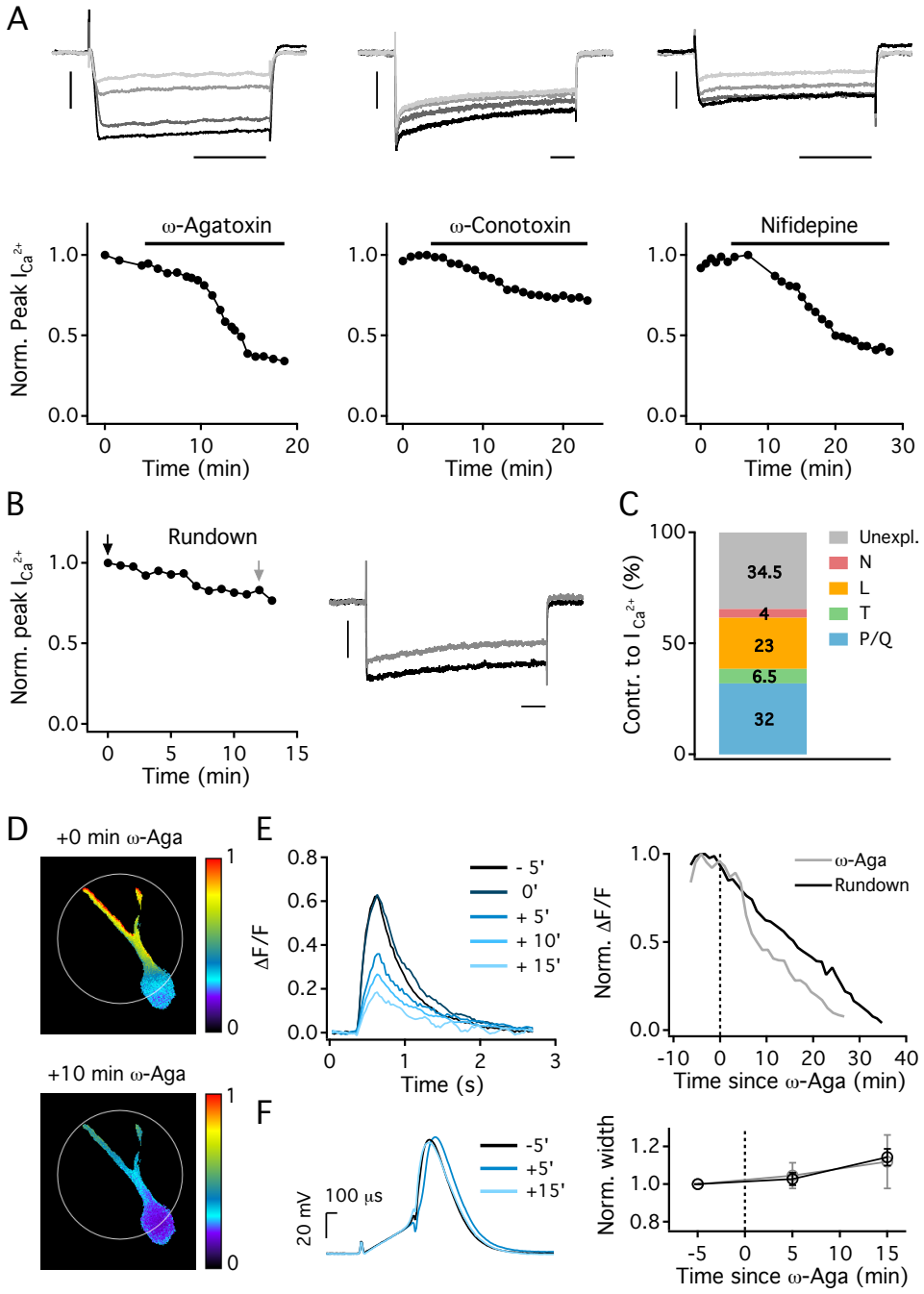

Figure 3. **A**. Whole-cell calcium current at different time intervals before and after the application of 200 nM ω-Agatoxin IVA in a P15 MSO neuron (*Left*), 1 µM ω-Conotoxin in a P13 MSO neuron (*Middle*) and 50 µM Nifedipine in a P15 MSO neuron (*Right*). *Below*: Normalised change in the peak whole-cell calcium current of cells in (*Top*). Solid bars show when the drug was washed in the bath. **B**. *Left*: Normalised change in the peak whole-cell calcium current in the absence of pharmacology ('rundown'). The black and grey arrows indicate trials at 0 and 12 minutes, respectively. *Right*: The whole-cell calcium current at the trials denoted by an arrow in (*Left*). **C**. Estimated contribution of calcium channel subtypes (%) to the whole-cell calcium current in P13 - P15 MSO neurons. All groups except 'Unexplained' are corrected for 26% rundown. **D**. AP-evoked dendritic calcium influx (ΔF/F) before (*Top*) and 10 min after bath application of ω-Agatoxin IVA (200 nM) (*Bottom*) in a P13 MSO neuron. **E**. *Left*: AP-evoked dendritic calcium influx (ΔF/F) of the cell in (D) at different time points before and after ω-Agatoxin IVA wash in. *Right*: AP-evoked dendritic ΔF/F (normalised to maximum) before and after ω-Agatoxin IVA wash in (grey). The same experiment in the absence of pharmacology in a P13 MSO neuron is plotted for comparison (black) (time adjusted to ω-Agatoxin IVA wash in). **F**: *Left*: Zoom in of APs which elicited the dendritic calcium influx shown in the 'rundown' cell shown in (E, right). *Right*: Average normalised AP width (from baseline) over time in 'Rundown' (black) and 'Agatoxin' (grey) cells. Error bars show the standard deviation.

NAE and in gerbils raised in OWN. All passive and active membrane properties tested changed considerably from P10 to P60, reflecting a substantial acceleration of voltage signalling. All active membrane properties were obtained from single AP trials in response to a 200 µm increasing and 300 µm decreasing current ramp at 10% above the current threshold. The shape of the AP changed substantially over the course of late postnatal development (Figure 4A). The current required to evoke an AP decreased between P10 (6.2 nA) and P14 (3.5 nA), before increasing again to mature levels (5.6 nA) (NAE n = 170; OWN n = 103) (Figure 4B). The repolarising phase of the AP was also strongly developmentally regulated (NAE n = 133; OWN n = 93). At P10, APs consistently displayed a depolarising after-potential as large as 11 mV. Only a day later, 8/15 cells displayed a depolarising after potential while 7/15 cells developed a small and prolonged afterhyperpolarisation. From P13 onwards all cells displayed an afterhyperpolarisation that progressively became larger and faster (Figure 4C). Alongside these changes, both the size and width of somatic APs decreased markedly from P10 (P10: 83 mV; 410 µs) to P60 (23.6 mV; 173 µs) (NAE n = 133; 132 OWN n = 93). While the decrease in AP size was fairly gradual, the AP width changed faster with a sharp transition between P11 and P13 (Figure 4D - E). We then generated I-V curves with alternating 250 ms current steps from -1 nA to +3.25 nA (NAE n = 156; OWN n = 115). While large voltage deflections were observed at steady-state before hearing onset, voltage responses became markedly smaller from P13 onwards. Interestingly, the initial decline of steady-state voltage deflections occurred earlier in response to negative current pulses than in response to positive current pulses (Figure 4F). Finally, both the input resistance (NAE n = 151; OWN n = 118) and the membrane time constant (NAE n = 150; OWN = 118) decreased substantially from P10 (112 MΩ; 8.1 ms) to P60 (4.8 MΩ; 436 µs) (Figures 4G - H). Importantly, all the parameters tested (except the membrane time constant) continued to decrease significantly between P18 and P60. Raising gerbils in OWN did not appear to induce substantial or consistent changes. Rather, we report only several instances of a significant difference (current threshold P17: Mann Whitney p = 0.027; AP width threshold P14: Unpaired T Test p = 0.047; P15: Unpaired T Test p = 0.007; I-V +3.25 nA P18: Mann Whitney p = 0.014; input resistance P18: Unpaired T Test p = 0.022). Except for the AP width, these significant differences occurred at only a single age. Taken together with the considerable variability at these ages, we did not elaborate on these significant differences further. Taken together, passive and active membrane properties of MSO neurons change substantially during development to promote rapid voltage signalling, and do not appear to be affected by exposure to OWN.

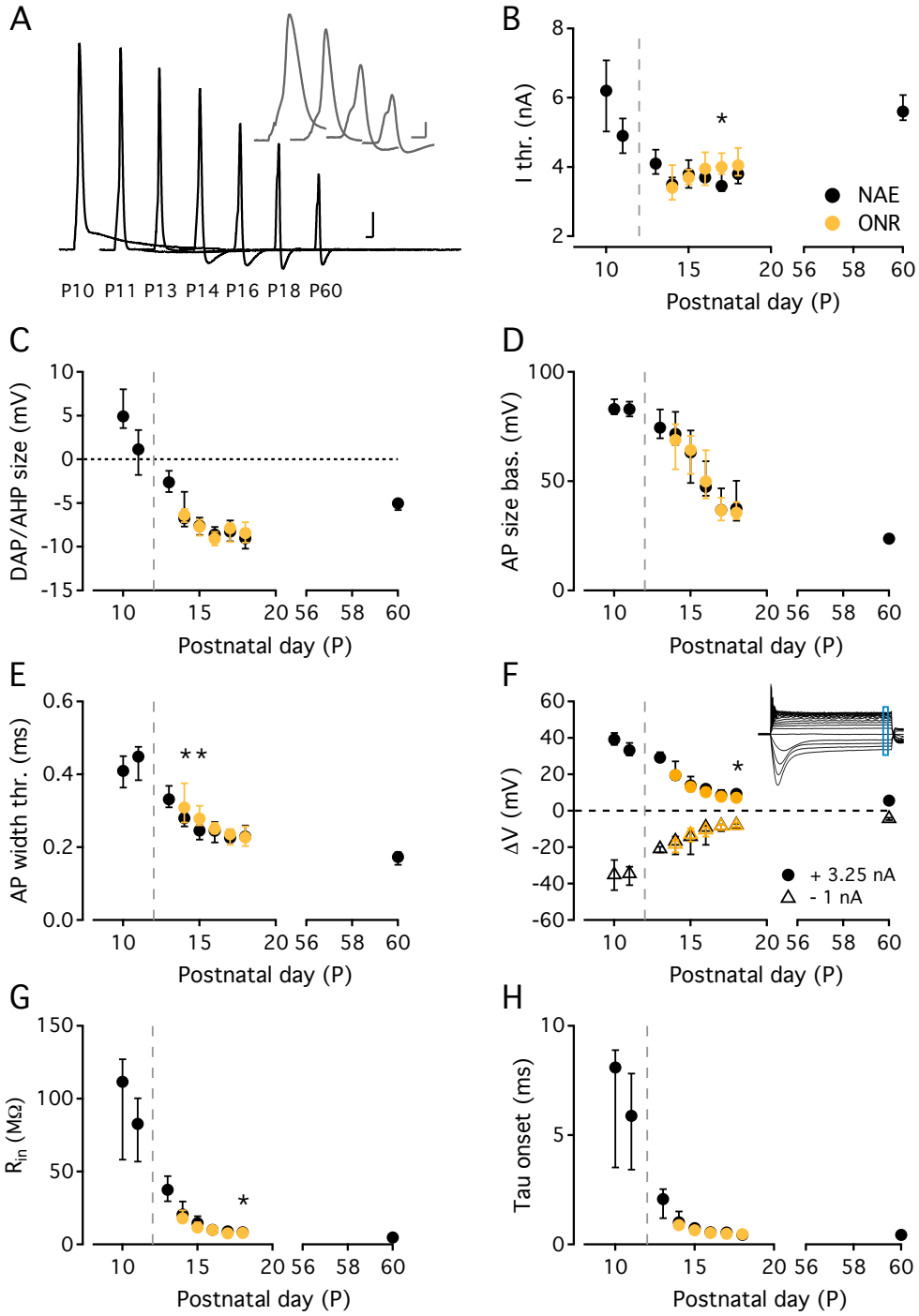

Figure 4. **A**. Shape of the AP at 10% above the current threshold throughout late postnatal development (P10 - P18) and at maturity (P60). Scale bar: 1 ms, 10 mV. *Inset*: close-up of the AP at P10, P13, P16 and P60. Scale bar: 0.5 ms, 10 mV. **B**. Change in the current threshold in response to a 200 µs increasing and 300 µs decreasing ramp stimulus during late postnatal development in gerbils raised in a NAE (black symbols) and in OWN (yellow symbols). **C**. Development of the depolarising after potential (DAP) or afterhyperpolarising potential (AHP) in response to a current stimulus at 10% above the current threshold. NAE: black symbols; OWN: yellow symbols. **D - E**. Developmental change in the AP size (from baseline) and AP width (from voltage threshold) in response to a current stimulus at 10% above the current threshold. NAE: black symbols; OWN: yellow symbols. **F**. Steady-state voltage deflection evoked by 200 ms current steps of -1 nA and +3.25 nA. NAE: black symbols; OWN: yellow symbols. *Inset*: example I-V curve in a P10 MSO neuron. The blue rectangle denotes the steady-state area from which values were measured. **G - H**. Change in the input resistance and membrane time constant throughout late postnatal development. NAE: black symbols; OWN: yellow symbols. All symbols show the median and the error bars represent the first and third quartiles. Significance at the $p < 0.05$ level is denoted with an asterisk. The dashed line in **B - H** represents hearing onset (P12).

3.4 Large VGCC-evoked dendritic calcium transients rapidly decrease shortly after hearing onset

As the shape of somatic APs of MSO cells is strongly developmentally regulated, it is likely that calcium signals driven by such regenerative voltage signals might also change during development. To test this possibility, we evoked somatic APs with current injections (200 µs increasing and 300 µs decreasing ramp) at 10% above the current threshold, which was repeatedly monitored throughout the recordings. We simultaneously imaged calcium signals in either the lateral or medial dendrite of the recorded cell. Dendritic calcium responses were measured in response to a single AP, or trains of 3, 10, and 25 APs at 100 Hz. All recordings were performed in the presence of blockers of glutamatergic, glycinergic and GABAergic synaptic transmission.

A large global calcium influx could be reliably evoked in MSO neurons at P13 (ΔF/F for 25 APs: 0.53) (Figure 5A). Even single APs were sufficient to evoke a dendritic calcium signal in all P10 and P11 cells, and in almost all P13 cells. However, by P18 only a fraction of cells displayed a small calcium response, and only in response to 10 or 25 APs (ΔF/F for 25 APs: 0.01) (Figure 5B). To identify when dendritic calcium signals driven by APs are first downregulated, we performed these experiments between P10 and P60 (n = 124). Given that calcium signals were only observed in response to 25 APs at P18, we restricted the following analysis to this stimulation condition. Before hearing onset, calcium signals were even larger than at P13 (ΔF/F P10: 0.65; P11: 0.51). Only a few days after hearing onset (P14), the calcium influx through VGCCs began to decline rapidly (P14: 0.27; P15: 0.14; P16: 0.04; P17: 0.02; P18: 0.01; P60: 0) (Figure 5C). Raising gerbils in OWN (n = 89) led to a slight but significant decrease in the amplitude of calcium transients at P17 and P18 (P17 Mann Whitney $p = 0.043$; P18 Mann Whitney $p = 0.029$) (Figure 5C, yellow symbols). While a calcium event could always be evoked in response to 25 APs between P10 and P14, only 46.2% of cells evoked displayed a calcium event in response to the same stimulation at P18 (Figure 5D). Interestingly, the occurrence of calcium events declined more rapidly in gerbils exposed to OWN, with only 28.6% and 18.7% of cells displaying a calcium event at P17 and P18, respectively (compared to 66.7% and 46.2% in gerbils raised in a NAE) (Figure 5D, yellow symbols). Furthermore, the spatial profile of the calcium event along the imaged dendrite also appeared to change during development (n = 97). Before hearing onset, the largest calcium responses were almost always observed at distal locations (P10 = 61.2 µm). However, from P15 onwards, calcium signals peaked at more proximal locations (P15 = 32.3 µm) (one-way ANOVA with Tukey's Multiple Comparison Test $p<0.05$ for P11, P13 vs P17 and P11, P13 vs P18; significance not shown on graph for clarity) (Figure 5E - F).

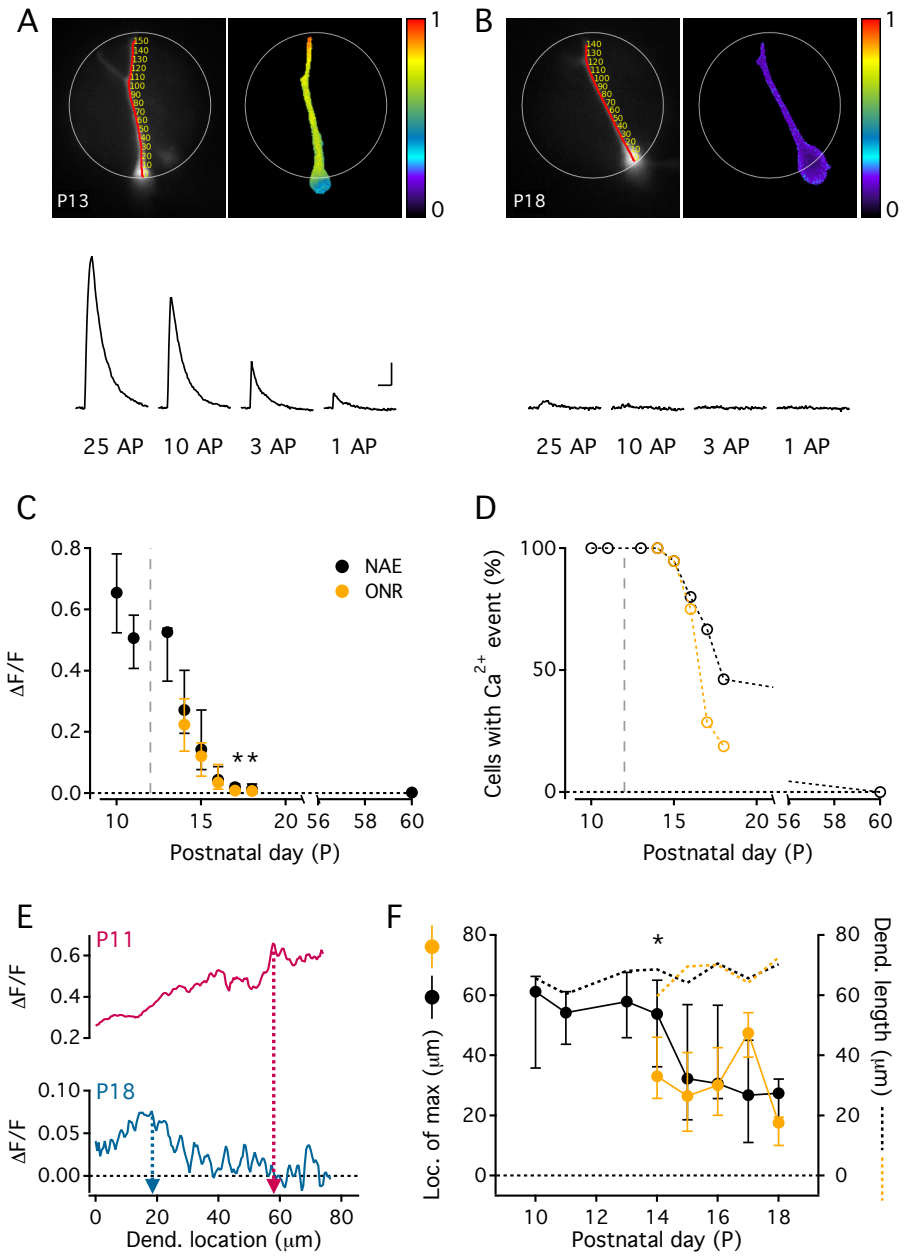

Figure 5. **A**. Dendritic calcium transient evoked by a train of 25 APs at 10% above the current threshold in a P13 MSO neuron. *Top*: Dendrite filled with OGB-1 as visualised during recordings (*left*) and colour mapped for ΔF/F (*right*). Numbers in the left panel denote the location along the dendrite (pixels). The white circle shows the location of the circular field stop. *Bottom*: Dendritic calcium transients (ΔF/F) in response to trains of 25, 10 and 3 APs (100 Hz) and in response to 1 AP in the same P13 neuron. The calcium signal was averaged over the length of the visible dendrite. Scale bar: 500 ms, 0.1 ΔF/F. **B**. Same as in A in a P18 neuron. Note that a calcium transient could only be evoked in response to a train of 25 APs. **C**. Development of the dendritic calcium influx evoked by 25 APs at 10% above the current threshold in gerbils raised in a NAE (black symbols) and in gerbils raised in OWN (yellow symbols). The dashed line represents hearing onset (P12). **D**. Percentage of cells that display a dendritic calcium event in response to 25 APs throughout late postnatal development. NAE: black symbols; OWN: yellow symbols. The dashed line represents hearing onset (P12). **E**. Amplitude of dendritic calcium transients (ΔF/F) along the dendrite of a P11 (*top*, pink) and P18 (*bottom*, blue) neuron (NAE) in response to 25 APs. In both cases, dendritic location '0 μm' represents the soma. Dashed arrows denote the dendritic location corresponding to the maximal ΔF/F value. **F**. Developmental change in the dendritic location of the maximum ΔF/F in response to 25 APs in cells that displayed a calcium event. Dendritic location '0 μm' represents the soma. The dashed lines represent the median dendritic lengths of the dataset. NAE: black symbols; OWN: yellow symbols. All filled symbols represent the median and the error bars represent the first and third quartiles. Significance at the $p < 0.05$ level is denoted with an asterisk.

Importantly, while Figure 5E shows an example of a P18 cell with a larger ΔF/F in proximal regions, many P15 - P18 cells displayed calcium signals which varied only little along the dendrite (not shown). Thus, the developmental change in peak ΔF/F may reflect a loss of distal calcium signals rather than a distal to proximal shift of calcium responses. Our finding that larger calcium signals were located distally before P15 did not simply result from an age-dependent difference in the dendritic length of neurons (Figure 5F, dotted lines). It also did not appear to be due to a smaller volume of distal dendritic branches. Dividing the change in calcium influx by the amplitude of a structural marker (Alexa 594) yielded a similar developmental profile (not shown). Finally, raising gerbils in OWN (n = 56) resulted in a more somatically biased peak ΔF/F at P14 (P14 NAE: 53.77 µm, P14 OWN: 33.05 µm, Unpaired T Test p = 0.033) (Figure 5F, yellow symbols). In summary, large global calcium signals which increased with distance from the soma could be evoked through VGCCs in MSO dendrites before hearing onset. Only two days after hearing onset, however, dendritic calcium signals decreased rapidly and could no longer be evoked at P60. Noise exposure appeared to accelerate the downregulation of calcium signals through VGCCs, as seen by a smaller amplitude of calcium signals and a decrease in the fraction of cells that could elicit a calcium event.

4. Discussion

How does activity guide the establishment of precise, functional circuits during critical phases of development? In the auditory brainstem, the basic innervation and tonotopy of excitatory and inhibitory inputs are established well before the onset of sound evoked activity (Kandler and Friauf, 1993; Kil et al., 1995). While many functional and structural refinements take place before hearing onset (Sanes and Friauf, 2000; Sanes, 1993; Kim and Kandler, 2003; Hoffpauir et al., 2010; Case et al., 2011), they continue in an activity-dependent manner after hearing onset (Sanes and Siverls, 1991; Sanes, Song, et al., 1992; Sanes, Markowitz, et al., 1992; Magnusson et al., 2005; Kapfer et al., 2002; Werthat et al., 2008; Kandler, Clause, et al., 2009). Calcium is involved in many forms of activity-dependent refinements of excitatory and inhibitory circuits (Malenka and Bear, 2004). Here, we show that large, global dendritic calcium signals through VGCCs can be reliably elicited by somatic APs in MSO neurons before and at hearing onset. Shortly after hearing onset, however, dendritic calcium signals decrease markedly in amplitude until they can only be evoked in a fraction of cells at P18, and are completely absent at P60. The loss of dendritic calcium signals through VGCCs was accompanied by a drastic decrease in AP size and width, as well as a considerable acceleration of voltage signalling. Furthermore, the whole-cell calcium current decreased over the same developmental period, and a low voltage-activated T-Type current present before hearing

onset was rapidly downregulated by P15. Overall, these findings suggest the existence of a short time window after hearing onset for sensory-driven, calcium-dependent circuit refinements.

The rapid loss of dendritic calcium signals from P14 onwards is consistent with a strong attenuation of APs as they backpropagate into the soma and dendrites of MSO neurons, in part due to a rapid increase in the expression of low voltage-activated potassium channels (Scott, Mathews, et al., 2005; Scott, Hage, et al., 2007). Before P14, however, large global dendritic calcium signals could be elicited reliably even in response to a single AP, suggesting APs backpropagate effectively at these stages (see Winters and Golding (2017)). In pyramidal and cartwheel cells of the dorsal cochlear nucleus of P10 - P18 rats, somatic APs generate dendritic calcium responses through VGCCs which differentially require the activation of Na^+ channels (Molitor and Manis, 2003). Whether the dendritic calcium responses before hearing onset described here depend on the active backpropagation of Na^+ spikes remains to be tested experimentally. At P60 somatic APs never elicited a calcium event through VGCCs at the soma or dendrite. Although a calcium current is still present, it is unlikely to be activated by the small somatic APs that elicit a depolarisation of only $\sim$25 mV from rest. However, VGCCs may still contribute to calcium entry following sufficiently large local dendritic depolarisations evoked by synaptic activity. The inability of somatic APs to elicit calcium entry through VGCCs at mature stages may serve to limit temporal distortions during synaptic integration.

4.1 Role of calcium signalling in the activity-dependent refinement of brainstem circuits

Large calcium responses have also been observed in the lateral superior olive (LSO) early in development. Suprathreshold stimulation of neonatal MNTB - LSO synapses generates global calcium responses which are dependent on the backpropagation of APs (Kullmann and Kandler, 2008). In turn, stimulation of glutamatergic afferents to neonatal LSO neurons evokes calcium responses through a differential activation of ionotropic and metabotropic glutamate receptors depending on the stimulation pattern and amplitude (Ene, 2003). These robust calcium responses parallel an early phase of growth of LSO dendrites and MNTB arbors (Sanes and Friauf, 2000) as well as functional synaptic silencing and strengthening (Kim and Kandler, 2003). Interestingly, a form of long-term depression (LTD) at the gerbil inhibitory MNTB-LSO synapse was found to be calcium-dependent and, importantly, restricted to a specific developmental period (Kotak and Sanes, 2000). The progressive loss of dendritic calcium signals in MSO neurons described here may therefore form the basis of a temporally restricted form of activity-dependent elimination and/or stabilisation of synaptic inputs, a phase rapidly followed by the implementation of mechanisms

that promote synaptic stability (Lyckman et al., 2008). In support of a role of VGCCs in activity-dependent refinements, global dendritic calcium responses driven by backpropagating APs are a retrograde marker of postsynaptic activity, which together with closely timed synaptic activity can lead to synaptic strengthening or elimination (Zhang et al., 1998; Dan and Poo, 2006; Feldman, 2012). The gradual loss of calcium from distal dendritic locations, in particular, might be an important mechanism mediating the appropriate spatial reorganisation of inputs to the MSO. In parallel to the loss of AP-evoked calcium through VGCCs, large synaptically-evoked calcium signals through AMPA and NMDA receptors are also downregulated shortly after hearing onset in MSO neurons (personal communication, Sarah Gleiss).

4.2 Development and pharmacology of the whole-cell calcium current

The whole-cell calcium current was strongly downregulated during development, further contributing to the progressively limited calcium signalling in MSO neurons. Postsynaptic voltage-dependent calcium currents were largely driven by P/Q- and L-Type channels, similar to that in the LSO of mice (Jurkovicova-Tarabova et al., 2012). L-Type channels are generally expressed in the somatodendritic compartment where they are involved in activity-dependent changes in gene transcription (Greer and Greenberg, 2008), and may thus play a role in activity-dependent circuit refinements. It will be important to assess the relative contribution of calcium channel subtypes at other developmental stages, particularly before hearing onset. A large low voltage-activated calcium current — presumably mediated by T-Type channels — was reliably elicited in P10 and P11 neurons. At these stages, it comprised $\sim$25% of the whole-cell calcium current, but was rapidly downregulated shortly after hearing onset. Interestingly, stimulating the inhibitory inputs to immature gerbil LSO neurons elicits prolonged IPSPs followed by a rebound depolarisation, possibly mediated by a low voltage-activated calcium current (Sanes, 1993). A similar developmental profile of a low threshold-activated calcium current was reported in acutely dissociated rat CA1 and CA3 cells (Thompson and Wong, 1991). In fact, in several types of neurons, low voltage-activated calcium channels are transiently expressed during embryonic stages and shortly after birth (Mynlieff and Beam, 1992; Gu and Spitzer, 1993; Chambard et al., 1999; Kirmse et al., 2005; Autret et al., 2005; Levic et al., 2007), where they regulate differentiation and neuronal growth (Spitzer et al., 2000; Lory et al., 2006).

Accumulating evidence also demonstrates an important role of T-Type channels in several forms of excitatory and inhibitory synaptic plasticity (Leresche and Lambert, 2016). For example, given their low voltage activation, T-Type channels can act synergistically with LGICs by contributing

to synaptic depolarisations mediated by AMPARs, thereby enhancing the activation of NMDARs and boosting calcium influx (Leresche and Lambert, 2016). In the visual cortex, a form of long-term potentiation (LTP) thought to mediate the experience-dependent potentiation of open eye responses following monocular deprivation depends on T-Type channels (Yoshimura et al., 2008). The amplitude of Ni^{2+}-sensitive T-Type currents ($Ca_v3.2$) peaks during the critical period before decreasing at adulthood, a process which is prevented by dark rearing (Horibe et al., 2014). A role of sensory experience in regulating the expresion of T-Type channels in the MSO is also possible, given their strong developmental downregulation around hearing onset, which occurs faster following noise exposure. In several brain regions, T-Type channels are expressed on distal dendrites, where they amplify distal synaptic inputs (Christie et al., 1995; Isomura et al., 2002; Crandall et al., 2010; Rudolph et al., 2015) and enhance the amplitude of backpropagating APs (Leresche and Lambert, 2016). Interestingly, AP-evoked calcium responses reported here were larger at distal dendritic locations between P10 and P14, but no longer from P15 onwards. This developmental profile is remarkably similar to the development of the low voltage-activated calcium current (lost from P15 onwards), hinting at a possible localisation of T-Type channels in distal dendrites. Further experiments are needed to assess the cellular localisation of T-Type channels in developing MSO neurons.

Finally, given that T-Type calcium channels require a hyperpolarisation to relieve steady-state inactivation (Cueni et al., 2009), they could constitute an interesting mechanism allowing inhibitory responses to modulate calcium signals. In support of this idea, dendritic calcium signals driven by APs in the nucleus laminaris of embryonic chicks double in amplitude when elicited from a more hyperpolarised membrane potential, reflecting the recruitment of a low-threshold calcium current (Blackmer et al., 2009). Given the voltage-dependent properties of T-Type channels, large calcium signals should preferentially occur when inhibition precedes a depolarisation provided by excitation or a backpropagating AP. Thus, at least until a few days after hearing onset, hyperpolarising inhibition to the MSO could harness second messenger systems normally evoked by excitation by interacting with T-Type channels. In turn, such an interaction may play a role in the refinement of inhibitory synapses (Kapfer et al., 2002).

4.3 Activity-dependent refinement of excitation and inhibition to the MSO

An important question in development is how different activity patterns drive the functional and structural reorganisation of neural circuits (Katz and Shatz, 1996). In the primary auditory cortex of rats, continuous moderate noise delays the development of mature frequency representation and

prolongs the critical period (Chang and Merzenich, 2003). Previous studies have demonstrated that exposure to omnidirectional white noise disrupts both a structural and a functional refinement of glycinergic inhibition in the gerbil MSO. First, omnidirectional white noise disrupts the normal rearrangement of glycinergic synapses to the soma of MSO neurons (Kapfer et al., 2002; Werthat et al., 2008). Second, the same stimulus prevents a developmental decrease in the size of evoked IPSCs and a decrease in the frequency of mIPSCs (Magnusson et al., 2005), and disrupts the development of mature ITD functions in the DNLL (Seidl, 2005). Taken together, these findings suggest that omnidirectional white noise disrupts a phase of synapse elimination of glycinergic inputs around hearing onset, maintaining glycinergic synapses in an immature functional and structural state. In contrast, we show that continuous noise exposure accelerates the maturation of calcium signalling in MSO neurons. While the amplitude of AP-evoked calcium responses did not change markedly, the proportion of cells without a calcium event was larger following noise exposure (see P17 and P18). Alongside these changes, excitatory transmission also appears to mature earlier following exposure to omnidirectional white noise, as shown by a larger size of single inputs and smaller synaptically-evoked calcium signals already at P14 (personal communication, Sarah Gleiss). Thus, while omnidirectional white noise delays (or prevents) the refinement of glycinergic inputs to the soma, it appears to *accelerate* the development of calcium signalling and the maturation of excitation. Our experiments raise the intriguing possibility that excitation and inhibition to the MSO may be differentially sensitive to different features of acoustic stimuli. Exposure to omnidirectional white noise not only masks binaural cues used for sound localisation, but also increases the overall level of acoustic activity, providing a higher drive to the auditory system. Specifically, while the refinement of inhibition is disrupted in the absence of relevant binaural cues (Kapfer et al., 2002), the high overall level of activity produced by noise exposure may selectively accelerate the development of excitation, leading to the faster development of calcium responses observed here. To dissect the influence of these stimulus parameters, these experiments could be repeated in an environment which disrupts binaural cues while decreasing the overall level of activity i.e. cochlear ablation or middle ear bone removal. If this procedure now delays the development of calcium signalling, it would favour the hypothesis that calcium signalling is sensitive to the overall level of acoustic activity. Manipulations of acoustic activity could be combined with immunohistochemistry against calcium-binding proteins to reveal and/or confirm changes in important phases of calcium signalling and homeostasis.

Recently, a form of long-term potentiation of glycinergic inputs (iLTP) was found in the MSO of gerbils. Interestingly, this form of iLTP is calcium- and NMDAR-dependent, and continues with diminishing efficacy up until the end of the third postnatal week (Winters and Golding, 2017).

While inhibition to the MSO may modulate calcium signals by interacting with T-Type channels, the refinement of glycinergic synapses may still depend on calcium-dependent signalling pathways recruited by excitation. Thus, an earlier loss of, or delay in calcium signalling may interfere with the elimination or stabilisation of synaptic inputs. An intriguing question yet to be answered is whether excitation and inhibition to the MSO refine in parallel and whether these processes share common cellular mechanisms.

Acknowledgements

Our interpretation of these results also derives from experiments on the development of synaptically-evoked dendritic calcium signals, performed by Sarah Gleiss. We thank Benedikt Grothe for valuable discussions and suggestions.

References

Ammer, J. J., Grothe, B., and Felmy, F. (2012). "Late postnatal development of intrinsic and synaptic properties promotes fast and precise signaling in the dorsal nucleus of the lateral lemniscus." In: *Journal of Neurophysiology* 107.4, pp. 1172–1185.

Autret, L., Mechaly, I., Scamps, F., Valmier, J., Lory, P., and Desmadryl, G. (2005). "The involvement of Ca v3.2/α 1HT-type calcium channels in excitability of mouse embryonic primary vestibular neurones". In: *The Journal of physiology* 567.1, pp. 67–78.

Bazwinsky-Wutschke, I., Härtig, W., Kretzschmar, R., and Rübsamen, R. (2016). "Differential morphology of the superior olivary complex of Meriones unguiculatus and Monodelphis domestica revealed by calcium-binding proteins". In: *Brain Structure and Function* 221.9, pp. 4505–4523.

Berridge, M. J. (1998). "Neuronal calcium signaling." In: *Neuron* 21.1, pp. 13–26.

Berridge, M. J., Bootman, M. D., and Roderick, H. L. (2003). "Calcium signalling: dynamics, homeostasis and remodelling". In: *Nature reviews. Molecular cell biology* 4.7, pp. 517–529.

Blackmer, T., Kuo, S. P., Bender, K. J., Apostolides, P. F., and Trussell, L. O. (2009). "Dendritic calcium channels and their activation by synaptic signals in auditory coincidence detector neurons." In: *Journal of Neurophysiology* 102.2, pp. 1218–1226.

Case, D. T., Zhao, X., and Gillespie, D. C. (2011). "Functional refinement in the projection from ventral cochlear nucleus to lateral superior olive precedes hearing onset in rat." In: *PLoS ONE* 6.6, e20756.

Chambard, J. M., Chabbert, C., Sans, A., and Desmadryl, G. (1999). “Developmental changes in low and high voltage-activated calcium currents in acutely isolated mouse vestibular neurons.” In: *The Journal of physiology* 518.Pt 1, pp. 141–149.

Chang, E. F. and Merzenich, M. M. (2003). “Environmental noise retards auditory cortical development.” In: *Science* 300.5618, pp. 498–502.

Chirila, F. V., Rowland, K. C., Thompson, J. M., and Spirou, G. A. (2007). “Development of gerbil medial superior olive: integration of temporally delayed excitation and inhibition at physiological temperature”. In: *The Journal of physiology* 584.1, pp. 167–190.

Christie, B. R., Eliot, L. S., Ito, K., Miyakawa, H., and Johnston, D. (1995). “Different Ca^{2+} channels in soma and dendrites of hippocampal pyramidal neurons mediate spike-induced Ca^{2+} influx.” In: *Journal of Neurophysiology* 73.6, pp. 2553–2557.

Crandall, S. R., Govindaiah, G., and Cox, C. L. (2010). “Low-Threshold Ca^{2+} Current Amplifies Distal Dendritic Signaling in Thalamic Reticular Neurons”. In: *Journal of Neuroscience* 30.46, pp. 15419–15429.

Cueni, L., Canepari, M., Adelman, J. P., and Lüthi, A. (2009). “Ca^{2+} signaling by T-type Ca^{2+} channels in neurons.” In: *Pflügers Archiv : European journal of physiology* 457.5, pp. 1161–1172.

Dan, Y. and Poo, M.-m. (2006). “Spike timing-dependent plasticity: from synapse to perception.” In: *Physiological Reviews* 86.3, pp. 1033–1048.

Ebbers, L. et al. (2015). “L-type Calcium Channel Ca v1.2 Is Required for Maintenance of Auditory Brainstem Nuclei”. In: *Journal of Biological Chemistry* 290.39, pp. 23692–23710.

Ene, F. A. (2003). “Glutamatergic Calcium Responses in the Developing Lateral Superior Olive: Receptor Types and Their Specific Activation by Synaptic Activity Patterns”. In: *Journal of Neurophysiology* 90.4, pp. 2581–2591.

Feldman, D. E. (2012). “The Spike-Timing Dependence of Plasticity”. In: *Neuron* 75.4, pp. 556–571.

Felmy, F. and Schneggenburger, R. (2004). “Developmental expression of the Ca2+-binding proteins calretinin and parvalbumin at the calyx of Held of rats and mice.” In: *European Journal of Neuroscience* 20.6, pp. 1473–1482.

Franklin, J. L. and Johnson, E. M. (1992). “Suppression of programmed neuronal death by sustained elevation of cytoplasmic calcium.” In: *Trends in neurosciences* 15.12, pp. 501–508.

Franzen, D. L., Gleiss, S. A., Berger, C., Kümpfbeck, F. S., Ammer, J. J., and Felmy, F. (2015). "Development and modulation of intrinsic membrane properties control the temporal precision of auditory brain stem neurons." In: *Journal of Neurophysiology* 113.2, pp. 524–536.

Friauf, E. (1993). "Transient appearance of calbindin-D28k-positive neurons in the superior olivary complex of developing rats". In: *Journal of Comparative Neurology* 334.1, pp. 59–74.

Gallin, W. J. and Greenberg, M. E. (1995). "Calcium regulation of gene expression in neurons: the mode of entry matters." In: *Current Opinion in Neurobiology* 5.3, pp. 367–374.

Greer, P. L. and Greenberg, M. E. (2008). "From Synapse to Nucleus: Calcium-Dependent Gene Transcription in the Control of Synapse Development and Function". In: *Neuron* 59.6, pp. 846–860.

Grothe, B., Pecka, M., and McAlpine, D. (2010). "Mechanisms of Sound Localization in Mammals". In: *Physiological Reviews* 90.3, pp. 983–1012.

Grothe, B. (2003). "Sensory systems: New roles for synaptic inhibition in sound localization". In: *Nature Reviews Neuroscience* 4.7, pp. 540–550.

Gu, X. and Spitzer, N. C. (1993). "Low-threshold Ca2+ current and its role in spontaneous elevations of intracellular Ca2+ in developing Xenopus neurons." In: *Journal of Neuroscience* 13.11, pp. 4936–4948.

Hassfurth, B., Grothe, B., and Koch, U. (2010). "The Mammalian Interaural Time Difference Detection Circuit Is Differentially Controlled by GABAB Receptors during Development". In: *The Journal of neuroscience : the official journal of the Society for Neuroscience* 30.29, pp. 9715–9727.

Hensch, T. K. (2005). "Critical period plasticity in local cortical circuits". In: *Nature Reviews Neuroscience* 6.11, pp. 877–888.

Hirtz, J. J., Boesen, M., et al. (2011). "Cav1.3 calcium channels are required for normal development of the auditory brainstem." In: *The Journal of neuroscience : the official journal of the Society for Neuroscience* 31.22, pp. 8280–8294.

Hirtz, J. J., Braun, N., Griesemer, D., Hannes, C., Janz, K., Löhrke, S., Müller, B., and Friauf, E. (2012). "Synaptic refinement of an inhibitory topographic map in the auditory brainstem requires functional Cav1.3 calcium channels." In: *The Journal of neuroscience : the official journal of the Society for Neuroscience* 32.42, pp. 14602–14616.

Hoffpauir, B. K., Kolson, D. R., Mathers, P. H., and Spirou, G. A. (2010). “Maturation of synaptic partners: functional phenotype and synaptic organization tuned in synchrony”. In: *The Journal of physiology* 588.22, pp. 4365–4385.

Horibe, S., Tarusawa, E., Komatsu, Y., and Yoshimura, Y. (2014). “Ni^{2+}-sensitive T-type Ca^{2+} channel currents are regulated in parallel with synaptic and visual response plasticity in visual cortex”. In: *Neuroscience research* 87, pp. 33–39.

Isomura, Y., Fujiwara-Tsukamoto, Y., Imanishi, M., Nambu, A., and Takada, M. (2002). “Distance-dependent Ni(2+)-sensitivity of synaptic plasticity in apical dendrites of hippocampal CA1 pyramidal cells.” In: *Journal of Neurophysiology* 87.2, pp. 1169–1174.

Iwasaki, S., Momiyama, A., Uchitel, O. D., and Takahashi, T. (2000). “Developmental changes in calcium channel types mediating central synaptic transmission.” In: *The Journal of neuroscience : the official journal of the Society for Neuroscience* 20.1, pp. 59–65.

Iwasaki, S. and Takahashi, T. (1998). “Developmental changes in calcium channel types mediating synaptic transmission in rat auditory brainstem”. In: *The Journal of physiology* 509.2, pp. 419–423.

Jonas, P. and Burnashev, N. (1995). “Molecular mechanisms controlling calcium entry through AMPA-type glutamate receptor channels”. In: *Neuron* 15.5, pp. 987–990.

Jurkovicova-Tarabova, B., Griesemer, D., Pirone, A., Sinnegger-Brauns, M. J., Striessnig, J., and Friauf, E. (2012). “Repertoire of high voltage-activated Ca^{2+} channels in the lateral superior olive: functional analysis in wild-type, Cav1.3-/-, and Cav1.2DHP-/- mice”. In: *Journal of Neurophysiology* 108.2, pp. 365–379.

Kandler, K. and Friauf, E. (1993). “Pre- and postnatal development of efferent connections of the cochlear nucleus in the rat.” In: *The Journal of Comparative Neurology* 328.2, pp. 161–184.

Kandler, K., Clause, A., and Noh, J. (2009). “Tonotopic reorganization of developing auditory brainstem circuits”. In: *Nature Neuroscience* 12.6, pp. 711–717.

Kapfer, C., Seidl, A. H., Schweizer, H., and Grothe, B. (2002). “Experience-dependent refinement of inhibitory inputs to auditory coincidence-detector neurons”. In: *Nature Neuroscience* 5.3, pp. 247–253.

Katz, L. C. and Shatz, C. J. (1996). “Synaptic activity and the construction of cortical circuits.” In: *Science* 274.5290, pp. 1133–1138.

Khurana, S., Liu, Z., Lewis, A. S., Rosa, K., Chetkovich, D., and Golding, N. L. (2012). "An essential role for modulation of hyperpolarization-activated current in the development of binaural temporal precision." In: *The Journal of neuroscience : the official journal of the Society for Neuroscience* 32.8, pp. 2814–2823.

Kil, J., Kageyama, G. H., Semple, M. N., and Kitzes, L. M. (1995). "Development of ventral cochlear nucleus projections to the superior olivary complex in gerbil." In: *The Journal of Comparative Neurology* 353.3, pp. 317–340.

Kim, G. and Kandler, K. (2003). "Elimination and strengthening of glycinergic/GABAergic connections during tonotopic map formation". In: *Nature Neuroscience* 6.3, pp. 282–290.

Kirmse, K., Grantyn, R., and Kirischuk, S. (2005). "Developmental downregulation of low-voltage-activated Ca 2+channels in Cajal-Retzius cells of the mouse visual cortex". In: *European Journal of Neuroscience* 21.12, pp. 3269–3276.

Koike-Tani, M., Saitoh, N., and Takahashi, T. (2005). "Mechanisms underlying developmental speeding in AMPA-EPSC decay time at the calyx of Held." In: *The Journal of neuroscience : the official journal of the Society for Neuroscience* 25.1, pp. 199–207.

Kotak, V. C. and Sanes, D. H. (2000). "Long-lasting inhibitory synaptic depression is age- and calcium-dependent." In: *The Journal of neuroscience : the official journal of the Society for Neuroscience* 20.15, pp. 5820–5826.

Kullmann, P. H. M. and Kandler, K. (2008). "Dendritic Ca^{2+} responses in neonatal lateral superior olive neurons elicited by glycinergic/GABAergic synapses and action potentials". In: *Neuroscience* 154.1, pp. 338–345.

Leresche, N. and Lambert, R. C. (2016). "T-type calcium channels in synaptic plasticity." In: *Channels*, pp. 1–19.

Levic, S., Nie, L., Tuteja, D., Harvey, M., Sokolowski, B. H. A., and Yamoah, E. N. (2007). "Development and regeneration of hair cells share common functional features." In: *Proceedings of the National Academy of Sciences of the United States of America* 104.48, pp. 19108–19113.

Lohmann, C., Ilic, V., and Friauf, E. (1998). "Development of a topographically organized auditory network in slice culture is calcium dependent." In: *Journal of neurobiology* 34.2, pp. 97–112.

Lohmann, C. and Friauf, E. (1996). "Distribution of the calcium-binding proteins parvalbumin and calretinin in the auditory brainstem of adult and developing rats". In: *Journal of Comparative Neurology* 367.1, pp. 90–109.

Lory, P., Bidaud, I., and Chemin, J. (2006). “T-type calcium channels in differentiation and proliferation.” In: *Cell calcium* 40.2, pp. 135–146.

Lyckman, A. W., Horng, S., Leamey, C. A., Tropea, D., Watakabe, A., Van Wart, A., McCurry, C., Yamamori, T., and Sur, M. (2008). “Gene expression patterns in visual cortex during the critical period: synaptic stabilization and reversal by visual deprivation.” In: *Proceedings of the National Academy of Sciences of the United States of America* 105.27, pp. 9409–9414.

Magee, J. C. and Johnston, D. (1997). “A synaptically controlled, associative signal for Hebbian plasticity in hippocampal neurons.” In: *Science* 275.5297, pp. 209–213.

Magnusson, A. K., Kapfer, C., Grothe, B., and Koch, U. (2005). “Maturation of glycinergic inhibition in the gerbil medial superior olive after hearing onset.” In: *The Journal of physiology* 568.Pt 2, pp. 497–512.

Malenka, R. C. and Bear, M. F. (2004). “LTP and LTD: an embarrassment of riches.” In: *Neuron* 44.1, pp. 5–21.

Markram, H. (1997). “Regulation of Synaptic Efficacy by Coincidence of Postsynaptic APs and EPSPs”. In: *Science* 275.5297, pp. 213–215.

Markram, H., Helm, P. J., and Sakmann, B. (1995). “Dendritic calcium transients evoked by single back-propagating action potentials in rat neocortical pyramidal neurons.” In: *The Journal of physiology* 485.1, pp. 1–20.

Michaelsen, K. and Lohmann, C. (2010). “Calcium dynamics at developing synapses: mechanisms and functions”. In: *European Journal of Neuroscience* 32.2, pp. 218–223.

Molitor, S. C. and Manis, P. B. (2003). “Dendritic Ca^{2+} transients evoked by action potentials in rat dorsal cochlear nucleus pyramidal and cartwheel neurons.” In: *Journal of Neurophysiology* 89.4, pp. 2225–2237.

Mynlieff, M. and Beam, K. G. (1992). “Developmental expression of voltage-dependent calcium currents in identified mouse motoneurons.” In: *Developmental biology* 152.2, pp. 407–410.

Nakamura, Y. and Takahashi, T. (2007). “Developmental changes in potassium currents at the rat calyx of Held presynaptic terminal”. In: *The Journal of physiology* 581.3, pp. 1101–1112.

Rudolph, S., Hull, C., and Regehr, W. G. (2015). “Active Dendrites and Differential Distribution of Calcium Channels Enable Functional Compartmentalization of Golgi Cells.” In: *The Journal of neuroscience : the official journal of the Society for Neuroscience* 35.47, pp. 15492–15504.

Sanes, D. H. (1993). “The development of synaptic function and integration in the central auditory system.” In: *The Journal of neuroscience : the official journal of the Society for Neuroscience* 13.6, pp. 2627–2637.

Sanes, D. H. and Friauf, E. (2000). “Development and influence of inhibition in the lateral superior olivary nucleus.” In: *Hearing research* 147.1-2, pp. 46–58.

Sanes, D. H., Markowitz, S., Bernstein, J., and Wardlow, J. (1992). “The influence of inhibitory afferents on the development of postsynaptic dendritic arbors.” In: *The Journal of Comparative Neurology* 321.4, pp. 637–644.

Sanes, D. H. and Siverls, V. (1991). “Development and specificity of inhibitory terminal arborizations in the central nervous system.” In: *Journal of neurobiology* 22.8, pp. 837–854.

Sanes, D. H., Song, J., and Tyson, J. (1992). “Refinement of dendritic arbors along the tonotopic axis of the gerbil lateral superior olive.” In: *Brain research. Developmental brain research* 67.1, pp. 47–55.

Scott, L. L., Hage, T. A., and Golding, N. L. (2007). “Weak action potential backpropagation is associated with high-frequency axonal firing capability in principal neurons of the gerbil medial superior olive”. In: *The Journal of physiology* 583.2, pp. 647–661.

Scott, L. L., Mathews, P. J., and Golding, N. L. (2005). “Posthearing developmental refinement of temporal processing in principal neurons of the medial superior olive.” In: *The Journal of neuroscience : the official journal of the Society for Neuroscience* 25.35, pp. 7887–7895.

Seidl, A. H. (2005). “Development of Sound Localization Mechanisms in the Mongolian Gerbil Is Shaped by Early Acoustic Experience”. In: *Journal of Neurophysiology* 94.2, pp. 1028–1036.

Simms, B. A. and Zamponi, G. W. (2014). “Neuronal Voltage-Gated Calcium Channels: Structure, Function, and Dysfunction”. In: *Neuron* 82.1, pp. 24–45.

Smith, A. J., Owens, S., and Forsythe, I. D. (2000). “Characterisation of inhibitory and excitatory postsynaptic currents of the rat medial superior olive.” In: *The Journal of physiology* 529 Pt 3, pp. 681–698.

Spitzer, N. C., Lautermilch, N. J., Smith, R. D., and Gomez, T. M. (2000). “Coding of neuronal differentiation by calcium transients”. In: *BioEssays* 22.9, pp. 811–817.

Steinert, J. R., Postlethwaite, M., Jordan, M. D., Chernova, T., Robinson, S. W., and Forsythe, I. D. (2010). “NMDAR-mediated EPSCs are maintained and accelerate in time course during

maturation of mouse and rat auditory brainstem in vitro". In: *The Journal of physiology* 588.3, pp. 447–463.

Taschenberger, H. and von Gersdorff, H. (2000). "Fine-tuning an auditory synapse for speed and fidelity: developmental changes in presynaptic waveform, EPSC kinetics, and synaptic plasticity." In: *The Journal of neuroscience : the official journal of the Society for Neuroscience* 20.24, pp. 9162–9173.

Thompson, S. M. and Wong, R. K. (1991). "Development of calcium current subtypes in isolated rat hippocampal pyramidal cells." In: *The Journal of physiology* 439, pp. 671–689.

Tong, H., Steinert, J. R., Robinson, S. W., Chernova, T., Read, D. J., Oliver, D. L., and Forsythe, I. D. (2010). "Regulation of Kv channel expression and neuronal excitability in rat medial nucleus of the trapezoid body maintained in organotypic culture". In: *The Journal of physiology* 588.9, pp. 1451–1468.

Werthat, F., Alexandrova, O., Grothe, B., and Koch, U. (2008). "Experience-dependent refinement of the inhibitory axons projecting to the medial superior olive". In: *Developmental Neurobiology* 68.13, pp. 1454–1462.

Winters, B. D. and Golding, N. L. (2017). "Developmentally Restricted Long-term Potentiation of Glycinergic Inhibition onto Neurons of the Medial Superior Olive". In: *Poster Session (PS 740), Association for Research in Otolaryngology*.

Withington-Wray, D. J., Binns, K. E., Dhanjal, S. S., Brickley, S. G., and Keating, M. J. (1990). "The Maturation of the Superior Collicular Map of Auditory Space in the Guinea Pig is Disrupted by Developmental Auditory Deprivation." In: *European Journal of Neuroscience* 2.8, pp. 693–703.

Yoshimura, Y., Inaba, M., Yamada, K., Kurotani, T., Begum, T., Reza, F., Maruyama, T., and Komatsu, Y. (2008). "Involvement of T-type Ca 2+channels in the potentiation of synaptic and visual responses during the critical period in rat visual cortex". In: *European Journal of Neuroscience* 28.4, pp. 730–743.

Zhang, L. I., Tao, H. W., Holt, C. E., Harris, W. A., and Poo, M. (1998). "A critical window for cooperation and competition among developing retinotectal synapses." In: *Nature* 395.6697, pp. 37–44.

4

DISCUSSION

4.1 CALCIUM-DEPENDENT REFINEMENTS IN THE DEVELOPING GERBIL MSO

Calcium is essential for the normal development of the auditory brainstem. Given its role as an important second messenger in neurons, calcium is also involved in many forms of activity-dependent circuit refinements. In neurons, functional and structural refinements are largely restricted to a critical period early in development marked by a heightened sensitivity to changes in sensory experience (Hensch, 2005). While mature circuits retain a certain degree of plasticity, changes in sensory experience no longer elicit such widespread changes in functional and structural organisation. For example, while exposure to omnidirectional white noise disrupts the ITD tuning of juvenile DNLL neurons, the same procedure has little or no effect in mature DNLL neurons (Seidl, 2005). Therefore, cellular mechanisms underlying circuit refinements are likely subject to developmental regulation. In the MSO, we found that large calcium signals reliably elicited at pre-hearing stages are rapidly downregulated within a week after the onset of hearing. At mature stages, calcium signals can no longer be elicited through VGCCs, but can to a small extent still be recruited by calcium-permeable AMPARs (personal communication, Sarah Gleiss). Thus, the developmental profile of calcium signalling in MSO neurons supports circuit refinements until approximately a week after hearing onset. In gerbils, glycinergic synapses undergo an activity-dependent structural and functional refinement during this developmental period, as shown by the rearrangement of glycinergic synapses to the soma (Kapfer et al., 2002; Werthat et al., 2008) and changes in inhibitory transmission (Magnusson et al., 2005).

4.1.1 *How does inhibition recruit calcium during development?*

While glutamatergic synapses can readily raise intracellular calcium through LGICs and VGCCs, it is less clear how inhibitory synapses recruit signalling pathways for refinement. In the auditory brainstem, the MNTB–LSO pathway has provided much insight into the cellular mechanisms underlying the activity-dependent refinement of inhibitory synapses. During the first postnatal week, synaptic connections are functionally eliminated and the remaining connections are strengthened (Kim and Kandler, 2003). After hearing onset, MNTB axons undergo a phase of structural pruning (Sanes and Siverls, 1991). These processes are separated by a week, reflecting the availability of distinct sets of

cellular mechanisms. As in many brain regions across different species, immature GABAergic/glycinergic synapses in the LSO are depolarising due to a high intracellular chloride concentration mediated by a delayed function of the K–Cl cotransporter (KCC2). After the first postnatal week, the activity of KCC2 gradually increases and GABA/glycinergic responses are hyperpolarising (rats: Kandler and Friauf (1995), Ehrlich et al. (1999), Kakazu et al. (1999), Balakrishnan et al. (2003), and Löhrke et al. (2005) (for a general review, see Ben-Ari (2002)). As a result, immature inhibitory synapses can evoke global calcium responses through VGCCs and even elicit APs (Kullmann and Kandler, 2001; Kullmann and Kandler, 2008). In the LSO, depolarising inhibitory responses parallel the phase of functional refinement (Kullmann and Kandler, 2001; Kullmann et al., 2002; Kullmann and Kandler, 2008). In turn, the phase of axonal pruning — the retraction of contact sites on terminals — occurs when inhibitory responses are hyperpolarising (Sanes and Friauf, 2000).

We found that a large T-Type calcium current is present in MSO neurons until a few days after hearing onset. Given that T-Type calcium channels require a prior hyperpolarisation to relieve steady-state inactivation (Cueni et al., 2009), they could constitute an interesting way for inhibition to influence calcium signals. This specific interaction could occur providing inhibition is hyperpolarising, and therefore requires an understanding of the development of inhibitory transmission in the gerbil MSO. Inhibitory responses switch from being depolarising to hyperpolarising in a sequential manner across different SOC nuclei (Löhrke et al., 2005) (for review see Milenkovic and Rübsamen (2011)). Importantly, most of these studies have been performed in rats. In gerbils, the depolarising to hyperpolarising switch has only been demonstrated in SBCs of the AVCN around P7 (Milenkovic et al., 2007; Witte et al., 2014). Although the transient depolarising effect of inhibitory circuits appears to be a conserved feature, discrepancies in its occurrence have been noted between species. For example, in rats the depolarising to hyperpolarising switch occurs uniformly throughout the LSO between P5–8 (Kandler and Friauf, 1995; Ehrlich et al., 1999; Löhrke et al., 2005). In gerbils, while the E_{IPSC} gradually shifts to more negative values until hearing onset in the medial (high-frequency) region of the LSO, it is already mature at P3 in the lateral (low-frequency) region (Kotak et al., 1998). Furthermore, intracellular recordings in the gerbil LSO display hyperpolarising synaptic potentials from P1 onwards (Sanes, 1993) (but see also Sanes and Friauf (2000)). While these discrepancies may result from experimental differences, they may also reflect important functional differences between species. Thus, the depolarising – hyperpolarising switch of inhibitory transmission may develop differently in gerbils, which are specialised for low-frequency hearing compared to rats. In support of this idea, the refinement of inhibitory synapses to the soma of MSO neurons of gerbils appears to be a specific adaptation for ITD encoding, as it does not occur in species not specialised for low-frequency hearing (Kapfer et al., 2002). A more detailed understanding of important transitions in inhibitory transmission in the gerbil MSO would shed light on the cellular mechanisms available to inhibition for activity-dependent refinement processes. If, as is suggested from the existing data, inhibitory responses are already hyperpolarising from an early stage in the gerbil MSO, they may recruit calcium and downstream signalling pathways by interacting with T-Type calcium channels. Consistent with this idea, MNTB-evoked hyperpolarisations in the LSO of neonatal gerbils elicit rebound depolarisations or APs (P1 – P8, 32°C), an effect that was speculated to involve a low-threshold calcium current (Sanes, 1993). Rebound depolarisations and APs following prolonged IPSPs have in fact been proposed as a cellular basis for the activity-dependent refinement of MNTB

arbors (Sanes and Takács, 1993). In the nucleus laminaris, the avian analogue of the mammalian MSO, AP-evoked calcium transients double in amplitude when elicited from -80 mV compared to from -60 mV, reflecting a recruitment of low-threshold calcium channels (Blackmer et al., 2009). While such responses would likely not occur given that GABAergic synapses in the nucleus laminaris are depolarising, these findings demonstrate that membrane hyperpolarisations can effectively modulate calcium levels.

Taken together, in the absence of depolarising inhibitory responses early in development, inhibition to the MSO could recruit calcium and downstream signalling pathways by providing the necessary hyperpolarisation to relieve T-Type channels from steady-state inactivation. T-Type calcium channels would therefore constitute an interesting mechanism allowing inhibition to trigger calcium-dependent refinements early in development. In this case, the relative timing of excitation and inhibition may be an important factor in determining the amplitude of calcium events.

4.1.2 *Role of T-Type channels in the developing MSO*

What is the functional role of the large but transient low-threshold calcium current in the MSO observed in our study? Some insight may be inferred from its developmental profile. The amplitude of the T-Type calcium current was very large before hearing onset (P10 – P11), and subsequently declined in amplitude until it was no longer detectable at P15. The presence of a transient low-threshold calcium current early in development has similarly been observed in other types of neurons, where low-threshold calcium channels generate spontaneous calcium elevations which correlate with neuronal growth, neuronal differentiation and changes in excitability (Gu and Spitzer, 1993; Chambard et al., 1999; Autret et al., 2005; Lory et al., 2006; Levic et al., 2007). In the chick, developing hair cells transiently exhibit a T-Type calcium current which promotes the emergence of spontaneous APs. Although they are gradually lost, T-Type currents transiently reappear in regenerating hair cells of adult chickens following hair cell loss (Levic et al., 2007), suggesting they may help reinstate immature processes in the mature system. Following unilateral cochlear ablation in immature gerbils, neurons in the contralateral LSO exhibit Ni^{+}-sensitive rebound depolarisations following membrane hyperpolarisation (P8 - P14, room temperature, compare to Sanes (1993)), suggesting a possible upregulation of a low-threshold calcium current (Kotak and Sanes, 1996). These effects were mostly observed before hearing onset, suggesting that altered spontaneous activity can influence low-threshold calcium currents. Therefore, the low voltage-activation of T-Type currents could serve to enhance the excitability of immature MSO neurons, facilitate calcium influx and promote neuronal growth, particularly before hearing onset when spontaneous activity is the main form of neuronal activity.

Given their ability to strongly influence calcium signals, T-Type channels have been implicated in various forms of synaptic plasticity (for review, see Leresche and Lambert (2016)). Thus, T-Type channels in the MSO may rather mediate changes in synaptic efficacy underlying circuit refinements, particularly at immature stages when synaptic kinetics are still relatively slow. Both

the excitatory and inhibitory projection to the LSO of rats undergo extensive functional refinement during the first postnatal week (Kim and Kandler, 2003; Case et al., 2011). In the gerbil MSO, while excitatory and inhibitory synaptic responses mature considerably after the onset of hearing (personal communication, Sarah Gleiss; Magnusson et al. (2005)), little is known about functional refinements before hearing onset. If such refinements take place in the MSO before hearing onset, T-Type channels may play a role. Alternatively, the large T-Type calcium current at pre-hearing stages may act as a stabilising signal, the absence of which shortly after hearing onset would allow circuit refinements to take place.

The rapid downregulation of the low-threshold calcium current around hearing onset in MSO neurons suggests that it may be regulated by the onset of acoustic experience. In layer 2/3 of the visual cortex, the development of a low-threshold calcium current has been found to correlate with periods of functional significance. Following monocular deprivation, responses from the non-deprived eye undergo a form of LTP mediated by $Ca_v3.2$ channels ($Ca_v3.2$ is a gene for T-Type channels) (Yoshimura et al., 2008). Both the amplitude of the $Ca_v3.2$ current and the expression of this form of LTP are largest during the critical period, before declining in adulthood. Interestingly, dark rearing prevents both the developmental decline of the $Ca_v3.2$ current and the expression of LTP (Horibe et al., 2014). In our experiments, exposure to omnidirectional white noise accelerated the development of both HVA and LVA calcium currents by approximately one day. Although subtle, these findings suggest that VGCCs in the MSO may be sensitive to changes in acoustic activity. If the T-Type current acts as a stabilising signal which prevents refinements before hearing onset, its earlier downregulation following omnidirectional white noise exposure would be expected to allow refinements to proceed earlier. Excitatory synaptic responses and calcium signals through LGICs appeared to mature faster following noise exposure (personal communication, Sarah Gleiss), suggesting this is a possibility. However, this does not appear to be the case for inhibition, as exposure to omnidirectional white noise was previously found to disrupt both the normal structural refinement of glycinergic synapses (Kapfer et al., 2002) and the development of glycinergic transmission (Magnusson et al., 2005).

While the amplitude of the T-Type calcium current decreases after hearing onset, it is still present at P13 and P14, suggesting a possible role in calcium-dependent refinements which depend on acoustic experience. For example, T-Type calcium channels may be involved in the experience-dependent pruning of axonal arbors or the reorganisation of synaptic inputs onto MSO neurons. In the MSO of gerbils, glycinergic synapses undergo an experience-dependent refinement during the first few days after hearing onset. As a result of this refinement, glycinergic synapses are eliminated from the distal dendrites and are confined to the soma and proximal dendrites of MSO neurons (Kapfer et al., 2002). This refinement is of functional importance as it appears to be a specific adaptation for ITD encoding (Kapfer et al., 2002). In mature MSO neurons, precisely timed inhibition tunes ITD sensitivity (Myoga et al., 2014) and blocking glycinergic inhibition *in vivo* shifts the maximal slope of ITD functions outside the physiological range (Brand et al., 2002; Pecka et al., 2008). Furthermore, the development of normal ITD tuning in the DNLL coincides with this structural refinement, and both are disrupted following omnidirectional white noise exposure (Kapfer et al., 2002; Seidl, 2005). Although correlative, these findings suggest that the structural refinement of glycinergic synapses may be necessary for appropriate ITD tuning. The refinement of glycinergic synapses to the

soma of MSO cells was speculated to involve a form of long-term plasticity which would strengthen appropriately timed synapses (Kapfer et al., 2002; Seidl, 2005). However, the mechanisms underlying such a refinement were unclear, particular given that inhibitory responses are likely hyperpolarising at that stage. The presence of a T-Type calcium current is very interesting in the context of this synaptic refinement. Given that T-Type calcium channels require a prior hyperpolarisation to relieve steady-state inactivation, a hyperpolarisation followed by a depolarisation should maximally activate T-Type channels, allowing a large influx of calcium. Thus, providing that synaptic kinetics are sufficiently slow with respect to the voltage-dependent kinetics of T-Type channels, the amplitude of calcium signals locally in the dendrite may depend on the relative timing between excitatory and inhibitory events. These local effects may interact further with backpropagating APs to elicit spike-timing dependent changes in synaptic efficacy (Magee and Johnston, 1997). A STDP based learning rule early in development has been put forward to explain the tuning asymmetry of MSO neurons. Specifically, the learning rule would strengthen inhibitory inputs activated before MSO spiking, and depress those active at the same time or after MSO spiking (Leibold and Hemmen, 2005). Here, by boosting calcium entry when a somatic hyperpolarisation is followed by a backpropagating AP, T-Type calcium channels could provide a mechanism by which inhibitory inputs active before MSO spiking are strengthened. The involvement of T-Type calcium channels would crucially depend on the kinetics of the voltage-dependent properties of T-Type calcium channels, which we did not assess in detail in the MSO. Moreover, it is unclear how such a mechanism could work *in vivo* upon high levels of spontaneous activity and when EPSPs and IPSPs display considerable temporal summation.

If T-Type calcium channels are involved in changes in synaptic efficacy early in development, their subcellular distribution is likely to reveal whether they participate in the strengthening or elimination of synaptic inputs. In hippocampal CA1 pyramidal cells where T-Type channels are localised in the distal dendrite, application of Ni^{+} (a blocker of R- and T-Type channels at low concentrations) inhibits LTP in a distance-dependent manner (Isomura et al., 2002). Thus, the cellular distribution of T-Type channels can regulate the ability to induce LTP/LTD along different areas of a dendrite. In our experiments, calcium signals peaked in the distal dendrite between P10 and P14, a phase coinciding with the presence of the low-threshold calcium current. Although correlative, these findings hint at a possible distal localisation of T-Type channels. A distal localisation of these channels would likely also increase space-clamp issues, particularly considering the concomittant developmental decrease in input resistance (Bar-Yehuda and Korngreen, 2008). Thus, the amplitude of the T-Type calcium current is possibly underestimated in our experiments, particularly at later developmental stages. Dual somatic and dendritic voltage-clamp experiments would be needed to estimate the contribution of T-Type channels more accurately as well as confirm their cellular distribution. A distal localisation of T-Type calcium channels may serve to amplify backpropagating voltage signals as in other brain regions (Christie et al., 1995; Magee and Johnston, 1995; Crandall et al., 2010; Rudolph et al., 2015).

Taken together, previous studies make a strong case for a role of T-Type calcium channels in activity-dependent refinements. First, T-Type channels are expressed in a developmentally restricted manner which can correlate with phases of functional importance (Lory et al., 2006; Cueni et al., 2009). Second, in several cell types these channels are expressed in specific cellular compartments, in

particular in distal dendrites. Third, T-Type channels are involved in different forms of excitatory and inhibitory LTP/LTD through interactions with LGICs (for review, see Leresche and Lambert (2016)). Finally, their activation and inactivation properties make them ideally suited to uniquely influence neuronal excitability (Cueni et al., 2009).

4.1.3 *Activity-dependent circuit refinements in the MSO*

Our findings demonstrate that calcium signalling is strongly developmentally regulated in MSO neurons. Before hearing onset, large global calcium events are elicited throughout the dendrite, with larger signals in the distal region. Shortly after hearing onset, VGCC-evoked calcium signals progressively decline in amplitude and can no longer be evoked at mature stages. Alongside these changes, the AMPAR-mediated component of the EPSC increases while the NMDAR component decreases, and synaptically-evoked calcium signals through both these receptors are downregulated shortly after hearing onset (personal communication, Sarah Gleiss). Recently, pairing high-frequency glycinergic and NMDAR-mediated PSPs with somatic APs was found to elicit LTP of glycinergic synapses (iLTP) in the MSO of gerbils (Winters and Golding, 2017). Specifically, this form of iLTP was found to depend on calcium entry through NMDARs, and decreased in efficacy during the third postnatal week (Winters and Golding, 2017). This developmental profile mirrors the decrease in AP size, the gradually limited AP backpropagation (Scott et al., 2007), and the loss of VGCC- and LGIC-evoked calcium signals. Interestingly, prolonged somatic depolarisations could rescue iLTP at later developmental stages (P30), suggesting that backpropagating APs may contribute to iLTP by relieving the Mg^{2+} block of NMDARs (Winters and Golding, 2017) or by facilitating the activation of VGCCs. The progressive decline in AP backpropagation during the week after hearing onset (Scott et al., 2007) may therefore preferentially activate proximal NMDARs. As a result, iLTP would more likely take place in the proximal and somatic region, following the rearrangement of glycinergic synapses (Kapfer et al., 2002). It remains to be tested how AMPARs — which can also provide the necessary depolarisation to relieve the Mg^{2+} block of NMDARs — would contribute to this refinement. The loss of distal VGCC-evoked calcium signals we observed could also potentially underlie a distal to proximal shift in the expression of iLTP. However, while VGCC-evoked calcium signals of a few P15 – P18 neurons peaked in more proximal regions, the majority of calcium signals at these stages were rather uniform along the dendrite. In fact, calcium signals seemed slightly smaller in the soma compared to the rest of the dendrite (not shown). During our VGCC imaging experiments, we only imaged a small portion of the soma as our aim was to image dendrites as far distally as possible. Future experiments could examine VGCC- and LGIC-evoked calcium signals in the soma in more detail. If the refinement of excitatory inputs to the MSO also relies on the coincidence of synaptic activity and bAPs, it would likely also be affected by the gradual decline in AP backpropagation. However, this does not appear to be the case, as excitatory synapses predominantly innervate the dendrites of MSO neurons. A learning rule underlying changes in synaptic efficacy of excitatory synapses remains to be tested.

In the findings above, calcium plays a role in the potentation of synapses. However, calcium can also mediate the elimination of synapses. In the gerbil LSO, two forms of inhibitory plasticity have been uncovered, which differ in their temporal expression. Before hearing onset, a form of calcium-dependent iLTD can be induced and is blocked by $GABA_BR$ antagonists (Kotak and Sanes, 2000; Kotak et al., 2001). After hearing onset, the same authors found a form of iLTP, which required postsynaptic depolarisation and was also blocked by $GABA_BR$ antagonists (Kotak and Sanes, 2014). Thus, calcium may participate in the LTP and/or LTD of inhibitory synapses at different developmental periods. In the gerbil MSO, higher VGCC-evoked calcium signals in the distal dendrite could for example mediate the elimination of distal synapses through a mechanism involving retrograde cannabinoid signalling, which is present at these developmental stages (Trattner et al., 2013). The loss of distal signals around P15 would however restrict this mechanism to before and shortly after hearing onset.

The involvement of $GABA_BRs$ in activity-dependent refinements in the LSO is interesting considering the developmental regulation of GABAergic transmission. Inhibition undergoes a transition from predominantly GABAergic to glycinergic transmission in the medial limb of the LSO of gerbils (Kotak et al., 1998), and $GABA_ARs$ contribute to the IPSC during the first week in the MSO of rats (Smith et al., 2000). In the gerbil MSO, $GABA_BRs$ differentially regulate neurotransmitter release of excitatory and inhibitory inputs during development. Furthermore, $GABA_BRs$ switch from a dendritic to a somatic localisation around hearing onset (Hassfurth et al., 2010). Interestingly, the membrane availability of $GABA_BRs$ has been shown to be regulated by glutamate (Vargas et al., 2008), suggesting that changes in overall activity levels, as following noise exposure, may influence $GABA_BR$ signalling and its downstream effects.

The finding that immature MSO neurons display efficient backpropagation (Winters and Golding, 2017), large LVA and HVA calcium currents and an NMDAR component early in development indicates that calcium signalling is most robust before and at hearing onset. However, the increase in the size of single excitatory fibres (personal communication, Sarah Gleiss) and the refinement of glycinergic synapses take place (or at least continue) after hearing onset (Kapfer et al., 2002; Magnusson et al., 2005). Thus, the onset of hearing may trigger a particular refinement mechanism, or a switch from one refinement mechanism to another. As mentioned earlier, large calcium signals before hearing onset may act as a stabilising signal which prevents circuit refinements. The rapid loss of calcium signals after hearing onset may then engage a phase of competition between excitatory and inhibitory inputs for access to this limited resource. Finally, it is possible that spontaneous activity before hearing onset mediates functional changes in synaptic efficacy, which are implemented on a structural level after hearing onset, as in the LSO of rats (Kim and Kandler, 2003; Kandler et al., 2009).

4.1.4 *Sensory experience differentially affects excitation and inhibition*

Exposure to omnidirectional white noise appears to accelerate the refinement of excitatory synaptic properties. In P14 neurons, both the size of the single EPSC and synaptically-evoked calcium signals resemble that of more mature stages (P17) following omnidirectional white noise exposure (personal communication, Sarah Gleiss). Along with the faster maturation of excitatory inputs, the proportion of P17 and P18 cells which could still evoke a calcium signal through VGCCs declined considerably following noise exposure. Thus, VGCC-evoked calcium signals may 'follow' excitatory synapses which are undergoing refinement. Interestingly, noise exposure appeared to accelerate the refinement of excitation without any change in the passive and active membrane properties of MSO neurons. Only the AP width was significantly larger at more than one day (P14 and P15) following noise exposure. Given the significant decrease of the T-Type current at P14, the larger AP width following noise exposure could reflect the presence of calcium-dependent potassium channels, which affect the repolarising phase of the AP. In layer 5 of the barrel cortex, sensory deprivation increases dendritic calcium electrogenesis without affecting passive and active membrane properties (Breton and Stuart, 2009). Thus, intrinsic membrane properties may be more robust to alterations in activity.

The pattern of acoustic experience has been shown to play an instructive role in the development of auditory circuits. In the primary auditory cortex, exposure to continuous white noise retards the emergence of topographic representational order and delays the closure of the critical period, allowing acoustically-driven plasticity to continue during adulthood (Chang and Merzenich, 2003). In contrast, exposure to pulsed white noise disrupts the normal development of tonotopicity and leads to broader tuning curves (Zhang et al., 2002). Similarly, synchronising the activity of auditory nerve fibres with repetitive broadband clicks reduces the frequency tuning of neurons in the central nucleus of the IC (Sanes and Constantine-Paton, 1983). In the MSO, masking binaural cues with continuous omnidirectional white noise prevents the normal rearrangement of glycinergic synapses to the soma (Kapfer et al., 2002; Werthat et al., 2008), and the normal development of glycinergic responses (Magnusson et al., 2005). Furthermore, the ITD tuning of DNLL neurons of gerbils raised for a limited time in omnidirectional white noise is similar to that of immature gerbils (Seidl, 2005). Taken together, this paradigm disrupts several important refinements, leaving the MSO in a functionally and structurally immature state. In contrast, omnidirectional white noise exposure appears to accelerate the development of excitatory transmission and calcium signalling, which in turn resemble more mature stages. Thus, our findings raise the possibility that the development of excitation and inhibition in the MSO may be differentially sensitive to different features of acoustic experience (overall level of activity vs. relevant binaural cues). Specifically, the faster maturation of excitatory transmission and calcium signalling may have resulted from the high overall level of activity upon continuous noise exposure. This hypothesis could be tested by repeating our experiments in an environment which disrupts binaural cues but now with low overall levels of acoustic activity e.g. cochlear ablation or middle ear bone removal. If this paradigm delays the development of calcium signalling, it would favour the hypothesis that calcium signalling is influenced by the overall level of acoustic activity, or level of synaptic drive. In support of this idea, a developmental decrease in an

NMDAR-mediated component in the visual cortex is prevented following dark rearing (Carmignoto and Vicini, 1992; Fox et al., 1992).

Even if the maturation of excitation and inhibition depend on distinct features of acoustic experience, they may still share common cellular mechanisms for refinement e.g. calcium. While T-Type calcium channels may allow inhibition to influence or even recruit calcium signals, their contribution to the rearrangement of glycinergic synapses would be limited to approximately 2 days after hearing onset. Thus, glycinergic inputs may also need to interact with excitation to access calcium-dependent signalling pathways needed for refinement. If extreme changes in overall acoustic activity accelerate or delay the development of calcium signalling, they may in turn affect calcium-dependent circuit refinements. Thus, the disruption of the glycinergic refinement following continuous exposure to omnidirectional white noise may simply reflect the earlier loss of calcium signals recruited by excitation. In disagreement with this, unilateral cochlear ablation also disrupts the refinement of glycinergic synapses (Kapfer et al., 2002). Although it is not known whether this procedure alters the development of calcium signalling in the MSO, unilateral cochlear ablation may provide a lower synaptic drive and hence delay calcium signalling. However, given that MSO neurons receive bilateral excitation and inhibition, it is difficult to speculate on the development of calcium signals following unilateral cochlear ablation. It would however be an important question to address, particularly given that excitatory inputs from both sides are anatomically segregated (Stotler, 1953; Lindsey, 1975; Smith et al., 1993). Another approach would be to assess the development of calcium signalling following bilateral middle ear bone removal (a reversible procedure such as earplugs would be preferable, but they are unfortunately not suitable for low frequencies). If a) this procedure delays the development of calcium signalling, and if b) the refinement of glycinergic synapses depends on calcium signals evoked by excitation, the refinement of glycinergic synapses may proceed normally, although perhaps with a different temporal profile. If not, this would provide further support that relevant binaural cues are required for the refinement of glycinergic synapses.

Alternatively, the refinement of glycinergic synapses may require relevant binaural cues *and* calcium recruited by excitation. To test this possibility, an important first step would be to establish whether extreme changes in the overall level of acoustic activity can influence the development of calcium signalling in a bidirectional manner. If so, the refinement of glycinergic synapses could be assessed in a paradigm which changes the overall level of acoustic activity without masking binaural cues. A normal refinement of glycinergic synapses upon both high and low levels of overall activity would favour the hypothesis that glycinergic synapses do not depend on calcium signals provided by excitation. If the refinement of glycinergic synapses is specifically disrupted upon high levels of overall activity, it would suggest that it depends not only on relevant binaural cues but also on calcium signals provided by excitation (which would be downregulated earlier in this condition). Conversely, if the glycinergic refinement requires calcium signals provided by excitation, low overall levels of activity may extend the time period during which the inhibitory refinement can take place. While such a paradigm may be difficult to implement (particularly in the case of low levels of overall activity) it would hopefully reveal whether excitation and inhibition share common mechanisms for refinement, and hence whether they mature in an interdependent manner.

While these experiments address how changes in acoustic experience influence circuit refinements, it will also be important to unravel the contribution of spontaneous activity. Unilateral cochlear ablation performed before hearing onset has been shown to disrupt the balance of excitatory and inhibitory transmission in the LSO of P8 – P14 gerbils (Kotak and Sanes, 1996). Specifically, functional denervation of the glycinergic pathway before hearing onset tipped the balance in favour of excitation. A decrease in the strength of glycinergic transmission was paralled by an increase and prolongation of EPSPs, largely attributable to an increase in the contribution of NMDARs and possibly the upregulation of a low-threshold calcium current (Kotak and Sanes, 1996). Given the presence of two additional inputs in the MSO, it is difficult to speculate on changes in the balance of excitation and inhibition following manipulations such as cochlear ablation. If important processes such as calcium signalling are similarly developmentally regulated in the LSO, this simpler circuit may also constitute a valid model to study activity-dependent circuit refinements in the MSO.

4.1.5 *Conclusions & Outlook*

The development of calcium signalling in the gerbil MSO supports the existence of calcium-dependent circuit refinements during a short time window after hearing onset. During this developmental period, glycinergic synapses are refined to the soma in an experience-dependent manner (Kapfer et al., 2002). A possible implication of this finding is that a somatic arrangement of glycinergic inputs leads to a favourable timing of inhibitory inputs relative to MSO spiking, which in turn is essential for ITD encoding (Kapfer et al., 2002; Seidl, 2005). The maintenance of somatic glycinergic synapses may reflect the elimination of distal inhibitory inputs. Alternatively, somatic glycinergic synapses may be selectively strengthened, and a form of iLTP has been recently found (Winters and Golding, 2017). Interestingly, the inhibitory refinement coincides with a decrease in the size of somatic APs, as well as their progressively limited backpropagation. Taken together, these observations suggest that the coincidence between the activation of glycinergic inputs and MSO spiking may be important for their refinement. If so, the progressive decline in AP backpropagation may eventually lead to the retention of glycinergic synapses at the soma.

The functional role of T-Type calcium channels in the MSO is an important question to address. Their strong developmental regulation around hearing onset is, in itself, interesting. Given their distinct voltage-dependent properties, T-Type channels may promote neuronal growth early in development by boosting calcium signals, enhance backpropagating voltage signals or even participate in activity-dependent changes in synaptic efficacy. Interestingly, T-Type calcium channels may constitute a way for hyperpolarising inhibition to modulate calcium signals. An interesting question for future research is whether T-Type calcium channels could potentially participate in the selection of inhibitory synapses which are active at a favourable time relative to MSO spiking. Slice experiments could be used to test how calcium signals differ in the presence or absence of a hyperpolarisation provided at various times relative to MSO spiking. A more in depth characterisation of calcium channel kinetics will also be required. Finally, assessing the full developmental profile and cellular

distribution of T-Type calcium channels in MSO neurons should provide more insight into their functional role.

4.2 PASSIVE MEMBRANE PROPERTIES DYNAMICALLY SHAPE VOLTAGE RESPONSES

Early in development, immature synaptic and membrane properties allow for larger temporal summation and hence larger integration windows, thereby promoting mechanisms underlying the refinement and stabilisation of circuits. However, these properties are not well suited to accommodate the high temporal precision required of the mature system. As a result, many developmental changes take place to mediate faster voltage signalling, including changes in the expression and conductance of ion channels (Scott et al., 2005; Bortone et al., 2006; Nakamura and Takahashi, 2007; Khurana et al., 2012), alterations in intrinsic and synaptic properties (Ahuja and Wu, 2000; Smith et al., 2000; Magnusson et al., 2005; Chirila et al., 2007; Hoffpauir et al., 2010; Ammer et al., 2012; Franzen et al., 2015), and changes in morphology (Rogowski and Feng, 1981; Rautenberg et al., 2009). While the role of voltage-gated conductances in shaping neuronal responses is studied in great detail, less is known about the relative contibution of passive membrane properties to the development of neuronal excitability and temporal precision in auditory brainstem neurons.

Based on passive membrane properties alone, the speed of voltage responses is defined by the membrane time constant of a neuron, a linear product of the input resistance and the membrane capacitance. Figure 4.1 simulates the voltage response of a neuron to the onset of a square pulse of a given current, based solely on these passive membrane properties. Different colours represent different combinations of input resistance and membrane capacitance. Several observations can be made based on this simplified illustration. First, at the beginning of the current step, the time taken to reach a particular voltage depends largely on the membrane capacitance (see red – orange traces vs. blue – green traces). In line with this, a current applied to a neuron must satisfy the requirement to charge the membrane capacitance. At a certain time point in the stimulation, the difference in input resistance will start to manifest itself more (e.g. the orange and red curves start to separate). Thus, the relative importance of the input resistance and the membrane capacitance not only depends on the duration of the stimulus, but also on where the voltage threshold is. Finally, the input resistance alone determines the voltage at steady-state, in accordance with Ohm's law. This very simplified simulation does not include the contribution of voltage-dependent conductances, and the relationships between passive properties are likely more complicated in response to very short current ramps. However, our findings in the VNLL fit the predictions of this simple model very well, illustrating the importance of passive membrane properties in shaping neuronal responses. For example, we found that while the addition of a leak conductance was very effective in changing the firing pattern of immature VNLL neurons to resemble that of mature stages, it did not strongly affect the AP waveform in response to short stimuli. In turn, the current threshold to short current injections correlated very well with the membrane capacitance, and was fairly insensitive to the addition of a leak conductance. An important relationship emerges from these findings: how the duration of a stimulus relates to the membrane time constant of a neuron. Thus, the relative influence of the membrane capacitance and

the input resistance on voltage responses depends on whether the stimulus comprises a small or large fraction of the membrane time constant. Given the much shorter membrane time constant of mature MSO neurons (~300 µs) compared to VNLL neurons (~3.5 ms), a stimulus which constitutes 5% of the membrane time constant of a VNLL neuron will constitute ~60% of the membrane time constant of a MSO neuron. Thus, even in response to very short stimuli, changes in input resistance will likely differentially affect the voltage response of MSO and VNLL neurons.

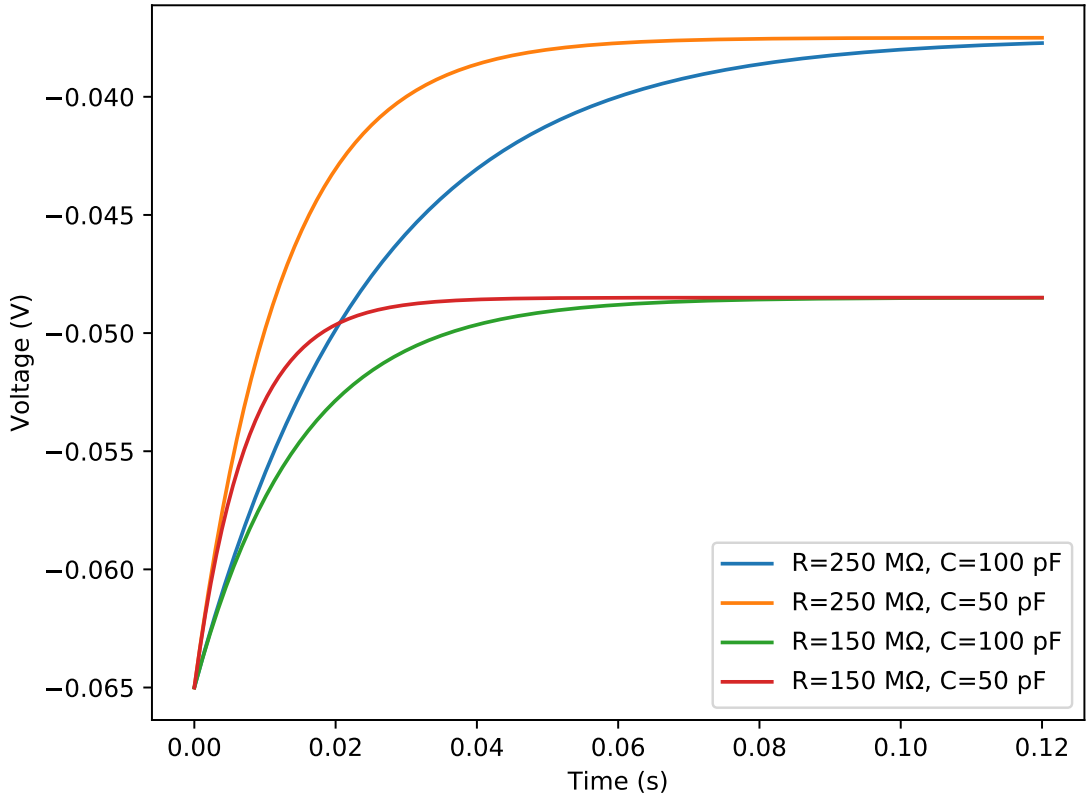

Figure 4.1: Voltage change from V_{rest} to V_{ss} in response to a current step. The different colours refer to different combinations of input resistance and membrane capacitance.

4.3 BIOPHYSICAL CHANGES UNDERLYING THE DEVELOPMENT OF TEMPORAL PRECISION

Many studies have demonstrated that a major factor governing AP precision is the balance and temporal sequence of voltage-dependent conductances underlying the EPSP near threshold (Fricker and Miles, 2000; Axmacher and Miles, 2004; Cudmore et al., 2010). Specifically, the precision

of EPSP–AP coupling depends on the shape of the EPSP at its maximum (Ammer et al., 2012), where high precision correlates with short EPSC decay times (Rodriguez-Molina et al., 2007). Thus, outward currents or conductances which curtail prolonged EPSPs at threshold decrease the jitter of AP generation and enhance AP precision (Fricker and Miles, 2000; Pouille and Scanziani, 2001; Gastrein et al., 2011; Wlodarczyk et al., 2013). In the MNTB, I_{KLVA} reduces the jitter and temporal window of AP generation (Gittelman, 2006). We found that changes in input resistance alone were sufficient to enhance the temporal precision of immature VNLL neurons to short current injections. The application of a leak conductance reduced the time the membrane potential spent close to threshold, and decreased the latency and jitter of APs. Consistent with this, developmental changes in passive membrane properties have been shown to influence the precision and jitter of AP generation in other regions (Cathala et al., 2003; Ammer et al., 2012). In the hippocampus, tonic GABA decreases the latency and jitter of AP generation through a decrease in the membrane time constant (Wlodarczyk et al., 2013). While tonic GABA application is very effective at enhancing the AP precision at threshold, the effect is negligeable at high stimulation intensities. Thus, background synaptic conductances or neuromodulations *in vivo* may play an important role in enhancing the AP precision of VNLL at threshold (Zsiros, 2005). Prolonged depolarisations by neuromodulators may further promote the appearance of an onset firing pattern by decreasing the input resistance and inactivating potassium currents (Berger et al., 2014; Franzen et al., 2015).

Both in MSO and VNLL neurons, changes in passive and active membrane properties promote the emergence of coincidence detector properties (Ratté et al., 2013). MSO neurons encode differences in the arrival time of sound at the two ears in the order or tens of microseconds with high precision. At mature stages, MSO neurons exhibit specialised membrane properties, as shown by their exceptionally low input resistance (~5 MΩ) and very short membrane time constant (~300 µs) (Scott et al., 2005; Couchman et al., 2010). Two well-balanced conductances contribute to the low input resistance at rest: a hyperpolarisation-activated mixed-cation conductance and a low-threshold potassium conductance (Scott et al., 2005; Khurana et al., 2011; Baumann et al., 2013). Interestingly, the development of I_h appears to slightly precede that of I_{KLVA}. Through their effect on the membrane time constant, these conductances accelerate voltage signalling and enhance the temporal precision of synaptic integration (Golding et al., 1995; Oertel et al., 2000; Scott et al., 2005; Khurana et al., 2011). Importantly, the extremely short membrane time constant of mature MSO neurons confers them with a high sensitivity to the arrival time of synaptic events. In turn, the high current threshold of mature MSO neurons (~5.5 nA) further imposes a requirement on synaptic events to arrive in close temporal register to evoke a suprathreshold response. At the same time, EPSCs are large and slower than the membrane time constant. Thus, MSO neurons act as neuronal integrators but are so rapid that they are also specialised for neuronal coincidence detection.

One of the most striking features of globular VNLL neurons has been reported in bats, where VNLLc neurons exhibit constant latency over varying stimulus intensities and frequencies (Covey and Casseday, 1991). The constant latency of VNLLc neurons has been suggested to arise from the coincidence of convergent inputs spanning a wide range of frequencies, and a high excitatory threshold (Covey and Casseday, 1991). The high excitatory threshold of VNLLc neurons is thought to contribute to short latencies, as it ensures that VNLLc neurons only respond when their inputs are

themselves well above threshold, when changes in latency are minimal (Covey and Casseday, 1991). The high temporal precision of VNLL neurons has been demonstrated in several other mammals, although fewer cells could be classified as constant latency responders (Recio-Spinoso and Joris, 2014). In juvenile gerbils, VNLL neurons are innervated by several calyceal endings, the coactivation of which is ideal to elicit a reliable suprathreshold response (Berger et al., 2014). Thus, juvenile VNLL neurons detect the coincident activation of broadly tuned octopus cells. At this stage, the low excitability and the presence of an A-type potassium current prevent the generation of an onset firing pattern (Berger et al., 2014). We found that VNLL neurons acquire their high temporal precision and characteristic onset firing pattern through changes in intrinsic membrane properties during development. Specifically, this transition is largely mediated by an increase in the density of potassium currents with slow inactivation kinetics, and a decrease in input resistance. Thus, as in other species investigated so far (Aitkin et al., 1970; Covey and Casseday, 1991; Batra and Fitzpatrick, 1999; Wu, 1999; Irfan et al., 2005; Zhang and Kelly, 2006; Recio-Spinoso and Joris, 2014; Caspari et al., 2015), mature VNLL neurons in gerbils also display highly precise onset responses. However, the current threshold of VNLL in response to physiologically relevant stimuli decreases during development. This change in excitability partly results from a developmental decrease in cell capacitance and changes in voltage-gated conductances. The decrease in current threshold seems at odds with the operational mode of a coincidence detector. As a result of this decrease in current threshold, VNLL neurons may respond to the coactivation of fewer inputs. If this is accompanied by a developemental increase in the size of synaptic responses, mature VNLL neurons may even respond to the activation of a single input. Given that the latency and jitter of AP generation decrease substantially with stimulation intensity (Axmacher and Miles, 2004; Rodriguez-Molina et al., 2007; Wlodarczyk et al., 2013), a low current threshold could promote short latencies and enhance AP precision by ensuring that VNLL cells respond well above threshold. It is unknown whether the number, arrangement and strength of these calyceal inputs changes during development. Recent studies report large all-or-none EPSCs in the VNLL of P22 mice, suggesting mature VNLL neurons may be innervated by a single excitatory calyceal fibre (Caspari et al., 2015; Baumann and Koch, 2017). While this should be tested using electron microscopy, the combination of a large all-or-none input and a low current threshold would ensure a high safety factor, promoting reliable synaptic transmission and high AP precision in the face of different acoustic conditions. However, it is difficult to reconcile this interpretation with the idea that constant latency arises from the convergence of broadly tuned inputs. Alternatively, while the high current threshold in juvenile neurons may be necessary to promote short latencies by ensuring inputs are responding well above threshold, this may not be necessary in mature VNLL neurons, where short latencies may rather be imparted by their specialised intrinsic properties.

4.3.1 *Conclusions & Outlook*

At immature stages, information transfer in the VNLL is gated by the timing of several presynaptic inputs and a low postsynaptic excitability. Here, endogenous neuromodulations may be particularly important to ensure the faithful transfer of information during levels of activity and dynamically

enhance the temporal precision of VNLL neurons. Our findings illustrate how developmental adaptations in intrinsic properties complement the coincidence detector properties of immature neurons. Specifically, developmental changes in passive and active membrane properties act in concert to generate the short latency onset responses and high temporal precision of mature VNLL neurons. Taken together, VNLL neurons are ideally suited to provide fast, broadband onset inhibition to the IC. An unresolved question is how synaptic properties mature in parallel with intrinsic membrane properties to mediate the high temporal precision of mature VNLL neurons.

4.4 GENERAL CONCLUSION

The establishment of a functional circuit requires a coordinated set of developmental changes in intrinsic and synaptic properties. In the auditory brainstem, such developmental refinements are particularly important given the high temporal precision required of mature neurons. While some of these changes appear to be relatively hardwired, others are influenced by acoustic experience. The developmental profile of calcium signalling in the MSO coincides with the onset of hearing and important circuit refinements known to take place at that time. Our findings show that while inhibition may influence or even recruit calcium signals early in development, this is likely limited to before and a few days after hearing onset. Thus, inhibition may need to interact with excitation to access calcium-dependent signalling pathways at later stages. Whether excitation and inhibition require common cellular mechanisms to mature — yet are differentially sensitive to distinct features of acoustic experience — will be an interesting question to address and may influence our interpretations relating to circuit refinements in the auditory system. Furthermore, an unresolved question is whether the large calcium signals before hearing onset simply promote growth in the immature circuit, or mediate functional changes in synaptic efficacy which are implemented on a structural level after the onset of acoustic experience. An important aspect of establishing a functional circuit is that auditory neurons must also acquire response properties which meet the functional requirements of the mature circuit. The exceptional temporal precision of globular VNLL neurons emerges through specific developmental interactions between passive and active membrane properties. While voltage-gated channels clearly play an important role in shaping voltage responses and shortening integrating times, our findings highlight the relative contribution of passive membrane properties, particularly in the context of different stimulation conditions e.g. neuromodulation vs. short synaptic stimulation. Integrating these findings with an understanding of how the pattern of input and synaptic properties develop will further our understanding of how auditory neurons acquire the high temporal precision required of the mature system.

Adams, J. C. (1979). 'Ascending projections to the inferior colliculus.' In: *The Journal of Comparative Neurology* 183.3, pp. 519–538.

Adams, J. C. (1997). 'Projections from octopus cells of the posteroventral cochlear nucleus to the ventral nucleus of the lateral lemniscus in cat and human'. In: *Auditory Neuroscience* 3(4), pp. 335–350.

Agmon-Snir, H., Carr, C. E., and Rinzel, J. (1998). 'The role of dendrites in auditory coincidence detection.' In: *Nature* 393.6682, pp. 268–272.

Agmon-Snir, H. and Segev, I. (1993). 'Signal delay and input synchronization in passive dendritic structures.' In: *Journal of Neurophysiology* 70.5, pp. 2066–2085.

Ahuja, T. K. and Wu, S. H. (2000). 'Developmental changes in physiological properties in the rat's dorsal nucleus of the lateral lemniscus.' In: *Hearing research* 149.1-2, pp. 33–45.

Aitkin, L. M., Anderson, D. J., and Brugge, J. F. (1970). 'Tonotopic organization and discharge characteristics of single neurons in nuclei of the lateral lemniscus of the cat.' In: *Journal of Neurophysiology* 33.3, pp. 421–440.

Ammer, J. J., Grothe, B., and Felmy, F. (2012). 'Late postnatal development of intrinsic and synaptic properties promotes fast and precise signaling in the dorsal nucleus of the lateral lemniscus.' In: *Journal of Neurophysiology* 107.4, pp. 1172–1185.

Ashida, G. and Carr, C. E. (2011). 'Sound localization: Jeffress and beyond'. In: *Current Opinion in Neurobiology* 21.5, pp. 745–751.

Autret, L., Mechaly, I., Scamps, F., Valmier, J., Lory, P., and Desmadryl, G. (2005). 'The involvement of Ca v3.2/α 1HT-type calcium channels in excitability of mouse embryonic primary vestibular neurones'. In: *The Journal of physiology* 567.1, pp. 67–78.

Axmacher, N. and Miles, R. (2004). 'Intrinsic cellular currents and the temporal precision of EPSP-action potential coupling in CA1 pyramidal cells.' In: *The Journal of physiology* 555.Pt 3, pp. 713–725.

Bal, R. and Oertel, D. (2001). 'Potassium currents in octopus cells of the mammalian cochlear nucleus.' In: *Journal of Neurophysiology* 86.5, pp. 2299–2311.

Balakrishnan, V., Becker, M., Löhrke, S., Nothwang, H. G., Güresir, E., and Friauf, E. (2003). 'Expression and function of chloride transporters during development of inhibitory neurotransmission in the auditory brainstem.' In: *The Journal of neuroscience : the official journal of the Society for Neuroscience* 23.10, pp. 4134–4145.

Bardo, S., Cavazzini, M. G., and Emptage, N. (2006). 'The role of the endoplasmic reticulum Ca2+ store in the plasticity of central neurons'. In: *Trends in Pharmacological Sciences* 27.2, pp. 78–84.

Barnes-Davies, M., Barker, M. C., Osmani, F., and Forsythe, I. D. (2004). 'Kv1 currents mediate a gradient of principal neuron excitability across the tonotopic axis in the rat lateral superior olive.' In: *European Journal of Neuroscience* 19.2, pp. 325–333.

Bar-Yehuda, D. and Korngreen, A. (2008). 'Space-Clamp Problems When Voltage Clamping Neurons Expressing Voltage-Gated Conductances'. In: *Journal of Neurophysiology* 99.3, pp. 1127–1136.

Batra, R. and Fitzpatrick, D. C. (1999). 'Discharge patterns of neurons in the ventral nucleus of the lateral lemniscus of the unanesthetized rabbit.' In: *Journal of Neurophysiology* 82.3, pp. 1097–1113.

Baumann, V. J. and Koch, U. (2017). 'Perinatal nicotine exposure impairs the maturation of glutamatergic inputs in the auditory brainstem'. In: *The Journal of physiology* 221, pp. 367–18.

Baumann, V. J., Lehnert, S., Leibold, C., and Koch, U. (2013). 'Tonotopic organization of the hyperpolarization-activated current (Ih) in the mammalian medial superior olive.' In: *Frontiers in Neural Circuits* 7, p. 117.

Bean, B. P. (2007). 'The action potential in mammalian central neurons'. In: *Nature Reviews Neuroscience* 8.6, pp. 451–465.

Behrend, O. and Schuller, G. (2000). 'The central acoustic tract and audio-vocal coupling in the horseshoe bat, Rhinolophus rouxi.' In: *European Journal of Neuroscience* 12.12, pp. 4268–4280.

Ben-Ari, Y. (2002). 'Excitatory actions of GABA during development: the nature of the nurture.' In: *Nature Reviews Neuroscience* 3.9, pp. 728–739.

Berger, C., Meyer, E. M. M., Ammer, J. J., and Felmy, F. (2014). 'Large Somatic Synapses on Neurons in the Ventral Lateral Lemniscus Work in Pairs'. In: 34.9, pp. 3237–3246.

Berntson, A. K. and Walmsley, B. (2008). 'Characterization of a potassium-based leak conductance in the medial nucleus of the trapezoid body.' In: *Hearing research* 244.1-2, pp. 98–106.

Berridge, M. J. (1998). 'Neuronal calcium signaling.' In: *Neuron* 21.1, pp. 13–26.

Berridge, M. J., Bootman, M. D., and Roderick, H. L. (2003). 'Calcium signalling: dynamics, homeostasis and remodelling'. In: *Nature reviews. Molecular cell biology* 4.7, pp. 517–529.

Blackmer, T., Kuo, S. P., Bender, K. J., Apostolides, P. F., and Trussell, L. O. (2009). 'Dendritic calcium channels and their activation by synaptic signals in auditory coincidence detector neurons.' In: *Journal of Neurophysiology* 102.2, pp. 1218–1226.

Bortone, D. S., Mitchell, K., and Manis, P. B. (2006). 'Developmental time course of potassium channel expression in the rat cochlear nucleus'. In: *Hearing research* 211.1-2, pp. 114–125.

Brand, A., Behrend, O., Marquardt, T., McAlpine, D., and Grothe, B. (2002). 'Precise inhibition is essential for microsecond interaural time difference coding.' In: *Nature* 417.6888, pp. 543–547.

Brandt, A., Striessnig, J., and Moser, T. (2003). 'CaV1.3 channels are essential for development and presynaptic activity of cochlear inner hair cells.' In: *The Journal of neuroscience : the official journal of the Society for Neuroscience* 23.34, pp. 10832–10840.

Breton, J.-D. and Stuart, G. J. (2009). 'Loss of sensory input increases the intrinsic excitability of layer 5 pyramidal neurons in rat barrel cortex'. In: *The Journal of physiology* 587.21, pp. 5107–5119.

Brew, H. M. and Forsythe, I. D. (1995). 'Two voltage-dependent K+ conductances with complementary functions in postsynaptic integration at a central auditory synapse.' In: *Journal of Neuroscience* 15.12, pp. 8011–8022.

Cant, N. B. and Hyson, R. L. (1992). 'Projections from the lateral nucleus of the trapezoid body to the medial superior olivary nucleus in the gerbil.' In: *Hearing research* 58.1, pp. 26–34.

Cao, X. J., Shatadal, S., and Oertel, D. (2007). 'Voltage-Sensitive Conductances of Bushy Cells of the Mammalian Ventral Cochlear Nucleus'. In: *Journal of Neurophysiology* 97.6, pp. 3961–3975.

Carbone, E. and Lux, H. D. (1984). 'A low voltage-activated, fully inactivating Ca channel in vertebrate sensory neurones.' In: *Nature* 310.5977, pp. 501–502.

Carmignoto, G. and Vicini, S. (1992). 'Activity-dependent decrease in NMDA receptor responses during development of the visual cortex.' In: *Science* 258.5084, pp. 1007–1011.

Case, D. T., Zhao, X., and Gillespie, D. C. (2011). 'Functional refinement in the projection from ventral cochlear nucleus to lateral superior olive precedes hearing onset in rat.' In: *PLoS ONE* 6.6, e20756.

Caspari, F., Baumann, V. J., Garcia-Pino, E., and Koch, U. (2015). 'Heterogeneity of Intrinsic and Synaptic Properties of Neurons in the Ventral and Dorsal Parts of the Ventral Nucleus of the Lateral Lemniscus'. In: *Frontiers in Neural Circuits* 9, p. 335.

Cathala, L., Brickley, S., Cull-Candy, S., and Farrant, M. (2003). 'Maturation of EPSCs and intrinsic membrane properties enhances precision at a cerebellar synapse.' In: 23.14, pp. 6074–6085.

Catterall, W. A. (2005). 'International Union of Pharmacology. XLVIII. Nomenclature and Structure-Function Relationships of Voltage-Gated Calcium Channels'. In: *Pharmacological reviews* 57.4, pp. 411–425.

Catterall, W. A. (2011). 'Voltage-gated calcium channels.' In: *Cold Spring Harbor perspectives in biology* 3.8, a003947.

Chambard, J. M., Chabbert, C., Sans, A., and Desmadryl, G. (1999). 'Developmental changes in low and high voltage-activated calcium currents in acutely isolated mouse vestibular neurons.' In: *The Journal of physiology* 518.Pt 1, pp. 141–149.

Chang, E. F. and Merzenich, M. M. (2003). 'Environmental noise retards auditory cortical development.' In: *Science* 300.5618, pp. 498–502.

Chirila, F. V., Rowland, K. C., Thompson, J. M., and Spirou, G. A. (2007). 'Development of gerbil medial superior olive: integration of temporally delayed excitation and inhibition at physiological temperature'. In: *The Journal of physiology* 584.1, pp. 167–190.

Christie, B. R., Eliot, L. S., Ito, K., Miyakawa, H., and Johnston, D. (1995). 'Different Ca^{2+} channels in soma and dendrites of hippocampal pyramidal neurons mediate spike-induced Ca^{2+} influx.' In: *Journal of Neurophysiology* 73.6, pp. 2553–2557.

Clapham, D. E. (2007). 'Calcium Signaling'. In: *Cell* 131.6, pp. 1047–1058.

Clark, G. M. (1969). 'The ultrastructure of nerve endings in the medial superior olive of the cat.' In: *Brain research* 14.2, pp. 293–305.

Clause, A., Kim, G., Sonntag, M., Weisz, C. J. C., Vetter, D. E., Rübsamen, R., and Kandler, K. (2014). 'The Precise Temporal Pattern of Prehearing Spontaneous Activity Is Necessary for Tonotopic Map Refinement'. In: *Neuron* 82.4, pp. 822–835.

Cormier, R. J., Greenwood, A. C., and Connor, J. A. (2001). 'Bidirectional synaptic plasticity correlated with the magnitude of dendritic calcium transients above a threshold.' In: *Journal of Neurophysiology* 85.1, pp. 399–406.

Couchman, K., Grothe, B., and Felmy, F. (2012). 'Functional localization of neurotransmitter receptors and synaptic inputs to mature neurons of the medial superior olive.' In: *Journal of Neurophysiology* 107.4, pp. 1186–1198.

Couchman, K., Grothe, B., and Felmy, F. (2010). 'Medial superior olivary neurons receive surprisingly few excitatory and inhibitory inputs with balanced strength and short-term dynamics.' In: *The Journal of neuroscience : the official journal of the Society for Neuroscience* 30.50, pp. 17111–17121.

Covey, E. and Casseday, J. H. (1986). 'Connectional basis for frequency representation in the nuclei of the lateral lemniscus of the bat Eptesicus fuscus.' In: *Journal of Neuroscience* 6.10, pp. 2926–2940.

Covey, E. and Casseday, J. H. (1991). 'The monaural nuclei of the lateral lemniscus in an echolocating bat: parallel pathways for analyzing temporal features of sound.' In: *The Journal of neuroscience : the official journal of the Society for Neuroscience* 11.11, pp. 3456–3470.

Cramer, K. S. and Gabriele, M. L. (2014). 'Axon guidance in the auditory system: multiple functions of Eph receptors.' In: *Neuroscience* 277, pp. 152–162.

Crandall, S. R., Govindaiah, G., and Cox, C. L. (2010). 'Low-Threshold Ca^{2+} Current Amplifies Distal Dendritic Signaling in Thalamic Reticular Neurons'. In: *Journal of Neuroscience* 30.46, pp. 15419–15429.

Cudmore, R. H., Fronzaroli-Molinieres, L., Giraud, P., and Debanne, D. (2010). 'Spike-time precision and network synchrony are controlled by the homeostatic regulation of the D-type potassium current.' In: *The Journal of neuroscience : the official journal of the Society for Neuroscience* 30.38, pp. 12885–12895.

Cueni, L., Canepari, M., Adelman, J. P., and Lüthi, A. (2009). 'Ca^{2+} signaling by T-type Ca^{2+} channels in neurons.' In: *Pflügers Archiv : European journal of physiology* 457.5, pp. 1161–1172.

Cynader, M. and Mitchell, D. E. (1980). 'Prolonged sensitivity to monocular deprivation in dark-reared cats'. In: *J Neurophysiol* 43.4, p. 1026.

Dodson, P. D., Barker, M. C., and Forsythe, I. D. (2002). 'Two heteromeric Kv1 potassium channels differentially regulate action potential firing.' In: *The Journal of neuroscience : the official journal of the Society for Neuroscience* 22.16, pp. 6953–6961.

Ebbers, L. et al. (2015). 'L-type Calcium Channel Ca v1.2 Is Required for Maintenance of Auditory Brainstem Nuclei'. In: *Journal of Biological Chemistry* 290.39, pp. 23692–23710.

Ehrlich, I., Lohrke, S., and Friauf, E. (1999). 'Shift from depolarizing to hyperpolarizing glycine action in rat auditory neurones is due to age-dependent Cl- regulation.' In: *The Journal of physiology* 520 Pt 1, pp. 121–137.

Englitz, B., Tolnai, S., Typlt, M., Jost, J., and Rübsamen, R. (2009). 'Reliability of synaptic transmission at the synapses of Held in vivo under acoustic stimulation.' In: *PLoS ONE* 4.10, e7014.

Feldman, D. E. (2012). 'The Spike-Timing Dependence of Plasticity'. In: *Neuron* 75.4, pp. 556–571.

Felmy, F. and Schneggenburger, R. (2004). 'Developmental expression of the Ca2+-binding proteins calretinin and parvalbumin at the calyx of Held of rats and mice.' In: *European Journal of Neuroscience* 20.6, pp. 1473–1482.

Finck, A., Schneck, C. D., and Hartman, A. F. (1972). 'Development of cochlear function in the neonate Mongolian gerbil (Meriones unguiculatus).' In: *Journal of comparative and physiological psychology* 78.3, pp. 375–380.

Ford, M. C., Alexandrova, O., Cossell, L., Stange-Marten, A., Sinclair, J., Kopp-Scheinpflug, C., Pecka, M., Attwell, D., and Grothe, B. (2015). 'Tuning of Ranvier node and internode properties in myelinated axons to adjust action potential timing'. In: *Nature Communications* 6, pp. 1–14.

Fox, K., Daw, N., Sato, H., and Czepita, D. (1992). 'The effect of visual experience on development of NMDA receptor synaptic transmission in kitten visual cortex.' In: *Journal of Neuroscience* 12.7, pp. 2672–2684.

Franken, T. P., Roberts, M. T., Wei, L., Golding, N. L., and Joris, P. X. (2015). 'In vivo coincidence detection in mammalian sound localization generates phase delays'. In: *Nature Neuroscience*, pp. 1–11.

Franks, K. M. and Isaacson, J. S. (2005). 'Synapse-Specific Downregulation of NMDA Receptors by Early Experience: A Critical Period for Plasticity of Sensory Input to Olfactory Cortex'. In: *Neuron* 47.1, pp. 101–114.

Franzen, D. L. *., Gleiss, S. A. *., Berger, C. *., Kümpfbeck, F. S., Ammer, J. J., and Felmy, F. (2015). 'Development and modulation of intrinsic membrane properties control the temporal precision of auditory brainstem neurons'. In: *Journal of Neurophysiology* 113(2), pp. 524–536.

Friauf, E. and Ostwald, J. (1988). 'Divergent projections of physiologically characterized rat ventral cochlear nucleus neurons as shown by intra-axonal injection of horseradish peroxidase.' In: *Experimental brain research. Experimentelle Hirnforschung. Expérimentation cérébrale* 73.2, pp. 263–284.

Friauf, E. (1993). 'Transient appearance of calbindin-D28k-positive neurons in the superior olivary complex of developing rats'. In: *Journal of Comparative Neurology* 334.1, pp. 59–74.

Fricker, D. and Miles, R. (2000). 'EPSP amplification and the precision of spike timing in hippocampal neurons.' In: *Neuron* 28.2, pp. 559–569.

Futai, K., Okada, M., Matsuyama, K., and Takahashi, T. (2001). 'High-fidelity transmission acquired via a developmental decrease in NMDA receptor expression at an auditory synapse.' In: *The Journal of neuroscience : the official journal of the Society for Neuroscience* 21.10, pp. 3342–3349.

Gastrein, P., Campanac, E., Gasselin, C., Cudmore, R. H., Bialowas, A., Carlier, E., Fronzaroli-Molinieres, L., Ankri, N., and Debanne, D. (2011). 'The role of hyperpolarization-activated cationic current in spike-time precision and intrinsic resonance in cortical neurons in vitro'. In: *The Journal of physiology* 589.15, pp. 3753–3773.

Geiger, J. R., Lübke, J., Roth, A., Frotscher, M., and Jonas, P. (1997). 'Submillisecond AMPA receptor-mediated signaling at a principal neuron-interneuron synapse.' In: *Neuron* 18.6, pp. 1009–1023.

Gittelman, J. X. (2006). 'Kv1.1-Containing Channels Are Critical for Temporal Precision During Spike Initiation'. In: *Journal of Neurophysiology* 96.3, pp. 1203–1214.

Glendenning, K. K., Brunso-Bechtold, J. K., Thompson, G. C., and Masterton, R. B. (1981). 'Ascending auditory afferents to the nuclei of the lateral lemniscus.' In: *The Journal of Comparative Neurology* 197.4, pp. 673–703.

Godfrey, D. A., Kiang, N. Y., and Norris, B. E. (1975). 'Single unit activity in the posteroventral cochlear nucleus of the cat.' In: *The Journal of Comparative Neurology* 162.2, pp. 247–268.

Goldberg, J. M. and Brown, P. B. (1969). 'Response of binaural neurons of dog superior olivary complex to dichotic tonal stimuli: some physiological mechanisms of sound localization.' In: *Journal of Neurophysiology* 32.4, pp. 613–636.

Golding, N. L., Robertson, D., and Oertel, D. (1995). 'Recordings from slices indicate that octopus cells of the cochlear nucleus detect coincident firing of auditory nerve fibers with temporal precision.' In: *Journal of Neuroscience* 15.4, pp. 3138–3153.

Goldstein, S. A., Bockenhauer, D., O'Kelly, I., and Zilberberg, N. (2001). 'Potassium leak channels and the KCNK family of two-P-domain subunits.' In: *Nature Reviews Neuroscience* 2.3, pp. 175–184.

Greer, P. L. and Greenberg, M. E. (2008). 'From Synapse to Nucleus: Calcium-Dependent Gene Transcription in the Control of Synapse Development and Function'. In: *Neuron* 59.6, pp. 846–860.

Grothe, B. (2000). 'The evolution of temporal processing in the medial superior olive, an auditory brainstem structure.' In: *Progress in neurobiology* 61.6, pp. 581–610.

Grothe, B. and Park, T. J. (2000). 'Structure and function of the bat superior olivary complex.' In: *Microscopy research and technique* 51.4, pp. 382–402.

Grothe, B., Pecka, M., and McAlpine, D. (2010). 'Mechanisms of Sound Localization in Mammals'. In: *Physiological Reviews* 90.3, pp. 983–1012.

Grothe, B., Schweizer, H., Pollak, G. D., Schuller, G., and Rosemann, C. (1994). 'Anatomy and projection patterns of the superior olivary complex in the Mexican free-tailed bat, Tadarida brasiliensis mexicana.' In: *The Journal of Comparative Neurology* 343.4, pp. 630–646.

Grothe, B. (2003). 'Sensory systems: New roles for synaptic inhibition in sound localization'. In: *Nature Reviews Neuroscience* 4.7, pp. 540–550.

Grothe, B. and Pecka, M. (2014). 'The natural history of sound localization in mammals–a story of neuronal inhibition.' In: *Frontiers in Neural Circuits* 8.65, p. 116.

Gu, X. and Spitzer, N. C. (1993). 'Low-threshold Ca2+ current and its role in spontaneous elevations of intracellular Ca2+ in developing Xenopus neurons.' In: *Journal of Neuroscience* 13.11, pp. 4936–4948.

Guinan, J. J., Norris, B. E., and Guinan, S. S. (1972). 'Single Auditory Units in the Superior Olivary Complex: II: Locations of Unit Categories and Tonotopic Organization'. In: *International Journal of Neuroscience* 4.4, pp. 147–166.

Gulledge, A. T., Kampa, B. M., and Stuart, G. J. (2005). 'Synaptic integration in dendritic trees'. In: *Journal of neurobiology* 64.1, pp. 75–90.

Hassfurth, B., Grothe, B., and Koch, U. (2010). 'The Mammalian Interaural Time Difference Detection Circuit Is Differentially Controlled by GABAB Receptors during Development'. In: *The Journal of neuroscience : the official journal of the Society for Neuroscience* 30.29, pp. 9715–9727.

Heffner, R. S. and Heffner, H. E. (1988). 'Sound localization and use of binaural cues by the gerbil (Meriones unguiculatus).' In: *Behavioral neuroscience* 102.3, pp. 422–428.

Hensch, T. K. (2005). 'Critical period plasticity in local cortical circuits'. In: *Nature Reviews Neuroscience* 6.11, pp. 877–888.

Hirtz, J. J. et al. (2011). 'Cav1.3 calcium channels are required for normal development of the auditory brainstem.' In: *The Journal of neuroscience : the official journal of the Society for Neuroscience* 31.22, pp. 8280–8294.

Hoffman, D. A., Magee, J. C., Colbert, C. M., and Johnston, D. (1997). 'K+ channel regulation of signal propagation in dendrites of hippocampal pyramidal neurons.' In: *Nature* 387.6636, pp. 869–875.

Hoffpauir, B. K., Kolson, D. R., Mathers, P. H., and Spirou, G. A. (2010). 'Maturation of synaptic partners: functional phenotype and synaptic organization tuned in synchrony'. In: *The Journal of physiology* 588.22, pp. 4365–4385.

Horibe, S., Tarusawa, E., Komatsu, Y., and Yoshimura, Y. (2014). 'Ni^{2+}-sensitive T-type Ca^{2+} channel currents are regulated in parallel with synaptic and visual response plasticity in visual cortex'. In: *Neuroscience research* 87, pp. 33–39.

Howell, D. M., Morgan, W. J., Jarjour, A. A., Spirou, G. A., Berrebi, A. S., Kennedy, T. E., and Mathers, P. H. (2007). 'Molecular guidance cues necessary for axon pathfinding from the ventral cochlear nucleus'. In: *The Journal of Comparative Neurology* 504.5, pp. 533–549.

Hubel, D. H. and Wiesel, T. N. (1965). 'Binocular interaction in striate cortex of kittens reared with artificial squint.' In: *Journal of Neurophysiology* 28.6, pp. 1041–1059.

Huffman, K. J. and Cramer, K. S. (2007). 'EphA4 misexpression alters tonotopic projections in the auditory brainstem'. In: *Developmental Neurobiology* 67.12, pp. 1655–1668.

Huffman, R. F. and Covey, E. (1995). 'Origin of ascending projections to the nuclei of the lateral lemniscus in the big brown bat, Eptesicus fuscus.' In: *The Journal of Comparative Neurology* 357.4, pp. 532–545.

Irfan, N., Zhang, H., and Wu, S. H. (2005). 'Synaptic transmission mediated by ionotropic glutamate, glycine and GABA receptors in the rat's ventral nucleus of the lateral lemniscus.' In: *Hearing research* 203.1-2, pp. 159–171.

Ismailov, I. (2004). 'The Kinetic Profile of Intracellular Calcium Predicts Long-Term Potentiation and Long-Term Depression'. In: *Journal of Neuroscience* 24.44, pp. 9847–9861.

Isomura, Y., Fujiwara-Tsukamoto, Y., Imanishi, M., Nambu, A., and Takada, M. (2002). 'Distance-dependent Ni(2+)-sensitivity of synaptic plasticity in apical dendrites of hippocampal CA1 pyramidal cells.' In: *Journal of Neurophysiology* 87.2, pp. 1169–1174.

Iwasaki, S., Momiyama, A., Uchitel, O. D., and Takahashi, T. (2000). 'Developmental changes in calcium channel types mediating central synaptic transmission.' In: *The Journal of neuroscience : the official journal of the Society for Neuroscience* 20.1, pp. 59–65.

Iwasaki, S. and Takahashi, T. (1998). 'Developmental changes in calcium channel types mediating synaptic transmission in rat auditory brainstem'. In: *The Journal of physiology* 509.2, pp. 419–423.

Jaffer, S., Vorobyov, V., Kind, P. C., and Sengpiel, F. (2012). 'Experience-dependent regulation of functional maps and synaptic protein expression in the cat visual cortex'. In: *European Journal of Neuroscience* 35.8, pp. 1281–1294.

Jeffress, L. A. (1948). 'A place theory of sound localization.' In: *Journal of comparative and physiological psychology* 41.1, pp. 35–39.

Jercog, P. E., Svirskis, G., Kotak, V. C., Sanes, D. H., and Rinzel, J. (2010). 'Asymmetric Excitatory Synaptic Dynamics Underlie Interaural Time Difference Processing in the Auditory System'. In: *PLoS biology* 8.6, e1000406–9.

Johnston, D., Christie, B. R., Frick, A., Gray, R., Hoffman, D. A., Schexnayder, L. K., Watanabe, S., and Yuan, L. L. (2003). 'Active dendrites, potassium channels and synaptic plasticity'. In: *Philosophical Transactions of the Royal Society B: Biological Sciences* 358.1432, pp. 667–674.

Johnston, D., Magee, J. C., Colbert, C. M., and Cristie, B. R. (1996). 'Active properties of neuronal dendrites.' In: *Annual review of neuroscience* 19.1, pp. 165–186.

Jonas, P. and Burnashev, N. (1995). 'Molecular mechanisms controlling calcium entry through AMPA-type glutamate receptor channels'. In: *Neuron* 15.5, pp. 987–990.

Joris, P. X., Carney, L. H., Smith, P., and Yin, T. C. (1994). 'Enhancement of neural synchronization in the anteroventral cochlear nucleus. I. Responses to tones at the characteristic frequency.' In: *Journal of Neurophysiology* 71.3, pp. 1022–1036.

Joshi, I. and Wang, L.-Y. (2002). 'Developmental profiles of glutamate receptors and synaptic transmission at a single synapse in the mouse auditory brainstem.' In: *The Journal of physiology* 540.Pt 3, pp. 861–873.

Kakazu, Y., Akaike, N., Komiyama, S., and Nabekura, J. (1999). 'Regulation of intracellular chloride by cotransporters in developing lateral superior olive neurons.' In: *The Journal of neuroscience : the official journal of the Society for Neuroscience* 19.8, pp. 2843–2851.

Kandler, K. and Friauf, E. (1993). 'Pre- and postnatal development of efferent connections of the cochlear nucleus in the rat.' In: *The Journal of Comparative Neurology* 328.2, pp. 161–184.

Kandler, K. and Friauf, E. (1995). 'Development of glycinergic and glutamatergic synaptic transmission in the auditory brainstem of perinatal rats.' In: *The Journal of neuroscience : the official journal of the Society for Neuroscience* 15.10, pp. 6890–6904.

Kandler, K., Clause, A., and Noh, J. (2009). 'Tonotopic reorganization of developing auditory brainstem circuits'. In: *Nature Neuroscience* 12.6, pp. 711–717.

Kapfer, C., Seidl, A. H., Schweizer, H., and Grothe, B. (2002). 'Experience-dependent refinement of inhibitory inputs to auditory coincidence-detector neurons'. In: *Nature Neuroscience* 5.3, pp. 247–253.

Karino, S., Smith, P., Yin, T. C. T., and Joris, P. X. (2011). 'Axonal Branching Patterns as Sources of Delay in the Mammalian Auditory Brainstem: A Re-Examination'. In: *Journal of Neuroscience* 31.8, pp. 3016–3031.

Katz, L. C. and Shatz, C. J. (1996). 'Synaptic activity and the construction of cortical circuits.' In: *Science* 274.5290, pp. 1133–1138.

Kelly, J. B., Adel, B. A. van, and Ito, M. (2009). 'Anatomical projections of the nuclei of the lateral lemniscus in the albino rat (rattus norvegicus)'. In: *The Journal of Comparative Neurology* 512.4, pp. 573–593.

Khurana, S., Liu, Z., Lewis, A. S., Rosa, K., Chetkovich, D., and Golding, N. L. (2012). 'An essential role for modulation of hyperpolarization-activated current in the development of binaural temporal precision.' In: *The Journal of neuroscience : the official journal of the Society for Neuroscience* 32.8, pp. 2814–2823.

Khurana, S., Remme, M. W. H., Rinzel, J., and Golding, N. L. (2011). 'Dynamic interaction of Ih and IK-LVA during trains of synaptic potentials in principal neurons of the medial superior olive.' In: *The Journal of neuroscience : the official journal of the Society for Neuroscience* 31.24, pp. 8936–8947.

Kil, J., Kageyama, G. H., Semple, M. N., and Kitzes, L. M. (1995). 'Development of ventral cochlear nucleus projections to the superior olivary complex in gerbil.' In: *The Journal of Comparative Neurology* 353.3, pp. 317–340.

Kim, G. and Kandler, K. (2010). 'Synaptic changes underlying the strengthening of GABA/glycinergic connections in the developing lateral superior olive.' In: *Neuroscience* 171.3, pp. 924–933.

Kim, G. and Kandler, K. (2003). 'Elimination and strengthening of glycinergic/GABAergic connections during tonotopic map formation'. In: *Nature Neuroscience* 6.3, pp. 282–290.

Kirkby, L. A., Sack, G. S., Firl, A., and Feller, M. B. (2013). 'A Role for Correlated Spontaneous Activity in the Assembly of Neural Circuits'. In: *Neuron* 80.5, pp. 1129–1144.

Kitzes, L. M., Kageyama, G. H., Semple, M. N., and Kil, J. (1995). 'Development of ectopic projections from the ventral cochlear nucleus to the superior olivary complex induced by neonatal ablation of the contralateral cochlea.' In: *The Journal of Comparative Neurology* 353.3, pp. 341–363.

Koike-Tani, M., Saitoh, N., and Takahashi, T. (2005). 'Mechanisms underlying developmental speeding in AMPA-EPSC decay time at the calyx of Held.' In: *The Journal of neuroscience : the official journal of the Society for Neuroscience* 25.1, pp. 199–207.

König, P., Engel, A. K., and Singer, W. (1996). 'Integrator or coincidence detector? The role of the cortical neuron revisited.' In: *Trends in neurosciences* 19.4, pp. 130–137.

Kopp-Scheinpflug, C., Lippe, W. R., Dörrscheidt, G. J., and Rübsamen, R. (2003). 'The medial nucleus of the trapezoid body in the gerbil is more than a relay: comparison of pre- and postsynaptic activity.' In: *Journal of the Association for Research in Otolaryngology* 4.1, pp. 1–23.

Kopp-Scheinpflug, C., Steinert, J. R., and Forsythe, I. D. (2011). 'Modulation and control of synaptic transmission across the MNTB.' In: *Hearing research* 279.1-2, pp. 22–31.

Kotak, V. C., DiMattina, C., and Sanes, D. H. (2001). 'GABA(B) and Trk receptor signaling mediates long-lasting inhibitory synaptic depression.' In: *Journal of Neurophysiology* 86.1, pp. 536–540.

Kotak, V. C., Korada, S., Schwartz, I. R., and Sanes, D. H. (1998). 'A developmental shift from GABAergic to glycinergic transmission in the central auditory system.' In: *The Journal of neuroscience : the official journal of the Society for Neuroscience* 18.12, pp. 4646–4655.

Kotak, V. C. and Sanes, D. H. (1996). 'Developmental influence of glycinergic transmission: regulation of NMDA receptor-mediated EPSPs.' In: *The Journal of neuroscience : the official journal of the Society for Neuroscience* 16.5, pp. 1836–1843.

Kotak, V. C. and Sanes, D. H. (2000). 'Long-lasting inhibitory synaptic depression is age- and calcium-dependent.' In: *The Journal of neuroscience : the official journal of the Society for Neuroscience* 20.15, pp. 5820–5826.

Kotak, V. C. and Sanes, D. H. (2014). 'Developmental expression of inhibitory synaptic long-term potentiation in the lateral superior olive.' In: *Frontiers in Neural Circuits* 8, p. 67.

Kuba, H., Koyano, K., and Ohmori, H. (2002). 'Development of membrane conductance improves coincidence detection in the nucleus laminaris of the chicken'. In: *The Journal of physiology* 540.2, pp. 529–542.

Kullmann, P. H. M. and Kandler, K. (2008). 'Dendritic Ca^{2+} responses in neonatal lateral superior olive neurons elicited by glycinergic/GABAergic synapses and action potentials'. In: *Neuroscience* 154.1, pp. 338–345.

Kullmann, P. H. and Kandler, K. (2001). 'Glycinergic/GABAergic synapses in the lateral superior olive are excitatory in neonatal C57Bl/6J mice.' In: *Brain research. Developmental brain research* 131.1-2, pp. 143–147.

Kullmann, P. H. M., Ene, F. A., and Kandler, K. (2002). 'Glycinergic and GABAergic calcium responses in the developing lateral superior olive.' In: *European Journal of Neuroscience* 15.7, pp. 1093–1104.

Kuwabara, N. and Zook, J. M. (1992). 'Projections to the medial superior olive from the medial and lateral nuclei of the trapezoid body in rodents and bats.' In: *The Journal of Comparative Neurology* 324.4, pp. 522–538.

Leao, R. N. (2003). 'Differences in Glycinergic mIPSCs in the Auditory Brain Stem of Normal and Congenitally Deaf Neonatal Mice'. In: *Journal of Neurophysiology* 91.2, pp. 1006–1012.

Leão, R. N., Berntson, A., Forsythe, I. D., and Walmsley, B. (2004). 'Reduced low-voltage activated K +conductances and enhanced central excitability in a congenitally deaf (dn/dn) mouse'. In: *The Journal of physiology* 559.1, pp. 25–33.

Leão, R. N., Sun, H., Svahn, K., Berntson, A., Youssoufian, M., Paolini, A. G., Fyffe, R. E. W., and Walmsley, B. (2006). 'Topographic organization in the auditory brainstem of juvenile mice is disrupted in congenital deafness'. In: *The Journal of physiology* 571.3, pp. 563–578.

Leibold, C. and Hemmen, J. L. van (2005). 'Spiking Neurons Learning Phase Delays: How Mammals May Develop Auditory Time-Difference Sensitivity'. In: *Physical Review Letters* 94.16, pp. 168102–4.

Leresche, N. and Lambert, R. C. (2016). 'T-type calcium channels in synaptic plasticity.' In: *Channels*, pp. 1–19.

Lesica, N. A., Lingner, A., and Grothe, B. (2010). 'Population Coding of Interaural Time Differences in Gerbils and Barn Owls'. In: *Journal of Neuroscience* 30.35, pp. 11696–11702.

Levic, S., Nie, L., Tuteja, D., Harvey, M., Sokolowski, B. H. A., and Yamoah, E. N. (2007). 'Development and regeneration of hair cells share common functional features.' In: *Proceedings of the National Academy of Sciences of the United States of America* 104.48, pp. 19108–19113.

Lindsey, B. G. (1975). 'Fine structure and distribution of axon terminals from the cochlear nucleus on neurons in the medial superior olivary nucleus of the cat.' In: *The Journal of Comparative Neurology* 160.1, pp. 81–103.

Lisman, J. (1989). 'A mechanism for the Hebb and the anti-Hebb processes underlying learning and memory.' In: *Proceedings of the National Academy of Sciences of the United States of America* 86.23, pp. 9574–9578.

Lohmann, C., Ilic, V., and Friauf, E. (1998). 'Development of a topographically organized auditory network in slice culture is calcium dependent.' In: *Journal of neurobiology* 34.2, pp. 97–112.

Lohmann, C. and Friauf, E. (1996). 'Distribution of the calcium-binding proteins parvalbumin and calretinin in the auditory brainstem of adult and developing rats'. In: *Journal of Comparative Neurology* 367.1, pp. 90–109.

Löhrke, S., Srinivasan, G., Oberhofer, M., Doncheva, E., and Friauf, E. (2005). 'Shift from depolarizing to hyperpolarizing glycine action occurs at different perinatal ages in superior olivary complex nuclei'. In: *European Journal of Neuroscience* 22.11, pp. 2708–2722.

Lory, P., Bidaud, I., and Chemin, J. (2006). 'T-type calcium channels in differentiation and proliferation.' In: *Cell calcium* 40.2, pp. 135–146.

Magee, J. C., Christofi, G., Miyakawa, H., Christie, B., Lasser-Ross, N., and Johnston, D. (1995). 'Subthreshold synaptic activation of voltage-gated Ca2+ channels mediates a localized Ca2+ influx into the dendrites of hippocampal pyramidal neurons.' In: *Journal of Neurophysiology* 74.3, pp. 1335–1342.

Magee, J. C. and Johnston, D. (1995). 'Synaptic activation of voltage-gated channels in the dendrites of hippocampal pyramidal neurons.' In: *Science* 268.5208, pp. 301–304.

Magee, J. C. and Johnston, D. (1997). 'A synaptically controlled, associative signal for Hebbian plasticity in hippocampal neurons.' In: *Science* 275.5297, pp. 209–213.

Magnusson, A. K., Kapfer, C., Grothe, B., and Koch, U. (2005). 'Maturation of glycinergic inhibition in the gerbil medial superior olive after hearing onset.' In: *The Journal of physiology* 568.Pt 2, pp. 497–512.

Maier, J. K., Kindermann, T., Grothe, B., and Klump, G. M. (2008). 'Effects of omnidirectional noise-exposure during hearing onset and age on auditory spatial resolution in the Mongolian gerbil (Meriones unguiculatus) — a behavioral approach'. In: *Brain research* 1220, pp. 47–57.

Maier, J. K. and Klump, G. M. (2006). 'Resolution in azimuth sound localization in the Mongolian gerbil (Meriones unguiculatus)'. In: *The Journal of the Acoustical Society of America* 119.2, pp. 1029–9.

Mainen, Z. F. and Sejnowski, T. J. (1996). 'Influence of dendritic structure on firing pattern in model neocortical neurons.' In: *Nature* 382.6589, pp. 363–366.

Malenka, R. C. and Bear, M. F. (2004). 'LTP and LTD: an embarrassment of riches.' In: *Neuron* 44.1, pp. 5–21.

Malenka, R. C., Kauer, J. A., Zucker, R. S., and Nicoll, R. A. (1988). 'Postsynaptic calcium is sufficient for potentiation of hippocampal synaptic transmission.' In: *Science* 242.4875, pp. 81–84.

Markram, H. (1997). 'Regulation of Synaptic Efficacy by Coincidence of Postsynaptic APs and EPSPs'. In: *Science* 275.5297, pp. 213–215.

Markram, H., Helm, P. J., and Sakmann, B. (1995). 'Dendritic calcium transients evoked by single back-propagating action potentials in rat neocortical pyramidal neurons.' In: *The Journal of physiology* 485.1, pp. 1–20.

Mathews, P. J., Jercog, P. E., Rinzel, J., Scott, L. L., and Golding, N. L. (2010). 'Control of submillisecond synaptic timing in binaural coincidence detectors by K(v)1 channels.' In: *Nature Publishing Group* 13.5, pp. 601–609.

McAlpine, D., Jiang, D., and Palmer, A. R. (2001). 'A neural code for low-frequency sound localization in mammals.' In: *Nature Neuroscience* 4.4, pp. 396–401.

McAlpine, D. and Grothe, B. (2003). 'Sound localization and delay lines – do mammals fit the model?' In: *Trends in neurosciences* 26.7, pp. 347–350.

McCobb, D. P. and Beam, K. G. (1991). 'Action potential waveform voltage-clamp commands reveal striking differences in calcium entry via low and high voltage-activated calcium channels.' In: *Neuron* 7.1, pp. 119–127.

Milenkovic, I. and Rübsamen, R. (2011). 'Development of the chloride homeostasis in the auditory brainstem.' In: *Physiological research* 60 Suppl 1, S15–27.

Milenkovic, I., Witte, M., Turecek, R., Heinrich, M., Reinert, T., and Rübsamen, R. (2007). 'Development of Chloride-Mediated Inhibition in Neurons of the Anteroventral Cochlear Nucleus of Gerbil (Meriones unguiculatus)'. In: *Journal of Neurophysiology* 98.3, pp. 1634–1644.

Myoga, M. H., Lehnert, S., Leibold, C., Felmy, F., and Grothe, B. (2014). 'Glycinergic inhibition tunes coincidence detection in the auditory brainstem'. In: *Nature Communications* 5, pp. 1–13.

Nakamura, P. A., Hsieh, C. Y., and Cramer, K. S. (2012). 'EphB signaling regulates target innervation in the developing and deafferented auditory brainstem'. In: *Developmental Neurobiology* 72.9, pp. 1243–1255.

Nakamura, Y. and Takahashi, T. (2007). 'Developmental changes in potassium currents at the rat calyx of Held presynaptic terminal'. In: *The Journal of physiology* 581.3, pp. 1101–1112.

Nayagam, D. A. X. (2005). 'Powerful, Onset Inhibition in the Ventral Nucleus of the Lateral Lemniscus'. In: *Journal of Neurophysiology* 94.2, pp. 1651–1654.

Nordeen, K. W., Killackey, H. P., and Kitzes, L. M. (1983). 'Ascending auditory projections to the inferior colliculus in the adult gerbil, Meriones unguiculatus.' In: *The Journal of Comparative Neurology* 214.2, pp. 131–143.

Nowycky, M. C., Fox, A. P., and Tsien, R. W. (1985). 'Three types of neuronal calcium channel with different calcium agonist sensitivity.' In: *Nature* 316.6027, pp. 440–443.

Oertel, D. (1997). 'Encoding of timing in the brain stem auditory nuclei of vertebrates.' In: *Neuron* 19.5, pp. 959–962.

Oertel, D. (1999). 'The role of timing in the brain stem auditory nuclei of vertebrates.' In: *Annual Review of Physiology* 61.1, pp. 497–519.

Oertel, D., Bal, R., Gardner, S. M., Smith, P., and Joris, P. X. (2000). 'Detection of synchrony in the activity of auditory nerve fibers by octopus cells of the mammalian cochlear nucleus.' In: *Proceedings of the National Academy of Sciences of the United States of America* 97.22, pp. 11773–11779.

Pecka, M., Brand, A., Behrend, O., and Grothe, B. (2008). 'Interaural Time Difference Processing in the Mammalian Medial Superior Olive: The Role of Glycinergic Inhibition'. In: *Journal of Neuroscience* 28.27, pp. 6914–6925.

Perkins, R. E. (1973). 'An electron microscopic study of synaptic organization in the medial superior olive of normal and experimental chinchillas.' In: *The Journal of Comparative Neurology* 148.3, pp. 387–415.

Pollak, G. D., Gittelman, J. X., Li, N., and Xie, R. (2011). 'Inhibitory projections from the ventral nucleus of the lateral lemniscus and superior paraolivary nucleus create directional selectivity of frequency modulations in the inferior colliculus: A comparison of bats with other mammals'. In: *Hearing research* 273.1-2, pp. 134–144.

Pouille, F. and Scanziani, M. (2001). 'Enforcement of temporal fidelity in pyramidal cells by somatic feed-forward inhibition.' In: *Science* 293.5532, pp. 1159–1163.

Ratté, S., Hong, S., De Schutter, E., and Prescott, S. A. (2013). 'Perspective'. In: *Neuron* 78.5, pp. 758–772.

Rautenberg, P. L., Grothe, B., and Felmy, F. (2009). 'Quantification of the three-dimensional morphology of coincidence detector neurons in the medial superior olive of gerbils during late postnatal development'. In: *The Journal of Comparative Neurology* 517.3, pp. 385–396.

Rayleigh, L. (1907). 'XII.On our perception of sound direction'. In: *Philosophical Magazine Series 6* 13.74, pp. 214–232.

Recio-Spinoso, A. and Joris, P. X. (2014). 'Temporal properties of responses to sound in the ventral nucleus of the lateral lemniscus.' In: *Journal of Neurophysiology* 111.4, pp. 817–835.

Rhode, W. S. and Greenberg, S. (1994). 'Encoding of amplitude modulation in the cochlear nucleus of the cat.' In: *Journal of Neurophysiology* 71.5, pp. 1797–1825.

Rhode, W. S., Oertel, D., and Smith, P. (1983). 'Physiological response properties of cells labeled intracellularly with horseradish peroxidase in cat ventral cochlear nucleus.' In: *The Journal of Comparative Neurology* 213.4, pp. 448–463.

Rhode, W. S. and Smith, P. (1986). 'Encoding timing and intensity in the ventral cochlear nucleus of the cat.' In: *Journal of Neurophysiology* 56.2, pp. 261–286.

Rietzel, H. J. and Friauf, E. (1998). 'Neuron types in the rat lateral superior olive and developmental changes in the complexity of their dendritic arbors.' In: *The Journal of Comparative Neurology* 390.1, pp. 20–40.

Roberts, M. T., Seeman, S. C., and Golding, N. L. (2013). 'A Mechanistic Understanding of the Role of Feedforward Inhibition in the Mammalian Sound Localization Circuitry'. In: *Neuron* 78.5, pp. 923–935.

Rodriguez-Molina, V. M., Aertsen, A., and Heck, D. H. (2007). 'Spike Timing and Reliability in Cortical Pyramidal Neurons: Effects of EPSC Kinetics, Input Synchronization and Background Noise on Spike Timing'. In: *PLoS ONE* 2.3, e319–11.

Rogowski, B. A. and Feng, A. S. (1981). 'Normal postnatal development of medial superior olivary neurons in the albino rat: a Golgi and Nissl study.' In: *The Journal of Comparative Neurology* 196.1, pp. 85–97.

Rose, C. R. and Konnerth, A. (2001). 'Stores not just for storage. intracellular calcium release and synaptic plasticity.' In: *Neuron* 31.4, pp. 519–522.

Rose, J. E., Brugge, J. F., Anderson, D. J., and Hind, J. E. (1967). 'Phase-locked response to low-frequency tones in single auditory nerve fibers of the squirrel monkey.' In: *Journal of Neurophysiology* 30.4, pp. 769–793.

Rudolph, S., Hull, C., and Regehr, W. G. (2015). 'Active Dendrites and Differential Distribution of Calcium Channels Enable Functional Compartmentalization of Golgi Cells.' In: *The Journal of neuroscience : the official journal of the Society for Neuroscience* 35.47, pp. 15492–15504.

Ryan, A. (1976). 'Hearing sensitivity of the mongolian gerbil, Meriones unguiculatis.' In: *The Journal of the Acoustical Society of America* 59.5, pp. 1222–1226.

Ryan, A. F., Woolf, N. K., and Sharp, F. R. (1982). 'Functional ontogeny in the central auditory pathway of the Mongolian gerbil. A 2-deoxyglucose study.' In: *Experimental*

brain research. Experimentelle Hirnforschung. Expérimentation cérébrale 47.3, pp. 428–436.

Saint Marie, R. L. and Baker, R. A. (1990). 'Neurotransmitter-specific uptake and retrograde transport of [3H]glycine from the inferior colliculus by ipsilateral projections of the superior olivary complex and nuclei of the lateral lemniscus.' In: *Brain research* 524.2, pp. 244–253.

Saint Marie, R. L., Shneiderman, A., and Stanforth, D. A. (1997). 'Patterns of gamma-aminobutyric acid and glycine immunoreactivities reflect structural and functional differences of the cat lateral lemniscal nuclei.' In: *The Journal of Comparative Neurology* 389.2, pp. 264–276.

Sanes, D. H. (1993). 'The development of synaptic function and integration in the central auditory system.' In: *The Journal of neuroscience : the official journal of the Society for Neuroscience* 13.6, pp. 2627–2637.

Sanes, D. H. and Constantine-Paton, M. (1983). 'Altered activity patterns during development reduce neural tuning'. In: *Science* 221.4616, pp. 1183–1185.

Sanes, D. H. and Friauf, E. (2000). 'Development and influence of inhibition in the lateral superior olivary nucleus.' In: *Hearing research* 147.1-2, pp. 46–58.

Sanes, D. H., Markowitz, S., Bernstein, J., and Wardlow, J. (1992a). 'The influence of inhibitory afferents on the development of postsynaptic dendritic arbors.' In: *The Journal of Comparative Neurology* 321.4, pp. 637–644.

Sanes, D. H. and Siverls, V. (1991). 'Development and specificity of inhibitory terminal arborizations in the central nervous system.' In: *Journal of neurobiology* 22.8, pp. 837–854.

Sanes, D. H., Song, J., and Tyson, J. (1992b). 'Refinement of dendritic arbors along the tonotopic axis of the gerbil lateral superior olive.' In: *Brain research. Developmental brain research* 67.1, pp. 47–55.

Sanes, D. H. and Takács, C. (1993). 'Activity-dependent refinement of inhibitory connections.' In: *European Journal of Neuroscience* 5.6, pp. 570–574.

Schneggenburger, R. and Forsythe, I. D. (2006). 'The calyx of Held'. In: *Cell and tissue research* 326.2, pp. 311–337.

Schofield, B. R. and Cant, N. B. (1997). 'Ventral nucleus of the lateral lemniscus in guinea pigs: cytoarchitecture and inputs from the cochlear nucleus.' In: *The Journal of Comparative Neurology* 379.3, pp. 363–385.

Scott, L. L., Hage, T. A., and Golding, N. L. (2007). 'Weak action potential backpropagation is associated with high-frequency axonal firing capability in principal neurons of the gerbil medial superior olive'. In: *The Journal of physiology* 583.2, pp. 647–661.

Scott, L. L., Mathews, P. J., and Golding, N. L. (2005). 'Posthearing developmental refinement of temporal processing in principal neurons of the medial superior olive.' In: *The Journal of neuroscience : the official journal of the Society for Neuroscience* 25.35, pp. 7887–7895.

Scott, L. L., Mathews, P. J., and Golding, N. L. (2010). 'Perisomatic voltage-gated sodium channels actively maintain linear synaptic integration in principal neurons of the medial superior olive.' In: *The Journal of neuroscience : the official journal of the Society for Neuroscience* 30.6, pp. 2039–2050.

Seidl, A. H. (2005). 'Development of Sound Localization Mechanisms in the Mongolian Gerbil Is Shaped by Early Acoustic Experience'. In: *Journal of Neurophysiology* 94.2, pp. 1028–1036.

Shatz, C. J. and Stryker, M. P. (1988). 'Prenatal tetrodotoxin infusion blocks segregation of retinogeniculate afferents.' In: *Science* 242.4875, pp. 87–89.

Shen, J.-x. and Yakel, J. L. (2009). 'Nicotinic acetylcholine receptor-mediated calcium signaling in the nervous system'. In: *Acta Pharmacologica Sinica* 30.6, pp. 673–680.

Shibata, S., Kakazu, Y., Okabe, A., Fukuda, A., and Nabekura, J. (2004). 'Experience-dependent changes in intracellular Cl- regulation in developing auditory neurons'. In: *Neuroscience research* 48.2, pp. 211–220.

Smith, A. J., Owens, S., and Forsythe, I. D. (2000). 'Characterisation of inhibitory and excitatory postsynaptic currents of the rat medial superior olive.' In: *The Journal of physiology* 529 Pt 3, pp. 681–698.

Smith, D. I. and Kraus, N. (1987). 'Postnatal development of the auditory brainstem response (ABR) in the unanesthetized gerbil.' In: *Hearing research* 27.2, pp. 157–164.

Smith, P., Joris, P. X., Carney, L. H., and Yin, T. C. (1991). 'Projections of physiologically characterized globular bushy cell axons from the cochlear nucleus of the cat.' In: *The Journal of Comparative Neurology* 304.3, pp. 387–407.

Smith, P., Joris, P. X., and Yin, T. C. (1993). 'Projections of physiologically characterized spherical bushy cell axons from the cochlear nucleus of the cat: evidence for delay lines to the medial superior olive.' In: *The Journal of Comparative Neurology* 331.2, pp. 245–260.

Smith, P., Joris, P. X., and Yin, T. C. (1998). 'Anatomy and physiology of principal cells of the medial nucleus of the trapezoid body (MNTB) of the cat.' In: *Journal of Neurophysiology* 79.6, pp. 3127–3142.

Smith, P., Massie, A., and Joris, P. X. (2005). 'Acoustic stria: Anatomy of physiologically characterized cells and their axonal projection patterns'. In: *The Journal of Comparative Neurology* 482.4, pp. 349–371.

Sommer, I., Lingenhöhl, K., and Friauf, E. (1993). 'Principal cells of the rat medial nucleus of the trapezoid body: an intracellular in vivo study of their physiology and morphology.' In: *Experimental brain research. Experimentelle Hirnforschung. Expérimentation cérébrale* 95.2, pp. 223–239.

Spangler, K. M., Warr, W. B., and Henkel, C. K. (1985). 'The projections of principal cells of the medial nucleus of the trapezoid body in the cat.' In: *The Journal of Comparative Neurology* 238.3, pp. 249–262.

Spitzer, M. W. and Semple, M. N. (1995). 'Neurons sensitive to interaural phase disparity in gerbil superior olive: diverse monaural and temporal response properties.' In: *Journal of Neurophysiology* 73.4, pp. 1668–1690.

Stange-Marten, A., Nabel, A. L., Sinclair, J. L., Fischl, M., Alexandrova, O., Wohlfrom, H., Kopp-Scheinpflug, C., Pecka, M., and Grothe, B. (2017). 'Input timing for spatial processing is precisely tuned via constant synaptic delays and myelination patterns in the auditory brainstem'. In: *Proceedings of the National Academy of Sciences of the United States of America* 595, pp. 201702290–8.

Steinert, J. R., Postlethwaite, M., Jordan, M. D., Chernova, T., Robinson, S. W., and Forsythe, I. D. (2010). 'NMDAR-mediated EPSCs are maintained and accelerate in time course during maturation of mouse and rat auditory brainstem in vitro'. In: *The Journal of physiology* 588.3, pp. 447–463.

Stellwagen, D. and Shatz, C. J. (2002). 'An instructive role for retinal waves in the development of retinogeniculate connectivity.' In: *Neuron* 33.3, pp. 357–367.

Stotler, W. A. (1953). 'An experimental study of the cells and connections of the superior olivary complex of the cat.' In: *The Journal of Comparative Neurology* 98.3, pp. 401–431.

Svirskis, G., Dodla, R., and Rinzel, J. (2003). 'Subthreshold outward currents enhance temporal integration in auditory neurons.' In: *Biological cybernetics* 89.5, pp. 333–340.

Svirskis, G., Kotak, V. C., Sanes, D. H., and Rinzel, J. (2002). 'Enhancement of signal-to-noise ratio and phase locking for small inputs by a low-threshold outward current in auditory neurons.' In: *The Journal of neuroscience : the official journal of the Society for Neuroscience* 22.24, pp. 11019–11025.

Swandulla, D. and Armstrong, C. M. (1988). 'Fast-deactivating calcium channels in chick sensory neurons.' In: *The Journal of general physiology* 92.2, pp. 197–218.

Swindale, N. V. (1981). 'Absence of ocular dominance patches in dark-reared cats.' In: *Nature* 290.5804, pp. 332–333.

Talavera, K. and Nilius, B. (2006). 'Biophysics and structure–function relationship of T-type Ca2+ channels'. In: *Cell calcium* 40.2, pp. 97–114.

Taschenberger, H. and von Gersdorff, H. (2000). 'Fine-tuning an auditory synapse for speed and fidelity: developmental changes in presynaptic waveform, EPSC kinetics, and synaptic plasticity.' In: *The Journal of neuroscience : the official journal of the Society for Neuroscience* 20.24, pp. 9162–9173.

Tolnai, S., Beutelmann, R., and Klump, G. M. (2017). 'Exploring binaural hearing in gerbils (Meriones unguiculatus) using virtual headphones.' In: *PLoS ONE* 12.4, e0175142.

Tong, H., Steinert, J. R., Robinson, S. W., Chernova, T., Read, D. J., Oliver, D. L., and Forsythe, I. D. (2010). 'Regulation of Kv channel expression and neuronal excitability in rat medial nucleus of the trapezoid body maintained in organotypic culture'. In: *The Journal of physiology* 588.9, pp. 1451–1468.

Trattner, B., Berner, S., Grothe, B., and Kunz, L. (2013). 'Depolarization-induced suppression of a glycinergic synapse in the superior olivary complex by endocannabinoids'. In: *Journal of neurochemistry* 34, pp. 78–90.

Tritsch, N. X., Rodriguez-Contreras, A., Crins, T. T. H., Wang, H. C., Borst, J. G. G., and Bergles, D. E. (2010). 'Calcium action potentials in hair cells pattern auditory neuron activity before hearing onset.' In: *Nature Publishing Group* 13.9, pp. 1050–1052.

Tritsch, N. X., Yi, E., Gale, J. E., Glowatzki, E., and Bergles, D. E. (2007). 'The origin of spontaneous activity in the developing auditory system.' In: *Nature* 450.7166, pp. 50–55.

Vale, C. and Sanes, D. H. (2002). 'The effect of bilateral deafness on excitatory and inhibitory synaptic strength in the inferior colliculus'. In: *European Journal of Neuroscience* 16.12, pp. 2394–2404.

Vale, C., Schoorlemmer, J., and Sanes, D. H. (2003). 'Deafness disrupts chloride transporter function and inhibitory synaptic transmission.' In: *Journal of Neuroscience* 23.20, pp. 7516–7524.

van der Heijden, M., Lorteije, J. A. M., Plauška, A., Roberts, M. T., Golding, N. L., and Borst, J. G. G. (2013). 'Directional hearing by linear summation of binaural inputs at the medial superior olive.' In: *Neuron* 78.5, pp. 936–948.

Vargas, K. J., Terunuma, M., Tello, J. A., Pangalos, M. N., Moss, S. J., and Couve, A. (2008). 'The availability of surface GABA B receptors is independent of gamma-aminobutyric acid but controlled by glutamate in central neurons.' In: *The Journal of biological chemistry* 283.36, pp. 24641–24648.

Vater, M., Covey, E., and Casseday, J. H. (1997). 'The columnar region of the ventral nucleus of the lateral lemniscus in the big brown bat (Eptesicus fuscus): synaptic arrangements and structural correlates of feedforward inhibitory function.' In: *Cell and tissue research* 289.2, pp. 223–233.

Vater, M. and Feng, A. S. (1990). 'Functional organization of ascending and descending connections of the cochlear nucleus of horseshoe bats.' In: *The Journal of Comparative Neurology* 292.3, pp. 373–395.

Verkhratsky, A. (2002). 'The endoplasmic reticulum and neuronal calcium signalling.' In: *Cell calcium* 32.5-6, pp. 393–404.

von Békésy, G. (1956). 'Current status of theories of hearing.' In: *Science* 123.3201, pp. 779–783.

von Gersdorff, H. and Borst, J. G. G. (2002). 'Short-Term Plasticity at the Calyx of Held'. In: *Nature Reviews Neuroscience* 3.1, pp. 53–64.

Warr, W. B. (1966). 'Fiber degeneration following lesions in the anterior ventral cochlear nucleus of the cat.' In: *Experimental neurology* 14.4, pp. 453–474.

Werthat, F., Alexandrova, O., Grothe, B., and Koch, U. (2008). 'Experience-dependent refinement of the inhibitory axons projecting to the medial superior olive'. In: *Developmental Neurobiology* 68.13, pp. 1454–1462.

Winters, B. D. and Golding, N. L. (2017). 'Developmentally Restricted Long-term Potentiation of Glycinergic Inhibition onto Neurons of the Medial Superior Olive'. In: *Poster Session, Association for Research in Otolaryngology*.

Winters, B. D., Jin, S.-X., Ledford, K. R., and Golding, N. L. (2017). 'Amplitude Normalization of Dendritic EPSPs at the Soma of Binaural Coincidence Detector Neurons of the Medial Superior Olive'. In: *Journal of Neuroscience* 37.12, pp. 3138–3149.

Witte, M., Reinert, T., Dietz, B., Nerlich, J., Rübsamen, R., and Milenkovic, I. (2014). 'Depolarizing chloride gradient in developing cochlear nucleus neurons: underlying mechanism and implication for calcium signaling.' In: *Neuroscience* 261, pp. 207–222.

Wlodarczyk, A. I., Xu, C., Song, I., Doronin, M., Wu, Y.-W., Walker, M. C., and Semyanov, A. (2013). 'Tonic GABAA conductance decreases membrane time constant and increases EPSP-spike precision in hippocampal pyramidal neurons.' In: *Frontiers in Neural Circuits* 7, p. 205.

Wolf, M., Schuchmann, M., and Wiegrebe, L. (2010). 'Localization dominance and the effect of frequency in the Mongolian Gerbil, Meriones unguiculatus'. In: *Journal of Comparative Physiology A* 196.7, pp. 463–470.

Woolf, N. K. and Ryan, A. F. (1984). 'The development of auditory function in the cochlea of the mongolian gerbil.' In: *Hearing research* 13.3, pp. 277–283.

Wu, S. H. (1999). 'Physiological properties of neurons in the ventral nucleus of the lateral lemniscus of the rat: intrinsic membrane properties and synaptic responses.' In: *Journal of Neurophysiology* 81.6, pp. 2862–2874.

Xiao, L., Michalski, N., Kronander, E., Gjoni, E., Genoud, C., Knott, G., and Schneggenburger, R. (2013). 'BMP signaling specifies the development of a large and fast CNS synapse'. In: *Nature Publishing Group* 16.7, pp. 856–864.

Yamada, R. (2005). 'Hyperpolarization-Activated Cyclic Nucleotide-Gated Cation Channels Regulate Auditory Coincidence Detection in Nucleus Laminaris of the Chick'. In: *Journal of Neuroscience* 25.39, pp. 8867–8877.

Yin, T. C. and Chan, J. C. (1990). 'Interaural time sensitivity in medial superior olive of cat.' In: *Journal of Neurophysiology* 64.2, pp. 465–488.

Yoshimura, Y., Inaba, M., Yamada, K., Kurotani, T., Begum, T., Reza, F., Maruyama, T., and Komatsu, Y. (2008). 'Involvement of T-type Ca 2+channels in the potentiation of synaptic and visual responses during the critical period in rat visual cortex'. In: *European Journal of Neuroscience* 28.4, pp. 730–743.

Zhang, H. and Kelly, J. B. (2006). 'Responses of neurons in the rat's ventral nucleus of the lateral lemniscus to monaural and binaural tone bursts.' In: *Journal of Neurophysiology* 95.4, pp. 2501–2512.

Zhang, L. I., Tao, H. W., Holt, C. E., Harris, W. A., and Poo, M. (1998). 'A critical window for cooperation and competition among developing retinotectal synapses.' In: *Nature* 395.6697, pp. 37–44.

Zhang, L. I., Bao, S., and Merzenich, M. M. (2002). 'Disruption of primary auditory cortex by synchronous auditory inputs during a critical period.' In: *Proceedings of the National Academy of Sciences of the United States of America* 99.4, pp. 2309–2314.

Zhao, M. and Wu, S. H. (2001). 'Morphology and physiology of neurons in the ventral nucleus of the lateral lemniscus in rat brain slices.' In: *The Journal of Comparative Neurology* 433.2, pp. 255–271.

Zhou, Y., Carney, L. H., and Colburn, H. S. (2005). 'A model for interaural time difference sensitivity in the medial superior olive: interaction of excitatory and inhibitory synaptic inputs, channel dynamics, and cellular morphology.' In: *The Journal of neuroscience : the official journal of the Society for Neuroscience* 25.12, pp. 3046–3058.

Zook, J. M. and Casseday, J. H. (1982). 'Origin of ascending projections to inferior colliculus in the mustache bat, Pteronotus parnellii.' In: *The Journal of Comparative Neurology* 207.1, pp. 14–28.

Zook, J. M. and Casseday, J. H. (1985). 'Projections from the cochlear nuclei in the mustache bat, Pteronotus parnellii.' In: *The Journal of Comparative Neurology* 237.3, pp. 307–324.

Zook, J. M. and Casseday, J. H. (1987). 'Convergence of ascending pathways at the inferior colliculus of the mustache bat, Pteronotus parnellii.' In: *The Journal of Comparative Neurology* 261.3, pp. 347–361.

Zsiros, V. (2005). 'Background Synaptic Conductance and Precision of EPSP-Spike Coupling at Pyramidal Cells'. In: *Journal of Neurophysiology* 93.6, pp. 3248–3256.

ABBREVIATIONS

AMPAR	α-amino-3-hydroxy-5-methyl-4-isoxazolepropionic acid receptor
AP	action potential
ATP	adenosine triphosphate
AVCN	anterior ventral cochlear nucleus
bAP	backpropagating AP
CN	cochlear nucleus
DNLL	dorsal nucleus of the lateral lemniscus
EPSC/P	excitatory postsynaptic current/potential
GABA	gamma-Aminobutyric acid
GBC	globular bushy cell
HVA	high voltage-activated
IC	inferior colliculus
ILD	interaural level difference
IPSC/P	inhibitory postsynaptic current/potential
ITD	interaural time difference
KCC2	K–Cl co-transporter
LGIC	ligand-gated ion channel
LNTB	lateral nucleus of the trapezoid body
LSO	lateral superior olive
LVA	low voltage-activated
MNTB	medial nucleus of the trapezoid body
MSO	medial superior olive
NMDAR	N-methyl-D-aspartic acid receptor
SBC	spherical bushy cell
SOC	superior olivary complex
STDP	spike timing dependent plasticity
VCN	ventral cochlear nucleus
VGCC	voltage-gated calcium channel
VNLL	ventral nucleus of the lateral lemniscus

ACKNOWLEDGEMENTS

So long and thanks for all the fish

— Douglas Adams

Firstly, thank you Felix for giving me the opportunity to work in your lab. I really enjoyed our many discussions which always gave me a new perspective on many topics. Thank you for your constant enthusiasm and support throughout my PhD, and for encouraging me to pursue my own ideas.

Thank you Benedikt for all your support throughout my PhD and for always taking the time to discuss my projects. I am very grateful to have been part of the GSN, which gave me the opportunity to meet many interesting people from exciting fields. I would also like to thank my other TAC members: Christian Leibold for making time for me whenever I popped my head around the door, and Mark Hübener for your many suggestions and great support throughout both my Masters and PhD in Munich. I would also like to thank the GSN administration team for always being there to sort out last minute administrative issues with a smile.

The crew in Hannover: many thanks to Linda, Alex, Nico and Sandra for your warm welcome every time I came up North.

Thank you Monika, Sabrina and Petra for your great assistance organising the litters for the noise box experiments. Also Andrea, Christian and Sven for helping me bring the noise box back to life.

Thanks to Jan Grewe and everyone at the G-Node for creating useful tools to help me analyse and visualise my imaging data.

Thank you Mike for always taking the time to help and offer advice.

This work wouldn't have been possible without the wonderful people in the Felmy lab who created such a supportive and fun atmosphere to work in. Julian, thank you for our many discussions during the VNLL project, which routinely ended with us being more confused than at the beginning. Alex, thanks for being a great desk neighbour and for teaming up with me to understand the intricacies of the MSO circuit. Thanks Franzi and Alisha for your advice, constant support and for teaching me most of what I know in German/Bavarian. *Dank eich recht schee!* Chrissi, thanks for your help and for getting me settled in the lab, and special thanks to Sarah for many fun moments at the setup during the MSO project.

I want to thank everyone in the Neurobiology department for many interesting discussions, for always being happy to help and for many good memories. Special thanks to Olga and Hilde for teaching me so much and for being lovely people to work with. Eli, thank you for getting me through the noise box experiments with a strategically well-timed piece of chocolate.

Of course I would like to thank my family for their enduring support and encouragement. Thank you also to Laurence and Olivia for your support and for making Munich feel like home.

Finally, thank you Christian for all your work on the MSO project, but most importantly for your unwavering intellectual and emotional support in the good and bad times. You were the glue that made everything stick together.

EIDESSTATTLICHE VERSICHERUNG/AFFIDAVIT

Hiermit versichere ich an Eides statt, dass ich die vorliegende Dissertation *Developmental refinements in temporally precise auditory brainstem circuits* selbstständig angefertigt habe, mich außer der angegebenen keiner weiteren Hilfsmittel bedient und alle Erkenntnisse, die aus dem Schrifttum ganz oder annähernd übernommen sind, als solche kenntlich gemacht und nach ihrer Herkunft unter Bezeichnung der Fundstelle einzeln nachgewiesen habe.

I hereby confirm that the dissertation *Developmental refinements in temporally precise auditory brainstem circuits* is the result of my own work and that I have only used sources or materials listed and specified in the dissertation.

München, im 24th July 2017
Munich, 24th July 2017

Delwen L. Franzen

AUTHOR CONTRIBUTIONS

The contributions of the authors Delwen L. Franzen (DLF), Sarah A. Gleiss (SAG), Christina Berger (CB), Franziska S. Kümpfbeck (FSK), Julian J. Ammer (JJA) and Felix Felmy (FF) to the study included in this thesis are as follows:

Franzen, D. L.*, Gleiss, S. A.*, Berger C.*, Kümpfbeck, F. S., Ammer, J. J. & Felmy, F. (2015). **Development and modulation of intrinsic membrane properties control the temporal precision of auditory brain stem neurons**. *J. Neurophysiol. 113(2)*, pp. 524-36. doi: 10.1152/jn.00601.2014. DLF, SAG, CB, FSK, JJA, and FF designed the research; DLF, SAG, CB, JJA, and FF performed the experiments; DLF, SAG, CB, FSK, JJA, and FF analysed the data and interpreted the results of the experiments; DLF, SAG, CB, FSK, and FF prepared the figures; DLF, JJA, and FF drafted the manuscript; DLF, SAG, CB, FSK, JJA, and FF edited and revised the manuscript; DLF, SAG, CB, FSK, JJA, and FF approved the final version of the manuscript.

We assert that the aforementioned author contributions are correct and accurate:

Prof. Dr. Felix Felmy

Delwen L. Franzen

Dr. Sarah A. Gleiss

Dr. Christina Berger

AUTHOR CONTRIBUTIONS

The contributions of the authors Delwen L. Franzen (DLF), Christian J. Kellner (CJK) and Felix Felmy (FF) to the study included in this thesis are as follows:

Franzen, D. L., Kellner, C. J. & Felmy, F. **Activity-dependent calcium signalling in MSO neurons during late postnatal development**. Manuscript in preparation. DLF and FF designed the research. DLF performed the experiments and analysed the electrophysiological and imaging data. CJK designed and implemented a custom-made program for the analysis of the imaging data. DLF drafted the manuscript included in this thesis with the help of FF.

We assert that the aforementioned author contributions are correct and accurate:

Prof. Dr. Felix Felmy

Delwen L. Franzen